

THESIS

SEDIMENTOLOGY, FACIES ARCHITECTURE, AND DIAGENESIS OF THE MIDDLE THREE FORKS FORMATION – NORTH DAKOTA, U.S.A.

Submitted by

Lauren A. Droege

Department of Geosciences

In partial fulfillment of the requirements

For the Degree of Master of Science

Colorado State University

Fort Collins, Colorado

Summer 2014

Master's Committee:

Advisor: Sven O. Egenhoff

Michael Ronayne
Monique Rocca

Copyright by Lauren A. Droege 2014

All Rights Reserved

ABSTRACT

SEDIMENTOLOGY, FACIES ARCHITECTURE, AND DIAGENESIS OF THE MIDDLE THREE FORKS FORMATION – NORTH DAKOTA, U.S.A.

The upper Devonian age middle Three Forks Formation in the North Dakota portion of the Williston Basin consists of a mixed carbonate-siliciclastic succession deposited in the mid- to inner-ramp portions of a low-angle epeiric ramp. Based on lithological and sedimentological characteristics, ten facies are recognized in the succession that are grouped into three facies associations (FAs). Laminated siliciclastic mudstones with silty dolostone intercalations (FA1) record deposition in the most distal, overall low-energy mid-ramp environment, whereas massive to well laminated clay clast-bearing silty dolostones (FA2) reflect sedimentation in a relatively high-energy inner-ramp setting. Mud-rich conglomerates with dolomite and clay clasts (FA3) occur in both inner- to mid-ramp settings throughout the study area, however these deposit types generally increase in abundance toward the basin margins. Halite pseudomorphs coupled with an overall low diversity of ichnofauna indicate that basin salinities were elevated at times during middle Three Forks Formation deposition.

Bedload transport processes are the dominant mechanism that led to deposition of FA1 and FA2 strata, evident in laminated siliciclastic mudstones as well as current and wave ripple-laminated silty dolostones, whereas mass gravity transport in which laminar flow processes dominated led to deposition of FA3 rocks. Recurring stacking of FA1 and FA2 strata reflect changes from low- to high-energy regimes and define up to six coarsening-upward parasequences throughout the study area, generally 1.0-5.5 m in thickness. In contrast, varying amounts of FA3 deposits

throughout the succession define five distinct stratigraphic intervals, herein termed Intervals 0-4, which reflect fluctuating climate conditions from overall humid to arid settings throughout the course of middle Three Forks Formation deposition. Intervals 0, 2, and 4 are generally characterized by high amounts of FA3 deposits, while Intervals 1 and 3 contain very few, if any, FA3 intercalations into overall well-preserved FA1 and FA2 beds.

The diagenetic history of the middle Three Forks Formation is complex and involves many different phases including: at least eight stages of dolomite, both replacement of a calcite precursor and dolomite cements that precipitated directly from aqueous solutions; anhydrite precipitation and replacement of dolomite; silicification of dolomite rhombs resulting in diagenetic quartz; pyrite framboids, concretions, and disseminated euhedral pyrite crystals; micro-intercrystalline, intercrystalline, intracrystalline, moldic, and linear dissolution porosity types.

Core descriptions, porosity estimation based on point-counting of forty-seven thin sections, isopach maps of potential “pay zones” throughout northwest North Dakota, as well as a complete lack of hydrocarbon residue in cores, suggest that reservoir quality of the middle Three Forks Formation is overall poor in this area, and few, if any, hydrocarbons have migrated to the middle Three Forks Formation from the overlying Bakken Formation.

ACKNOWLEDGEMENTS

I am thankful to Statoil for providing the financial support to carry out the research for this project. I am especially grateful to my advisor, Dr. Sven Egenhoff, for his continuous enthusiasm, guidance, and invaluable discussions throughout the course of this project, as well as the countless hours he spent reviewing and helping to improve my writing. I am also sincerely thankful to Heather Lowers at the USGS for her assistance with both the SEM and EDS Microbeam results. Many thanks to Julie LeFever at the NDGS for allowing us the time to log the several hundreds of feet worth of core necessary to the success of this project.

I would like to thank my thesis committee members, Dr. Sven Egenhoff, Dr. Mike Ronayne, and Dr. Monique Rocca for their insightful suggestions and comments that helped improve the quality of my thesis. I am also genuinely thankful to my comrades of the Colorado State University Sedimentology working group for their support as well as all of the laughs we enjoyed together along the way. I am very thankful to Anders J. Ipsen for all the love, encouragement, and patience throughout these past two years.

TABLE OF CONTENTS

ABSTRACT.....	ii
ACKNOWLEDGMENTS	iv
CHAPTER 1.0: INTRODUCTION	1
CHAPTER 2.0: GEOLOGICAL SETTING.....	4
CHAPTER 3.0: METHODOLOGY	10
CHAPTER 4.0: SEDIMENTOLOGY	14
4.1 Sedimentary Facies	15
4.2 Facies Association Descriptions	19
4.2.1 Facies Association 1	19
4.2.2 Facies Association 2	22
4.2.3 Facies Association 3	25
4.4.0 Facies Association Interpretations	27
4.4.1 Synsedimentary Deformation	28
4.4.2 Facies Association 1	28
4.4.3 Facies Association 2	30
4.4.4 Facies Association 3	31
CHAPTER 5.0: FACIES ARCHITECTURE	33
5.1 Middle Three Forks Formation Stratigraphy	33
5.2 Facies Distribution and Stacking Patterns	34
5.2.1 Interval 0	36
5.2.2 Interval 1	36
5.2.3 Interval 2	37

5.2.4 Interval 3	38
5.2.5 Interval 4	39
CHAPTER 6.0: DEPOSITIONAL MODEL	41
6.1 Inner-ramp and Mid-ramp Depositional Environments.....	42
6.2 Sediment Gravity Flows	44
CHAPTER 7.0 DIAGENESIS.....	45
7.1 Dolomite	45
7.1.1 Dolomite I.....	47
7.1.2 Dolomite II.....	47
7.1.3 Dolomite III through VIII	47
7.1.4 Dolomite Iron Concentrations.....	50
7.2 Quartz.....	51
7.3 Anhydrite	51
7.4 Pyrite	53
7.5.0 Porosity	55
7.5.1 Micro-intercrystalline Porosity	55
7.5.2 Intracrystalline Porosity	55
7.5.3 Intercrystalline Porosity	56
7.5.4 Moldic Porosity.....	56
7.5.5 Linear Dissolution Porosity	56
7.5.6 Porosity Distribution.....	58
7.6.0 Diagenetic History	59
7.6.1 Dolomite	59

7.6.2 Quartz.....	60
7.6.3 Anhydrite	61
7.6.4 Pyrite	61
7.6.5 Porosity	62
CHAPTER 8.0 DISCUSSION	64
8.1 Middle Three Forks Formation Depositional Environment.....	64
8.2 Halite Pseudomorphs as Indicators of Basinwide Hypersaline Conditions.....	65
8.3 Middle Three Forks Formation Dolomitization Model	66
8.4 Debrites and Mud-flow Deposits as Indicators of Variations in Climate During Deposition of the Middle Three Forks Formation	68
8.5 Lateral Distribution of Dolomitic Pay Zones: Implications for Petroleum Exploration.....	69
CHAPTER 9.0 CONCLUSIONS	77
REFERENCES	79
APPENDICES	87
Appendix 1: West-East Transect A-A' from western Williams County, North Dakota to eastern Mountrail County, North Dakota through the middle Three Forks Formation, Williston Basin	87
Appendix 2: West-East Transect B-B' from western Williams County, North Dakota and northern McKenzie County to eastern Mountrail County, North Dakota through the middle Three Forks Formation, Williston Basin.....	88

Appendix 3: North-South Transect C-C' from northern Mountrail County, North Dakota to central Mountrail County, North Dakota through the middle Three Forks Formation, Williston Basin	89
Appendix 4: North-South Transect D-D' northern Mountrail County, North Dakota to southern Mountrail County, North Dakota through the middle Three Forks Formation, Williston Basin	90
Appendix 5: Core Logs	91
Appendix 6: Thin Section Index	128
Appendix 7: Scanning Electron Microscope Report.....	130
Appendix 8: Electron Microprobe Quantitative Results	141

1.0 INTRODUCTION

The upper Devonian Three Forks Formation is one of the most important hydrocarbon plays in the Williston Basin, North Dakota, USA. Currently, there are 1141 horizontal wells drilled and completed in the Three Forks Formation (North Dakota Department of Mineral Resources, 2013). Estimated to contain approximately 2 billion barrels of recoverable oil (Nordeng and Helms, 2010), the Three Forks Formation will nearly double the amount of recoverable hydrocarbons in the Bakken petroleum system.

Currently, the target zone is exclusively the upper Three Forks Formation, as the upper 50 feet contain the largest proven reserves of oil in the formation (Nordeng and Helms, 2010). However, a similar dolomitic facies is ubiquitous in the central part of the Three Forks Formation where it is intercalated with debris flow units, referred to as the middle Three Forks Formation by Egenhoff et al. (2011). As a result of the close vicinity of the middle Three Forks Formation to the oil-charged upper Three Forks Formation and overlying lower Bakken Formation, hydrocarbons sourced by the lower Bakken Formation could have potentially migrated stratigraphically downward into the middle Three Forks Formation. Hydrocarbons that penetrated the middle Three Forks Formation would likely be stored within the dolomitic intervals, which have proven to be valuable reservoir targets in the upper Three Forks Formation.

Several studies on both outcrop and subsurface correlation of the Three Forks Formation in the USA and Canada have been performed since the 1950s (see Baillie, 1955; Sandberg and Hammond, 1958; Dumonceaux, 1984; Berwick, 2008; Gantyno, 2010; Nekhorosheva, 2011). Although the established model for sedimentation of the Three Forks Formation is that of deposition in a shallow epeiric sea (Dumonceaux, 1984; Gantyno, 2010; Nekhorosheva, 2011),

the unusual co-occurrence of the dolomites with siliciclastic matrix-supported conglomerates interpreted as debris flows (Egenhoff et al., 2011) has not been explored to date. Joint deposition of siliciclastics and carbonates within the same sedimentary system remains poorly understood (Wilson and Lokier, 2002), and has not been developed for siliciclastic matrix-supported conglomerates within shallow-marine dolomitic successions. While Mount (1984, 1985) already pointed out that mixed carbonate-siliciclastic systems are in fact common in the rock record, the mostly Bahamas-based research of the 1980s and early 1990s generally ignored this approach, as it did not apply to the isolated carbonate platform setting of any of the Bahaman Islands.

Mixed carbonate-siliciclastic settings, however, did gain increasing attention toward the mid-1990s and beyond (e.g. van Buchem et al., 2002; Woolfe and Larcombe, 1998). These deposits occur in attached carbonate platforms, mainly ramp systems, of all ages, and often represent one of the four mixing scenarios of carbonates and siliciclastics proposed by Mount (1984). However, none of these depositional models can explain the intercalation of siliciclastics and carbonates in the middle Three Forks Formation, where many of the clasts in the debris flows have originated from reworking of older dolomite beds. Therefore, the debris flows represent a unique form of intrabasinal erosion and re-deposition with most, if not all, of the clasts originating from the same depositional setting. The siliciclastic and carbonate facies are therefore not, as suggested by Mount (1984), deposited in adjacent facies belts, but instead represent episodic events driven most likely by rapidly changing climatic parameters in a succession that also underwent significant short-term sea-level fluctuations (Egenhoff et al., 2011).

The two primary goals of this study therefore are: (1) to evaluate the potential of the middle Three Forks Formation as a hydrocarbon reservoir, with a specific focus on the dolomitic

intervals, and (2) to develop a detailed sedimentological model of the middle Three Forks Formation that will allow prediction of thickness and regional distribution of dolomitic intervals as well as mixed siliciclastic-dolomitic intercalations to better understand the type of depositional setting.

Dolomitic intervals in the middle Three Forks Formation are likely thickest and most prevalent toward the basin center and thin toward the margins (Egenhoff et al., 2011). Therefore, this study focuses exclusively on twenty-two drill cores taken from the Three Forks Formation depocenter, in Mountrail, McKenzie, and Williams Counties, North Dakota. A total of forty-eight thin sections made from representative core samples are documented for texture, diagenetic characteristics, as well as porosity and composition quantification. This study therefore aims to understand the variety and interaction of processes that governed the deposition of the middle Three Forks Formation, which is most likely applicable to other similar mixed carbonate-siliciclastic reservoirs in the rock record.

2.0 GEOLOGICAL SETTING

The Williston Basin is an elliptical-shaped intracratonic sedimentary basin (Gerhard et al., 1990). Extending over an area of approximately 250,000 km² with a diameter of 560 km (Kent and Christopher, 1994), the basin includes much of northeastern Montana, southern Saskatchewan, and western North Dakota, with marginal areas extending into South Dakota, Manitoba and Alberta (Figure 1).

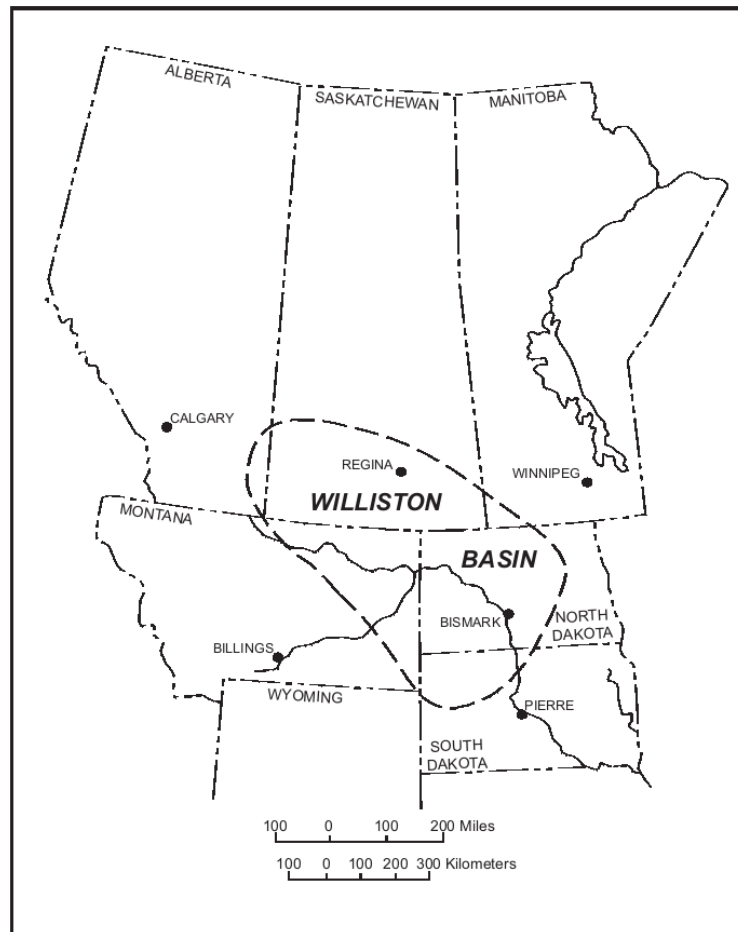


Figure 1. Map showing approximate extent of the Williston Basin in the United States and Canada (Pitman et al., 2001).

The evolution of the Williston Basin began in Cambrian times and continued through the Tertiary, represented by a Phanerozoic succession of sedimentary rocks that attain a maximum thickness of 4,900 m in the Watford deep, southeast of Williston, North Dakota (Gerhard et al., 1990). Pre-Pennsylvanian rocks are predominantly carbonates, with some intercalated clastic units and few evaporites, whereas post-Pennsylvanian rocks are mostly siliciclastic in character. The Paleozoic section hosts almost all of the oil and gas resources within the basin (Gerhard et al., 1990), which include the Bakken-Three Forks petroleum system (Figure 2).

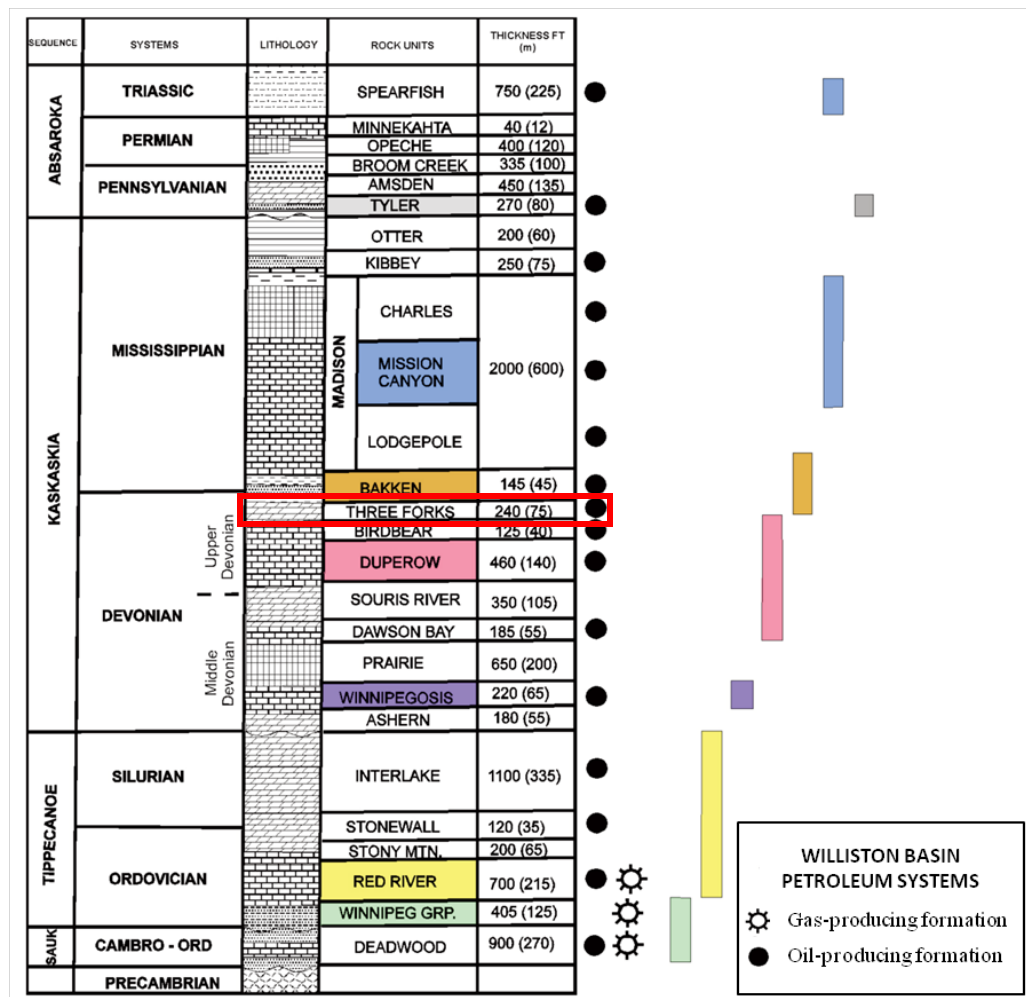


Figure 2. Stratigraphic column for Paleozoic and lower Mesozoic units in the Williston Basin. The USGS estimates at least seven petroleum systems within the Paleozoic and lower Mesozoic sections of the basin (Anna, 2011), whose extents are highlighted above. The Three Forks Formation is indicated by a red box. Modified from Anna (2011).

During the Late Devonian (Famennian) the North American craton was largely covered by an epeiric sea, and the Williston Basin was connected to the elongate Elk Point Basin in northwestern Alberta, Canada (Figure 3). At this time the location of the Williston Basin was near the equator and the climate was characterized by an overall hot climate with fluctuating arid and humid conditions (Egenhoff et al., 2011).

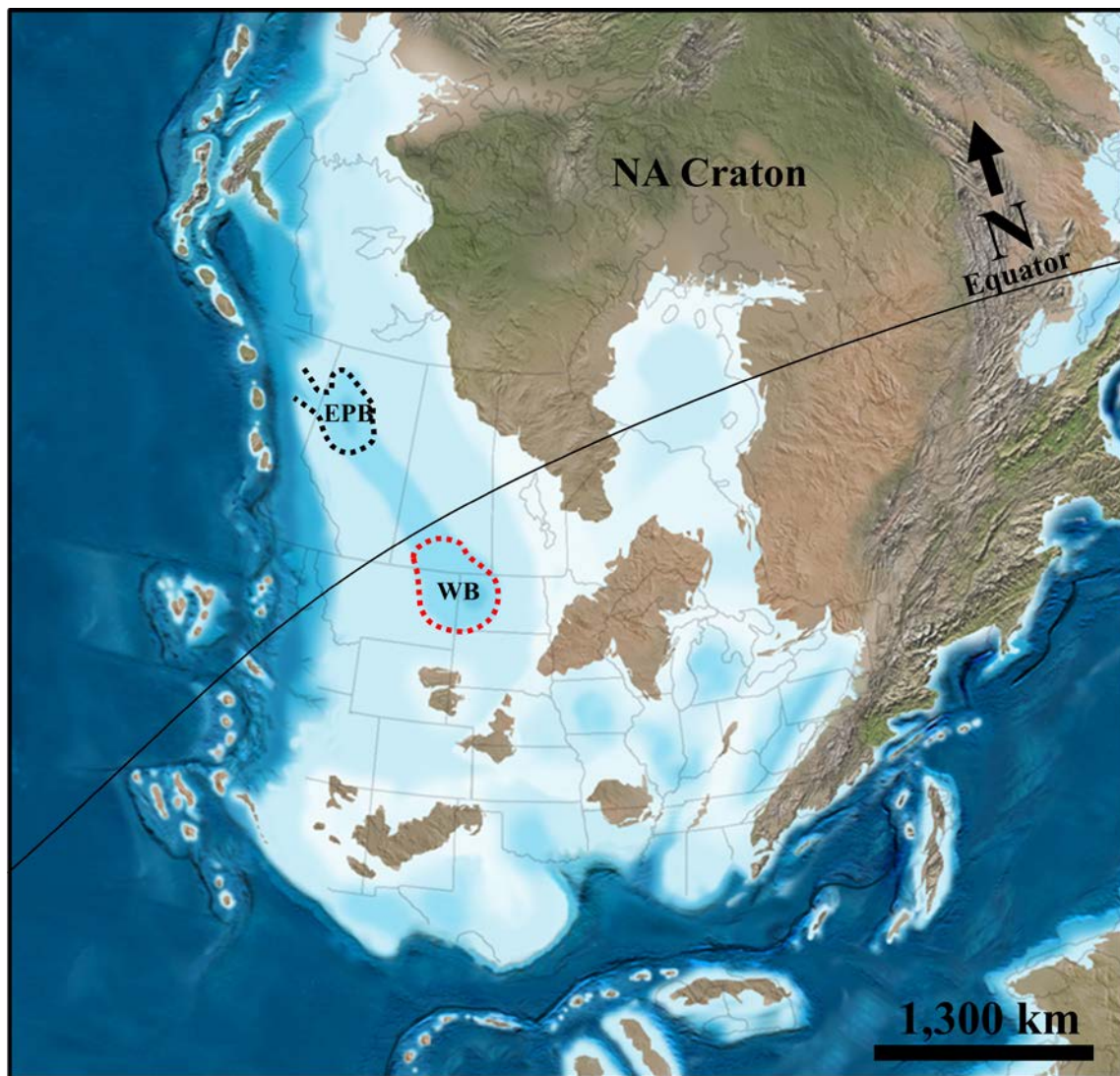


Figure 3. Paleogeography of North America during the Late Devonian (modified from R. Blakey's website: <http://www2.nau.edu/rcb7/namD360.jpg>.) The Williston Basin (WB) is indicated by the red dotted line and the Elk Point Basin (EPB) by the black dotted line.

Stratigraphically, the Three Forks Formation conformably overlies the Birdbear (“Nisku”) Formation (Heck et al., 2002). Deposited in subtidal to supratidal environments, the Birdbear Formation is generally divided into two units: (1) a lower part comprised of bedded, peloidal lime mudstone, and bedded to massive dolomite, and (2) an upper unit consisting of massive bedded dolomite, breccias, and anhydrite (Peterson and MacCary, 1987). The Three Forks Formation is overlain by the Bakken Formation, which is characterized by three informal members: a lower shale member, a middle mixed carbonate-siliciclastic member, and an upper shale member (LeFever et al., 1991; Smith and Bustin, 2000; Egenhoff and Fishman, 2013). The middle member reflects deposition in a shallow-water marine environment (Smith and Bustin, 2000), while the upper and lower members represent deposition in an offshore marine environment during periods of sea-level rise (Webster, 1984; Smith and Bustin, 2000; Pitman et al., 2001). An unconformity exists at the Three Forks-Bakken contact toward the basin margins, but near the basin center the contact is conformable (Sonnenberg and Pramudito, 2009).

Although the Three Forks Formation outcrops in South Dakota, northern Wyoming, and eastern Montana, it occurs solely in the subsurface throughout North Dakota, reaching a maximum thickness of 82 m in southwestern Mountrail County and thinning to zero thickness to the east-southeast (LeFever, 2008). Since the 1960s, various nomenclature schemes have been applied to the Three Forks Formation (Figure 4). The subdivision of the formation in this study will follow Bottjer et al. (2011) and Egenhoff et al. (2011) who separate the Three Forks Formation into three distinct stratigraphic units based on lithology: (1) the lower Three Forks Formation, a basal unit comprised of red to brown-colored sand- to mudstones with varying amounts of anhydrite; (2) the middle Three Forks Formation, a succession of mostly matrix-supported conglomerates consisting of predominantly of dolomitic intraclasts with some intercalated levels of laminated to

massive dolomite; and (3) the upper Three Forks Formation, an upper unit consisting mostly of dolomitic rock with varying amounts of green siliciclastic mudstone.

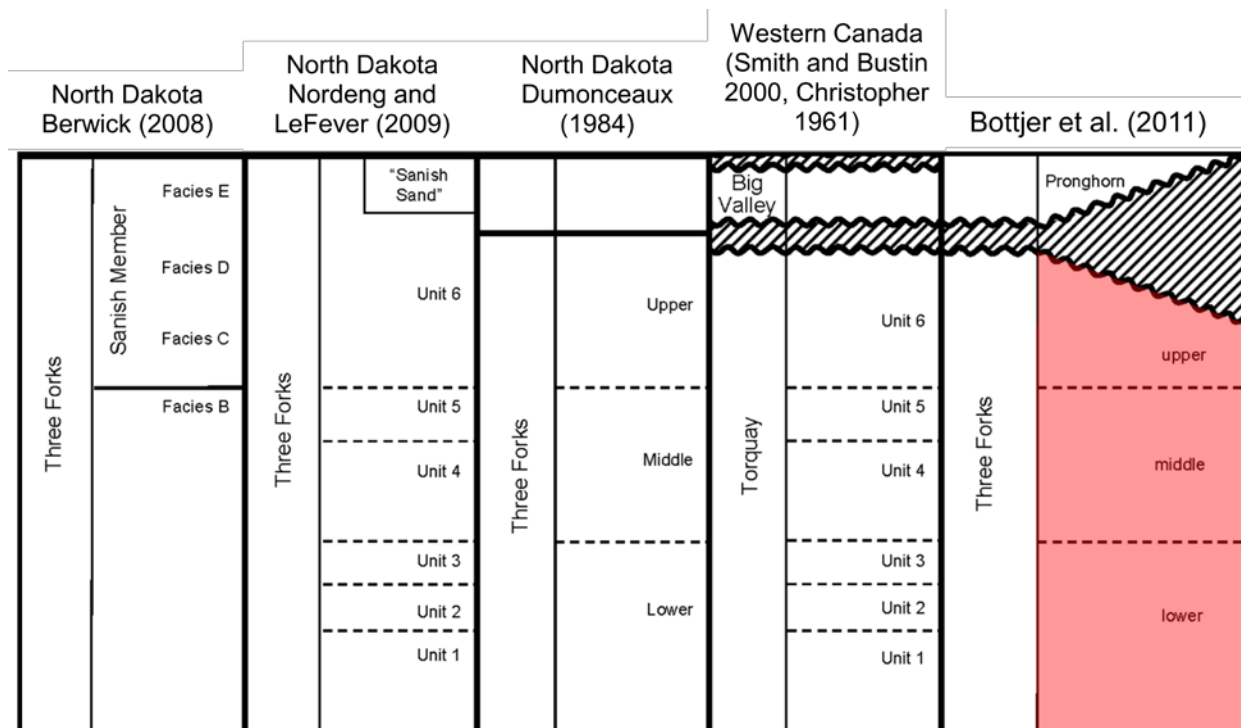


Figure 4. Correlation chart for the Three Forks Formation, Williston Basin, North Dakota, Montana, and Canada, with the nomenclature used in this study (highlighted in red) compared to subdivisions of previous workers. Not to scale. Modified from Bottjer et al. (2011).

The middle Three Forks Formation is comprised of two distinct facies: (1) dolomites with variable siliciclastic mudstone intercalations, similar to those found in the upper Three Forks Formation, and (2) mostly matrix-supported, and some clast-supported, siliciclastic conglomerates whose principle allochems are dolomite intraclasts (Dumonceaux, 1984; Egenhoff, 2011). Based on Dumonceaux (1984), dolomites with no mudstone intercalations are laminated, non-fossiliferous, and composed of dolomitic mud with variable amounts of detrital silt-size quartz particles. These features are representative of deposition in a supratidal setting, in which quartz-silt particles were transported into the environment by trade winds off the emergent

part of the craton (Dumonceaux, 1984). However, Bottjer et al. (2011), proposed that this “clean” dolomite facies represents deposition in a shallow marine subtidal to lower intertidal environment with rare subaerial exposure, evidenced by parallel to sub-parallel laminations, wavy laminations, and ripple cross-laminations. An increase in siliciclastic material within this dolomitic facies reflects deposition in an environment with fluctuating energy conditions in an intertidal to supratidal setting, according to Bottjer et al. (2011). Indicators of these environments include: uni- and bi-directional ripple cross-laminations, thin laterally continuous mudstone laminations, mud drapes, soft-sediment deformation, and dolomite rip-up clasts (Bottjer et al., 2011). The occurrence of siliciclastic matrix- and some clast-supported conglomerates is likely related to fluctuations in climate, and/or changes in sea-level (Egenhoff et al., 2011). Following Egenhoff et al. (2011), these conglomeratic facies are debris flows, likely initiated in the hinterland by flooding during humid conditions. Upon entering the basin, these predominantly siliciclastic debris flows eroded the supratidal/intertidal portion of the ramp, incorporating lithified to half-lithified dolomite clasts. The lack of conglomeratic facies is indicative of arid conditions in which little to no terrestrial sediment was transported into the basin.

3.0 METHODOLOGY

This study integrates detailed core log information from twenty-two drill cores available from the North Dakota Geological Survey (NDGS) Wilson M. Laird Core and Sample Library in Grand Forks, North Dakota (Table 1, Figure 5, Appendix 5). Cores are described at a fine scale (mm-cm) noting facies contacts, sedimentary structures and bedforms, and vertical stacking patterns. A total of forty-eight thin sections oriented perpendicular to bedding, most of them polished with five unpolished, are made from core samples of representative facies. The five unpolished slides are stained with Alizarin red S to distinguish calcite from dolomite, and potassium ferricyanide to detect ferrous iron, which is often substituted into the dolomite crystal lattice. All thin sections are impregnated with blue epoxy to aid with porosity identification. Using transmitted light microscopy, the composition, texture, fine-scale sedimentary structures, and diagenetic characteristics such as dolomitization and zoning of dolomite rhombohedra, of each thin section are documented. Each thin section is assigned a two-dimensional grid in which point-counting of 300 grid points allows for an objective estimation of composition and porosity volumes. These data help to properly document diagenetic features, correlate rock units, interpret depositional environments that were active during and soon after deposition, as well as to predict porosity trends within the middle Three Forks Formation.

Table 1. List of well with cores logged in this study. Note (*) indicates that this well is located outside of the study area and only thin section data (no core log data) is documented herein.

Original Operator	Original Well Name	Well File #
Brigham Oil and Gas, L.P.	Olson 10-15H 1-H	17513
Newfield Production Company	Heidi 1-4H	18413
Amerada Hess Corporation	Anderson Smith 1-26H	16083
Headingon Oil Company, LLC	Sakakawea Federal 13X-35	17067
Brigham Oil and Gas, L.P.	Anderson 28 1-H	17351
Hess Corporation	RS-Nelson-156-91 1423 H-1	16824
Hess Corporation	RS State C-157-90 3603 H-1	17071
Amerada Hess Corporation	State ND 1-11H	16160
EOG Resources, Inc.	Sidonia 1-06H	17676
Fidelity Exploration Company	Farhart 11-11H	17096
EOG Resources, Inc.	Bures 1-17H	16586
Fidelity Exploration Company	Deadwood Canyon Ranch 43-28H	16841
Whiting Oil and Gas Corporation	Braaflat 11-11H	17023
EOG Resources, Inc.	Liberty 2-11H	18101
Burlington Resources Oil and Gas Company	Washburn 44-36H	17309
SM Energy Company	Jaynes 16-12H	20022
Murex Petroleum Corporation	Junior 10-3H	21928
Hess Corporation	En-Person Observation 11-22	20315
North Plains Energy, LLC	Scanlan 3-5H	18770
Brigham Oil and Gas, L.P.	State 36-1 2H	19215
Hess Corporation	H. Bakken 12-07H	16565
North Plains Energy, LLC	Comford 9-12H	19060
Brigham Oil and Gas, L.P.*	Richardson 30 No. 1*	DN39564*

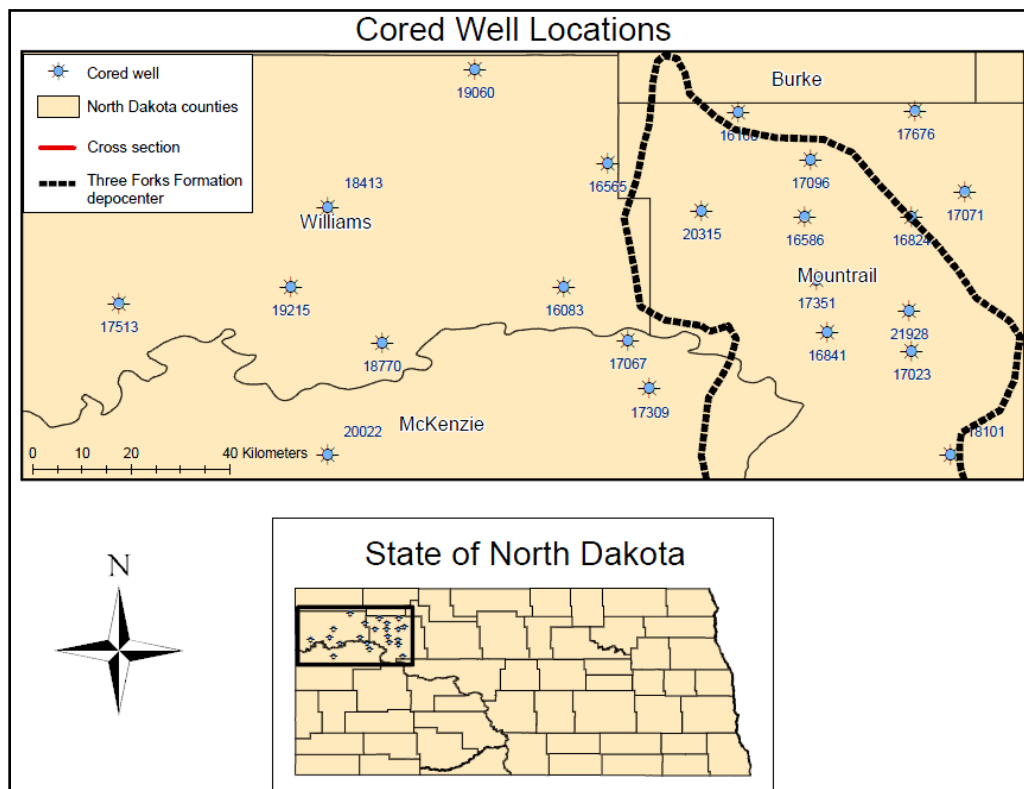


Figure 5. Map showing the well locations of cores used in this study (Table 1). Generalized middle Three Forks Formation depocenter referenced in text is shown by dashed line.

Micron-scale textural characteristics and diagenetic cements of selected thin sections are documented using a JEOL 5800V scanning electron microscope (SEM) equipped with an energy dispersive spectrometer (EDS). Also included is a quantitative elemental analysis of zoned dolomite crystals using a JEOL 8900 electron microprobe operated at 10kv, 30nA (cup) in which a focused electron beam bombards a specific point of interest on a sample. Upon bombardment of the electron beam, x-rays are produced. Each element produces x-rays with characteristic energies, therefore by counting the x-rays generated by each element in the sample and comparing that number to the number of x-rays generated by a standard of known composition, the chemical composition of a point of interest can be quantified. The x-rays were analyzed for the following elements: Ca (calcite), Mg (dolomite), Fe (hematite), Mn (rhodochrosite), S (barite), Si (quartz), Ba (barite) and Sr (celestite). To normalize elemental data, carbon was added as the difference from one hundred percent.

The majority of the rocks documented herein are dolomites. The Randazzo and Zachos (1983) scheme is used for classification of dolomite fabric and nomenclature, based on textures defined by Friedman (1965) (Figure 6). Dolomite crystal size is broken out into three divisions following Wright (1992): dolomicrostone (crystal size < 0.004 mm), dolomicrosparstone (crystal size 0.004 – 0.01 mm), and dolosparstone (crystal size > 0.01 mm). For classification of porosity in the middle Three Forks Formation a revised version of a scheme for porosity in carbonate rocks proposed by Choquette and Pray (1970) is applied. The modifications applied herein include: (1) “micro-intercrystalline porosity” which is defined as micron-scale pore space in between very fine-crystalline dolomite matrix crystals that is only detectable in thin sections impregnated with blue epoxy; (2) the term “moldic porosity” is defined as porosity created exclusively by fully dissolved dolomite crystals rather than dissolution of carbonate grains; (3)

“linear dissolution porosity” which refers to diffuse “bands” of porosity, typically less than 0.02 mm thick that appear to result from partial dissolution of fine-crystalline dolomite matrix.

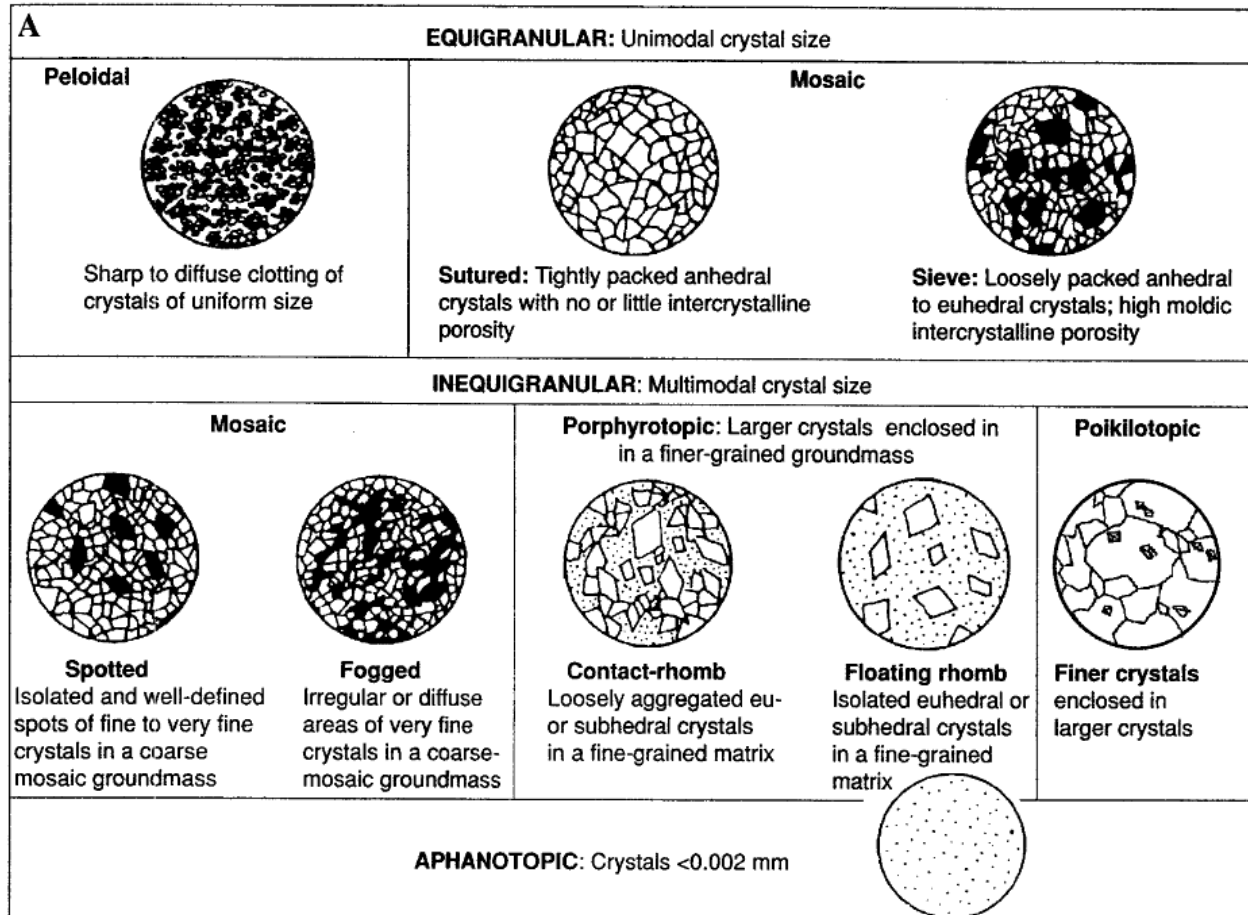


Figure 6. Classification of dolomite crystallization textures defined by Friedman (1965), modified by Randazzo and Zachos (1983), from Flügel (2004).

4.0 SEDIMENTOLOGY

The middle Three Forks Formation consists of three distinct rock types: (1) siliciclastic mudstones, (2) silty dolostones, and (3) mud-rich matrix-supported conglomerates. Detailed logging of twenty-two drill cores, as well as comprehensive analyses of forty-eight thin sections, enabled the middle Three Forks Formation to be further subdivided into ten facies (Table 2, Figure 7). Logs of these cored intervals are presented in four transects throughout the study area (Appendices 1-4). The ten facies are classified based on sedimentary structures observed at both a macroscopic and microscopic scale, relative amounts of carbonates to siliciclastics, and grain sizes.

Bioturbation is overall sparse throughout the middle Three Forks Formation. Nevertheless, multidirectional *Phycosiphon incertum* fecal strings (“Type B” following Egenhoff and Fishman, 2013), typically 0.1-0.2 mm across, frequently occur throughout laminated siliciclastic mudstones. Rarely-occurring spreiten-bearing U-shaped *Diplocraterion* burrows 0.75-1.0 mm wide are present in relatively coarse-grained, ripple-laminated facies (see Cornish, 1986).

4.1 Sedimentary Facies

Table 2. Summary of sedimentologic attributes of facies in the Middle Three Forks Formation.

Facies	Facies Thickness	Description and Sedimentary Structures	Composition	Interpretation
Laminated to massive siliciclastic mudstone (Facies 1)	0.2-30 mm	<ul style="list-style-type: none"> Planar to undulating, continuous to discontinuous laminae and laminasets, of uneven thickness normally graded In places, laminae are structureless and even thickness at the topmost portion of laminasets Dolomite-filled dykes, water escape structures, flame structures and faulting are common Halite pseudomorphs present locally Moderately bioturbated by <i>Phycosiphon incertum</i> 	<ul style="list-style-type: none"> 30-60% fine- to medium-crystalline dolomite 30-40% clay matrix 5-15% coarse silt-size detrital quartz 0-4% pyrite 	<ul style="list-style-type: none"> Planar laminae of uneven thickness indicate bedload transport Normally graded laminae indicate deposition from a waning flow Structureless, laminae of even thickness represent suspension settling under relatively tranquil conditions Dykes, water escape structures, flame structures, and faulting represent liquefaction and/or fluidization triggered by tectonism, likely earthquakes Halite pseudomorphs reflect highly saline conditions
Planar laminated siliciclastic mud-rich silty dolostone (Facies 2)	5-15 mm	<ul style="list-style-type: none"> Normally graded, planar to undulating, continuous laminae and laminasets of uneven thickness comprised of dolomite and subrounded detrital quartz grains Normal faults are common 	<ul style="list-style-type: none"> 10-60% medium- to coarse crystalline dolomite 50-60% clay matrix 5-30% coarse-silt to very fine sand-size detrital quartz 	<ul style="list-style-type: none"> Normally graded laminae indicate deposition by waning flows Laminae of uneven thickness indicate bedload transport
Massive silty dolostone (Facies 3)	5-150 mm	<ul style="list-style-type: none"> Relatively "clean" dolostone with little to no clay content Sub-rounded to elongate, 2-10 mm clay clasts in places Massive, no internal structures 	<ul style="list-style-type: none"> 60-90% medium- to coarse crystalline dolomite 3-20% clay clasts < 1-15% coarse-silt to very fine sand-size detrital quartz 0-4% pyrite 	<ul style="list-style-type: none"> Depositional process unclear due to obliteration of all sedimentary structures caused by liquefaction
Wave ripple-laminated silty dolostone (Facies 4a)	15-200 mm	<ul style="list-style-type: none"> Discontinuous to continuous cross-laminae and laminasets, showing bi-directional foresets Commonly capped by mud laminae (< 2 mm in thickness) within troughs that pinch out laterally into dolomite laminae Normal faults, sedimentary dykes, and water escape structures commonly disrupt lamination/bedding Basal scour surfaces are common Weakly bioturbated by <i>Diplocraterion</i> 	<ul style="list-style-type: none"> 70-90% medium- to coarse crystalline dolomite 2-20% clay clasts 10-20% coarse-silt to very fine sand-size detrital quartz 	<ul style="list-style-type: none"> Bi-directional foresets reflect bedload transport by wave action Mud laminae indicate deposition under low energy conditions Diminutive ichnofauna suggest stressful environment
Current ripple-laminated silty dolostone (Facies 4b)	10-75 mm	<ul style="list-style-type: none"> Discontinuous to continuous cross-laminae and laminasets, showing uni-directional foresets Climbing ripples in places Mud laminae (< 2 mm in thickness) commonly cap stoss side of ripples 0.2-1.0 mm sub-rounded clay clasts occur at the base of laminasets Weakly bioturbated by <i>Diplocraterion</i> 	<ul style="list-style-type: none"> 50-90% medium- to coarse crystalline dolomite 10-35% clay matrix 20% clay clasts 5-10% coarse-silt to very fine sand-size detrital quartz 0-3% pyrite 	<ul style="list-style-type: none"> Uni-directional foresets and sub-rounded clay clasts indicate bedload transport dominated by bottom currents Climbing ripples are representative of high influx of sediment Mud laminae reflect deposition under relatively low energy conditions Diminutive ichnofauna suggest stressful environment

Facies	Facies Thickness	Description and Sedimentary Structures	Composition	Interpretation
Planar-laminated silty dolostone (Facies 5)	15-40 mm	<ul style="list-style-type: none"> •Relatively "clean" planar-laminated dolostone •Sub-rounded coarse silt- to very fine sand-size quartz grains occur at base of laminae •Few 1-2 mm clay clasts oriented parallel to bedding in places •Locally occurring subrounded 2-5 mm dolomite clasts 	<ul style="list-style-type: none"> •70-90% medium- to coarse crystalline dolomite •10-15% siliciclastic clay clasts •5-15% coarse-silt to- very fine sand-size detrital quartz 	<ul style="list-style-type: none"> •Deposition occurred under high energy, upper flow regime conditions •Clay clasts indicate bedload transport
Dolomite clast-bearing siliciclastic mud- to siltstone (Facies 6a)	50-1500 mm	<ul style="list-style-type: none"> •Few (< 10%) poorly sorted 0.05-3 mm sub-angular dolomite clasts in siliciclastic mud- to siltstone matrix •Some dolomite clasts are elongate and have a smeared appearance that tapers at each end of the long axis, oriented parallel to bedding •Locally occurring pyrite •Elongate, discontinuous 2 - 15 mm clay laminae and some 2-10 mm angular clay clasts arranged roughly parallel to bedding in places 	<ul style="list-style-type: none"> •30-40% fine- to medium crystalline dolomite •40-50% clay and fine silt matrix •2-10% dolomite clasts •0-20% siliciclastic clay clasts 	<ul style="list-style-type: none"> •Minimal amount of relatively small clasts oriented parallel to bedding in clay- to- silt matrix is indicative of mud flow as dominant transport mechanism
Matrix-supported conglomerate (Facies 6b)	50-2000 mm	<ul style="list-style-type: none"> •Abundant 2-40 mm angular to sub-rounded dolomite clasts, commonly laminated, often poorly sorted •Inverse grading in places •Siliciclastic silt- to- mudstone matrix •Pyrite is present locally •5-20 mm angular clay clasts in places 	<ul style="list-style-type: none"> •20-40% medium- to coarse-crystalline dolomite •40-80% clay and fine silt matrix •20-50% dolomite clasts •20-60% siliciclastic clay clasts 	<ul style="list-style-type: none"> •Cohesive clay-rich matrix supported and transported clasts within a gravity mass flow •Inverse grading in places, of abundant poorly sorted clasts is reflective of debris flow as dominant transport mechanism
Matrix- to- clast-supported conglomerate in dolomite-rich matrix (Facies 7)	75-900 mm	<ul style="list-style-type: none"> •Abundant 5 - 25 mm elongate, sub-angular clay clasts, oriented roughly parallel to bedding, in brown dolomitic matrix •Roundish, bulbous 10-15 mm dolomite clasts with pillow-like shape in places •Locally occurring dolomite-filled clastic dykes •Siliciclastic silt- to- mudstone matrix 	<ul style="list-style-type: none"> •30-40% medium- to coarse-crystalline dolomite •0-10% clay and silt matrix •10-40% dolomite clasts •30-60% siliciclastic clay clasts 	<ul style="list-style-type: none"> •Clay clasts are intrabasinal rip-up clasts •Dolomite matrix represents liquified dolomite beds •Clasts oriented parallel to bedding is indicative of transport within gravity mass flow •Chaotic distribution of clasts, clastic dykes , and liquified dolomite beds represent disruption caused by earthquake shaking
Clast-supported conglomerate in siliciclastic silt- to clay-rich matrix (Facies 8)	25-600 mm	<ul style="list-style-type: none"> •Irregularly pillow-shaped bulbous 2-40 mm dolomite clasts, commonly with edges along the long axis that taper parallel to bedding •Dolomite clasts are randomly oriented in places, commonly laminated •Elongate to sub-angular 5-30 mm clay clasts oriented roughly parallel to bedding •Siliciclastic silt- to- mudstone matrix 	<ul style="list-style-type: none"> •0-10% medium- to coarse-crystalline dolomite •30-40% clay and silt matrix •30-60% dolomite clasts •30-60% siliciclastic clay clasts 	<ul style="list-style-type: none"> •Siliciclastic silt- to- mudstone matrix reflects liquified mudstone beds •Soft, pillow-shaped dolomite clasts represent half-lithified dolomite that was transported in a cohesive clay-rich matrix as gravity mass flow

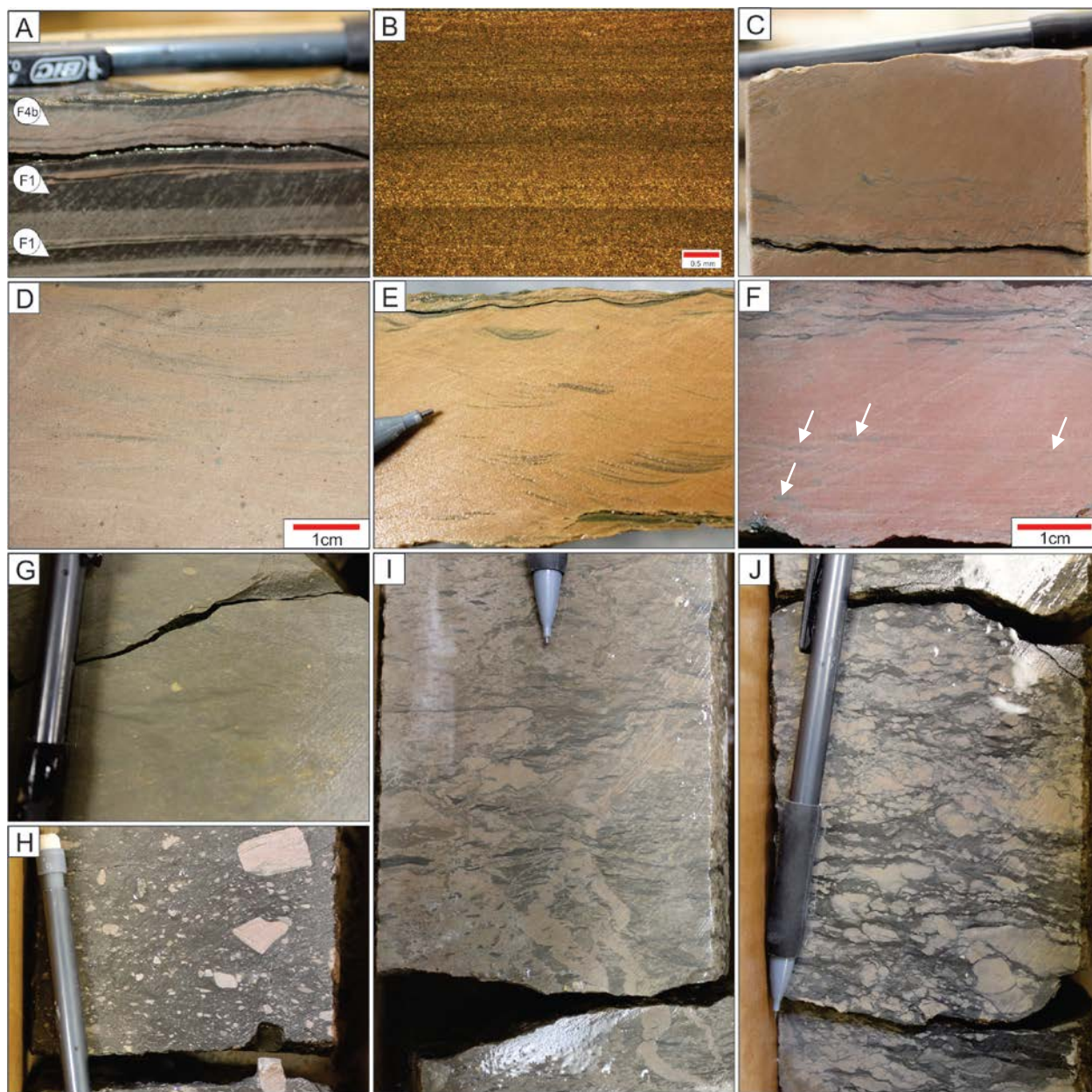


Figure 7. Facies of the Middle Three Forks Formation. **(A)** Core photograph of laminated siliciclastic mudstone (F1) intercalated with current ripple-laminated silty dolostone (F4b) (North Plains Energy Comfort 9-12H, 9780.7 ft). **(B)** Thin section photomicrograph showing normal grading in planar laminated siliciclastic mud-rich silty dolostone in plane-polarized light (F2) (Brigham Oil and Gas, L.P. Olson 10-15 1-H, 10716.9 ft). **(C)** Core photograph illustrating the structureless fabric of massive silty dolostone (F3) (North Plains Energy, LLC Comfort 9-12H, 9792.3 ft). **(D)** Core photograph showing bi-directional cross-lamination in wave ripple-laminated silty dolostone (F4a) (Brigham Oil and Gas, L.P. Anderson 28 1-H, 10214.5 ft). **(E)** Core photograph highlighting uni-directional cross-lamination in current ripple-laminated silty dolostone (F4b) (Hess Corporation H. Bakken 12-07H, 9783.5 ft). **(F)** Core photograph illustrating relatively “clean” planar laminated silty dolostone with few 1-3 mm clay clasts (white arrows) oriented parallel to bedding in planar laminated dolomitic siltstone (F5) (Fidelity Exploration and Production Company Farhart 11-11H, 9791.0 ft). **(G)** Core photograph showing sparse 0.5-2 mm, sub-rounded dolomite clasts and elongate, 5-20 mm clay clasts in green siliciclastic matrix (F6a) (Hess Corporation H. Bakken 12-07H, 9755.3 ft). **(H)** Core photograph illustrating the chaotic distribution of 1-25 mm, sub-angular to sub-rounded, dolomitic clasts, laminated in places, in dark gray to green siliciclastic matrix (F6b) (Murex Petroleum

Corporation Junior 10-3H, 9944.3 ft). **(I)** Core photograph highlighting elongate, 5-20 mm sub-angular clay clasts and few roundish, pillow-shaped dolomite clasts in light brown dolomitic matrix (F7) (North Plains Energy, LLC Scanlan 3-5H, 11151.3 ft). **(J)** Core photograph showing 2-35 mm roundish, pillow-shaped dolomite clasts associated with elongate 5-20 mm sub-angular clay clasts in a dark gray to green siliciclastic mud to silt matrix (F8) (North Plains Energy, LLC Scanlan 3-5H, 11158.3).

4.2 Facies Associations

The ten facies in Table 2 are classified into three facies associations (Table 3) that are described in detail below.

Table 3. Summary of facies associations and corresponding facies in the middle Three Forks Formation.

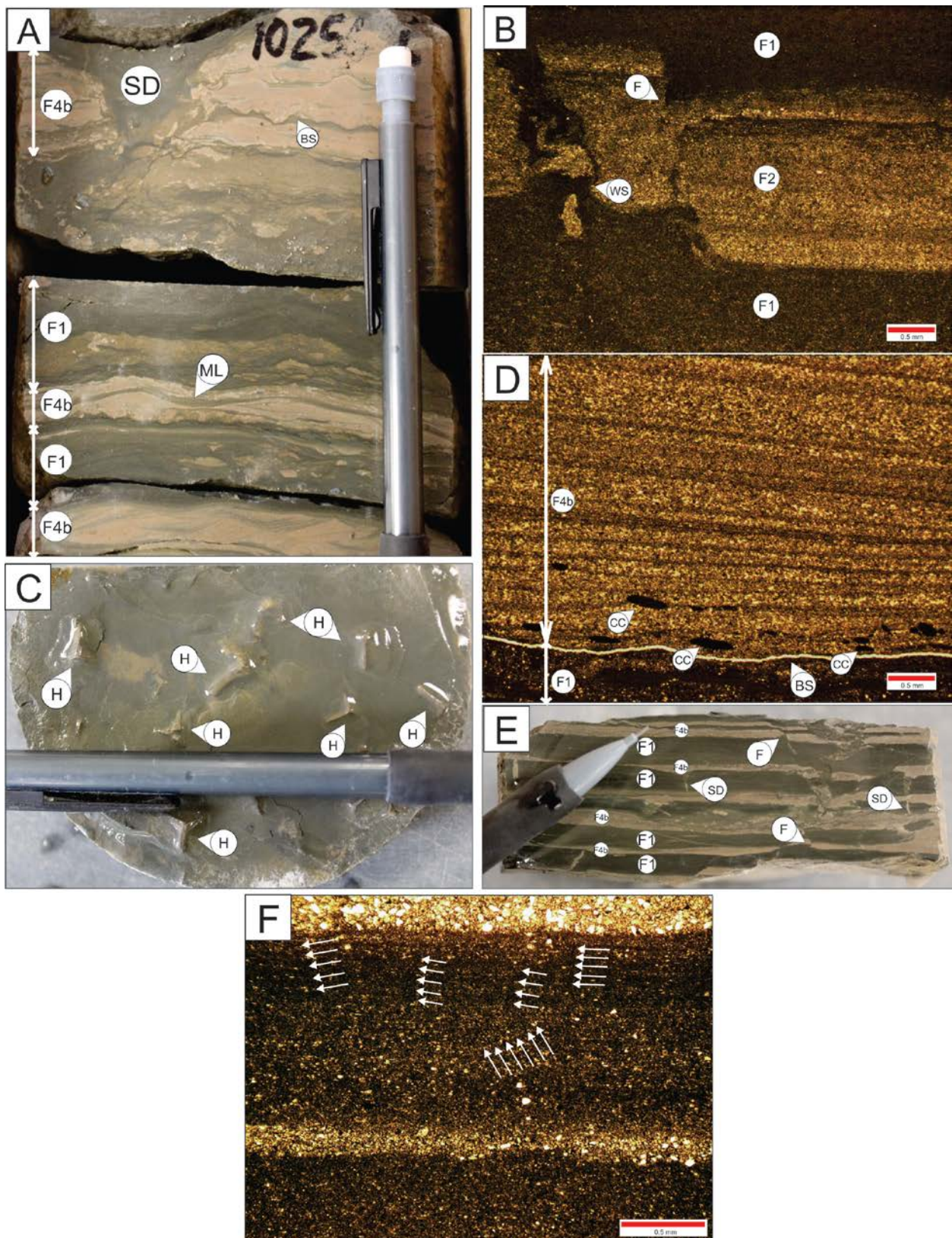
Facies Associations	Facies
Facies Association 1: Laminated siliciclastic mudstone with silty dolostone intercalations	Facies 1: Laminated to massive siliciclastic mudstone Facies 2: Planar laminated siliciclastic mud-rich silty dolostone Facies 3: Massive silty dolostone Facies 4b: Current ripple-laminated silty dolostone Facies 8: Clast-supported conglomerate in siliciclastic silt- to clay-rich matrix
Facies Association 2: Massive to well laminated clay clast-bearing silty dolostone	Facies 3: Massive silty dolostone Facies 4a: Wave ripple-laminated silty dolostone Facies 4b: Current ripple-laminated silty dolostone Facies 5: Planar-laminated silty dolostone Facies 7: Matrix- to clast-supported conglomerate in dolomite-rich matrix
Facies Association 3: Mud-rich conglomerate with dolomite and clay clasts	Facies 6a: Dolomite clast-bearing siliciclastic mud- to- siltstone Facies 6b: Matrix-supported conglomerate

4.2.1 Facies association 1: Laminated to Massive Siliciclastic Mudstone With Silty Dolostone Intercalations

Laminated siliciclastic mudstone with silty dolostone intercalations (FA 1) forms vertically continuous units that range in thickness from 300-900 mm. It consists of well laminated, normally graded siliciclastic mudstones intercalated with well laminated silty dolostones (Figure 8A). In places, otherwise continuous siliciclastic mudstone laminae of even thickness are moderately disturbed by multidirectional *Phycosiphon incertum* fecal strings (Figure 8F). Although dolomicrosparstone to dolosparstone (classification based on Wright, 1992) makes up most of the rock in FA1 (50-70%), approximately 30-40% of the bulk rock volume is comprised of siliciclastic clay-size material. Silty dolostone intercalations frequently show downlapping, uni-directional laminae and laminasets (Figure 8A, 8D), that are comprised of both

dolomicrosparstone to dolosparstone and coarse silt- to- very fine-sand size sub-rounded detrital quartz grains. Many of the troughs within the cross-laminated silty dolostones are capped by 1-2 mm thick siliciclastic mud laminae (Figure 8A). In places, silty dolostones are structureless, showing little to no well-preserved sedimentary fabric. The basal surfaces of silty dolostones are mostly sharp and irregular, and are commonly lined with 0.2-1.0 mm sub-rounded clay clasts (Figure 8D). Rocks of FA1 sometimes appear in the form of clast-supported conglomerates in which 5-30 mm sub-rounded to bulbous, pillow-shaped dolomite clasts are oriented roughly parallel to bedding in a green siliciclastic silt- to mudstone matrix. Dolomite-filled dykes, normal faults, water-escape structures, and load casts are common sedimentary structures within FA1 (Figure 8A, 8B, 8E). Halite pseudomorphs preserved as dolomite are also locally present, generally found on interfaces of siliciclastic mudstones and dolostones (Figure 8C). These features are most common in mud-rich intervals and occur in several stratigraphic horizons throughout FA1.

Figure 8 (next page). Examples of laminated siliciclastic mudstone with dolomitic siltstone intercalations (facies association 1). **(A)** Core photograph of laminated siliciclastic mudstone (F1) intercalated with current ripple-laminated silty dolostone (F4b). Note basal scour surfaces (BS) at base of silty dolostones, mud laminae (ML) that occur in troughs of ripples, and the mud-filled sedimentary dyke (SD) oriented perpendicular to bedding (Hess Corporation EN-Person Observation 11-22, 10,256.6 ft). **(B)** Optical micrograph of planar laminated siliciclastic mud-rich silty dolostone (F2) intercalated with laminated siliciclastic mudstone (F1). Photograph also shows a normal fault (F) that offsets individual beds and water-escape structure (WS) that disrupts bedding (Brigham Oil and Gas L.P. Anderson 28 1-H, 10219.4 ft). **(C)** Core photograph showing halite pseudomorphs (H) on the base of a laminated siliciclastic mudstone (F1) bedding plane (North Plains Energy, LLC Comford 9-12H, 9786.5 ft). **(D)** Optical micrograph of current ripple-laminated silty dolostone (F4b) overlying laminated siliciclastic mudstone (F1). Note the scour surface (BS) and sub-rounded clay clasts (CC) at the base of the laminated ripple-laminated silty dolostone (Headington Oil Company LLC Sakakawea Federal 13X-35, 9914.0 ft). **(E)** Core photograph showing abundant dolomite-filled sedimentary dykes (SD) and faults offsetting laminated siliciclastic mudstone (F1) and current ripple-laminated silty dolostone (F4b) beds (Hess Corporation EN-Person Observation 11-22, 10230.9 ft). **(F)** Optical micrograph of laminated siliciclastic mudstone (F1) in which *Phycosiphon incertum* fecal strings disrupt continuous laminae of even thickness (arrows) (Brigham Oil and Gas Richardson 30 No.1, 8418.7ft).



4.2.2 Facies association 2: Massive to Well Laminated Clay Clast-Bearing Silty Dolostone

Massive to well laminated clay clast-bearing silty dolostone (FA 2) forms continuous vertical sections that range from 75-900 mm in thickness, representing approximately 20% of the middle Three Forks Formation bulk rock volume. It has a structureless to well laminated fabric and consists of 40-90% dolomicrosparstone to dolosparstone and 5-20% sub-rounded coarse silt- to- very fine sand-size detrital quartz grains, with 2-21% siliciclastic clay-size material, mostly in the form of 0.2-5.0 mm rip-up clasts. However, few relatively thin siliciclastic mudstone laminae (0.5-4 mm) occur locally intercalated with “clean” dolomite beds. In places, FA2 rocks appear as matrix- to- clast-supported conglomerates that contain abundant 5-10 mm elongate sub-angular clay clasts oriented roughly parallel to bedding in a dolomite-rich matrix. Detrital quartz grains and dolomite crystals in the laminated silty dolostones generally appear to be normally graded, and comprise of one of two types of cross-lamination: downlapping, bi-directional and uni-directional laminae (Figure 9B-E). The basal portions of downlapping cross-laminasets generally consist of concentrations of coarse silt- to- very fine sand-size detrital quartz grains, whereas toward the top of each cross-laminaset detrital quartz is overall scarce (Figure 9D). Clast-bearing planar to undulating horizontally laminated silty dolostones are also present in FA2, but are not as common as the cross-laminated silty dolostones. Laminae in clast-bearing planar to undulating horizontally laminated silty dolostones are largely comprised of dolomicrosparstone to dolosparstone and sub-rounded coarse silt- to- very fine sand-size detrital quartz grains that, similar to the cross-laminated silty dolostones, appear to be normally graded with quartz content overall decreasing toward the top of each laminaset. In general, the amount of detrital quartz grains is higher throughout FA2 than in FA1. Irregular scour surfaces are common at the base of cross-laminated facies (Figure 9D). Although bioturbation is rare to

completely absent in FA2 rocks, locally-occurring, discrete U-shaped *Diplocraterion* burrows disrupt otherwise well-preserved uni- and- bi-directional cross-lamination in places (Figure 9A). A burrow-mottled fabric that completely obliterates all primary laminated structures also occurs locally, however it is important to note that this fabric is very uncommon as well. Synsedimentary deformation features such as water-escape structures, ball-and-pillow structures, slumping (e.g. flow-folds) (Figure 9B), and convolute lamination are prevalent throughout the massive to well laminated clay clast-bearing silty dolostone. Halite pseudomorphs preserved as dolomite locally occur on interfaces of siliciclastic mudstones and dolostones within FA2, however these features are not as prevalent in FA2 as FA1.

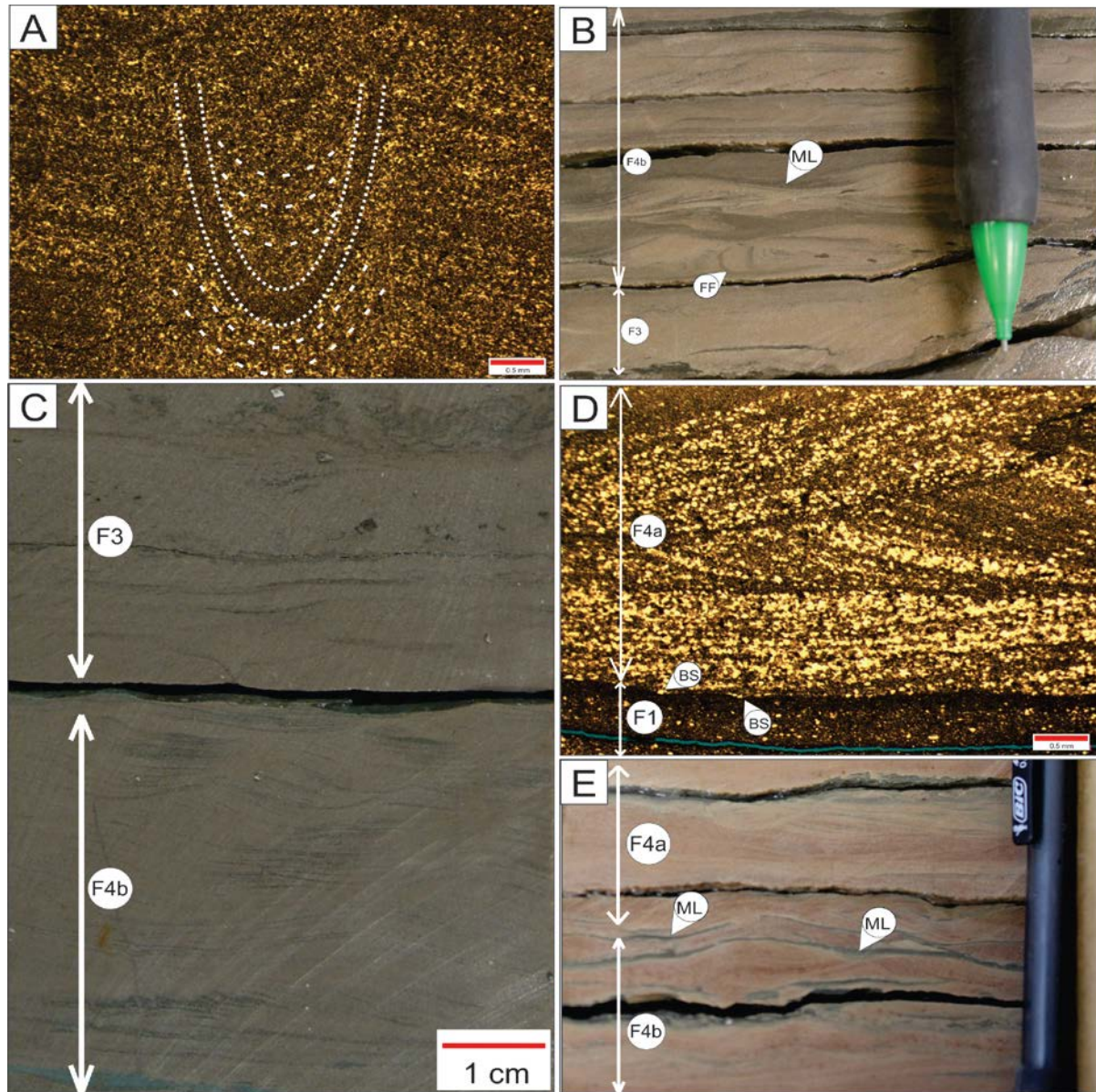
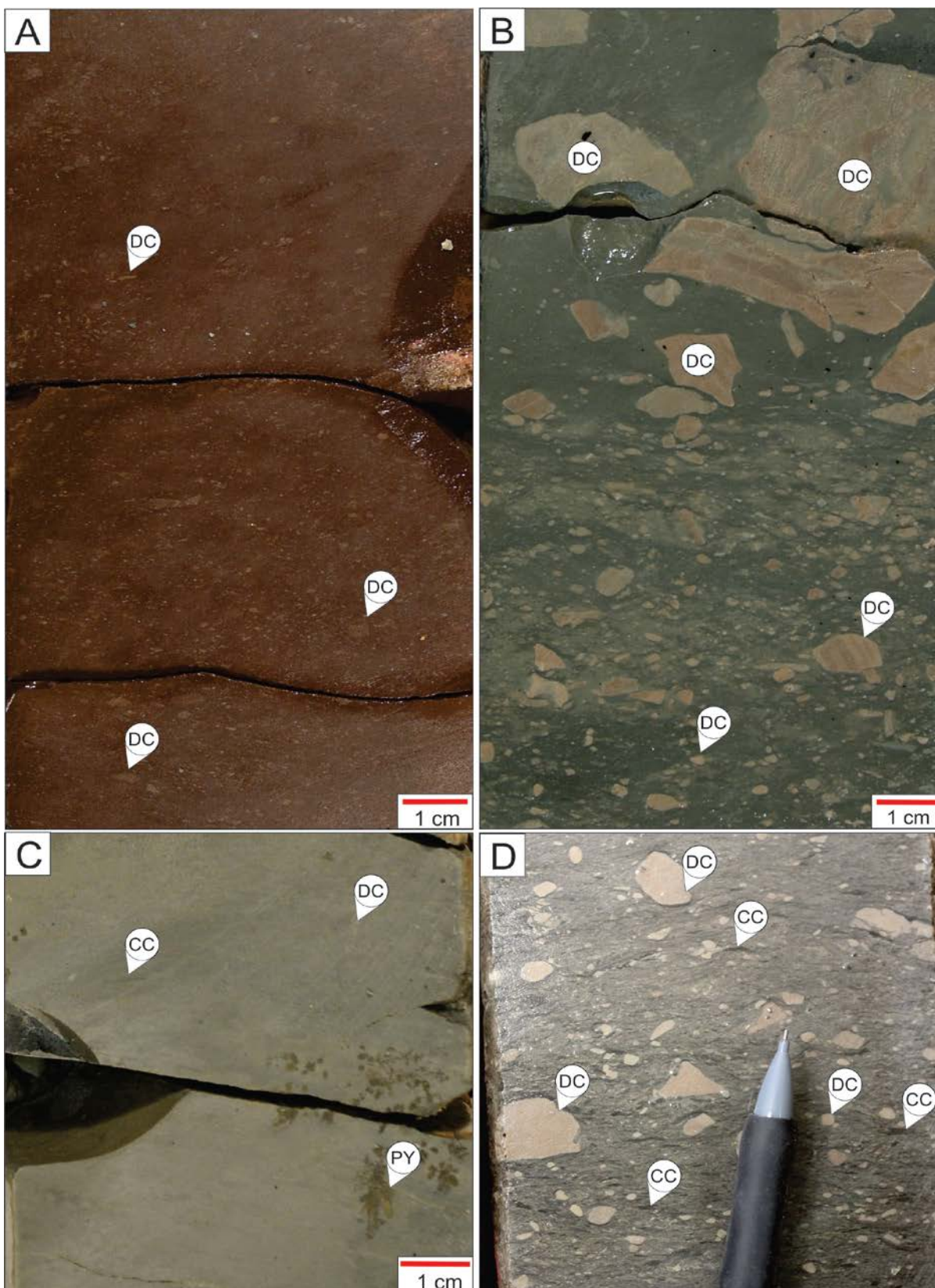


Figure 9. Examples of relatively “clean” massive to well laminated clay clast-bearing dolomitic siltstone (facies association 2). **(A)** Optical micrograph of wave ripple-laminated silty dolostone (F4a) showing sprieten-bearing, U-shaped *Diplocraterion* trace fossil. Spreiten is indicated by the wide-spaced dashed lines and U-shaped dwelling tube is shown by the tightly-spaced dashed lines (North Plains Energy, LLC. Comford 9-12H, 9784.2 ft). **(B)** Core photograph showing massive silty dolostone (F4b) and current ripple-laminated silty dolostone (F4b) capped by thin mudstone laminae (ML). Note synsedimentary deformation in the form of a flow fold (FF) (Burlington Resources Oil and Gas Company LP Washburn 44-36H, 10603.5 ft). **(C)** Core photograph of current ripple-laminated silty dolostone (F4b) overlain by massive silty dolostone (F3) (Amerada Hess Corporation State ND 1-11H, 9588.0 ft). **(D)** Optical micrograph showing laminated siliciclastic mudstone (F1) overlain by bi-directional downlapping foresets of wave ripple-laminated silty dolostone (F4a). Note the scour surface (BS) (SM Energy Company Jaynes 16-12H, 11180.9 ft). **(E)** Core photograph of wave ripple-laminated silty dolostone (F4a) and current ripple-laminated silty dolostone (F4b) capped by thin mudstone laminae (ML) (Hess Corporation H. Bakken 12-07H, 9784.9 ft).

4.2.3 Facies association 3: Mud-Rich Conglomerate with Dolomite and Clay Clasts

Mud-rich conglomerate with dolomite and clay clasts (FA 3) is the most abundant facies association and represents approximately 70% of the bulk rock volume. Units of this facies association measure from 20 mm beds intercalated into dolomite and mudstone beds, to units that reach up to 5000 mm in thickness. The matrix is primarily comprised of clay- to- silt-size siliciclastic material. Principle allochems include: (1) sub-angular to sub-rounded 0.5-40 mm dolomite clasts that in places show preserved lamination, and (2) elongate to sub-angular 5-30 mm clay clasts, commonly oriented parallel to bedding (Figure 10A-D). Pyrite crystals 0.25-0.75 mm in size are also common (Figure 10D). Matrix-supported intervals that are comprised of less than 10% clasts contain sub-millimeter- to- 3 mm poorly sorted sub-angular dolomite clasts. These matrix-supported intervals that contain few to no clasts (< 10%) are in places structureless, or may show fining-upward trends or coarsening-upward trends. Contrarily, matrix-supported intervals that are comprised of abundant (> 10%), relatively large dolomite clasts (2-40 mm) are often poorly sorted and chaotically distributed, with common inverse grading. Overall, clast-rich matrix-supported units are less common than the clast-poor matrix-supported intervals. Basal contacts of FA3 are abrupt, commonly showing irregular scour surfaces. Although present throughout the study area, thicknesses and distribution patterns of FA3 are highly variable.

Figure 10 (next page). Examples of mud-rich matrix-supported conglomerate with dolomite and clay clasts (facies association 3). (A) Core photograph of dolomite clast-bearing siliciclastic silt- to- mudstone (F6a) showing relatively small, sub-angular dolomite clasts (DC) that have an overall structureless fabric (EOG Resources, Inc. Sidonia 1-06H, 8875.4 ft). (B) Core photograph of matrix-supported conglomerate (F6b) comprised of relatively large sub-angular to sub-rounded dolomite clasts (DC) randomly distributed in a siliciclastic silt- to- mudstone matrix (EOG Resources, Inc. Sidonia 1-06H, 8826.0 ft). (C) Core photograph of dolomite clast-bearing siliciclastic silt- to- mudstone (F6a) showing relatively small, sub-angular dolomite clasts (DC) and locally occurring concentrated “clusters” of pyrite crystals (PY) (Brigham Oil and Gas, L.P. State 36-1 2H, 10858.0). (D) Core photograph of matrix-supported conglomerate (F6b) comprised of poorly sorted, relatively large sub-angular to sub-rounded dolomite clasts (DC) and elongate sub-angular clay clasts (CC) oriented roughly parallel to bedding in a siliciclastic silt- to- mudstone matrix (North Plains Energy, LLC Comford 9-12H, 9768.2 ft).



4.4 Interpretation of Facies Associations

The three facies associations identified in the middle Three Forks Formation reflect deposition by two predominant processes: (1) bedload transport and (2) mass gravity transport. In places, deposition by suspension settling is recorded, yet evidence of this process is relatively uncommon. Throughout the middle Three Forks Formation, the abundance of uni-directional and bi-directional foresets within cross-stratified silty dolostone units, as well as locally occurring planar- to- undulating lamination of siliciclastic mud- to siltstones and silty dolostones indicate deposition by bedload processes. In contrast, the abundance of mud-rich matrix-supported conglomerates with dolomite and clay clasts intercalated into silty dolostone and siliciclastic mudstone units, suggests that time-equivalent laminar sediment gravity flows transported dolomite and clay clasts derived from older sediments and rocks within the basin, in a cohesive clay- to- silt-rich matrix (c.f. Marr et al, 2001; Niedoroda et al., 2007; Talling et al., 2012). Where present, rocks that record deposition by suspension settling are comprised of structureless, relatively thin (0.1-0.2 mm) mudstone laminae of even thickness situated at the top of planar-laminated normally graded mud-rich beds.

Traditionally, depositional processes that form primary sedimentary structures, such as planar lamination and ripple cross-lamination, have been described and interpreted based on the size of detrital grains (e.g. Harms et al., 1975). Although detrital grains, such as quartz and clay minerals, do occur throughout the middle Three Forks Formation, the majority of rocks in the succession are comprised of authigenic dolomite. This authigenic dolomite is interpreted to be replacement dolomite, that is post-depositional in origin, and formed from in-situ recrystallization of a precursor, likely calcite. As a result, most of the original grains that formed primary sedimentary fabrics have since been altered, and in places entirely obliterated due to

complete mole-per-mole dolomite replacement of calcite (c.f. Sibley and Gregg, 1987; Machel, 2005). However, sedimentary structures comprised largely of authigenic dolomite remain well-preserved in the middle Three Forks Formation, despite the fact that most of the original grain boundaries are no longer discernible. Nevertheless, identification and interpretation of primary sedimentary structures in the middle Three Forks Formation is based largely on the occurrence, size, and arrangement of unaltered detrital grains, such as quartz and clay minerals, as well as the overall textural trends of authigenic dolomite crystals.

4.4.1 Synsedimentary Deformation

Synsedimentary deformation features such as massive rock fabric, water escape structures, sedimentary injection dykes, ball-and-pillow structures, and convolute bedding occur extensively throughout FA1 and FA2 rocks. These features are often associated with abundant faulting (normal and reverse), therefore their formation is attributed to one of two underlying earthquake-induced processes: (1) fluidization, whereby upward-moving water produces a fluid drag on overlying sediments, or (2) liquefaction, the process in which granular material is temporarily transformed from a solid into a liquefied state (Levi et al., 2006; Sims, 2012).

4.4.2 Facies Association 1: Laminated to Massive Siliciclastic Mudstone With Silty Dolostone Intercalations

Ripple-cross-stratified silty dolostone beds that are intercalated with planar to undulating mud- to- siltstone beds are typical characteristics of fluctuating energy conditions, between fair weather and storm wave base (Burchette and Wright, 1992; Flügel, 2004). An overall low energy setting dominated by bedload processes is reflected in planar to undulating lamina and laminasets of uneven thickness comprised predominantly of clay- to- silt-size siliciclastic grains

(c.f. Egenhoff and Fishman, 2013). Nevertheless, these mudstone laminae are commonly normally graded comprised of a relatively coarse-grained base that grades into a fine-grained upper portion, recording initial high energy conditions that waned over time. The gradation of these bedload-dominated mudstones into continuous siliciclastic mudstone laminae of even thickness suggests a transition to relatively tranquil conditions in which deposition by suspension settling prevailed. Frequently occurring cross-laminated silty dolostone intercalations reflect episodic high energy conditions, in which bedload was also the dominant transport mechanism, as indicated by downlapping laminasets and irregular basal scour surfaces. The presence of 0.2-3.0 mm sub-rounded clay rip-up clasts oriented roughly parallel to bedding at the base of cross-stratified silty dolostone laminasets further suggests erosion of the seafloor by high-energy currents. Dolomite-filled halite pseudomorphs on the interfaces of siliciclastic mudstones and dolostones reflect deposition in a restricted hypersaline environment (Decima et al., 1988; Martill et al., 2007; Rouchy et al., 2001). The overall lack of ichnofauna, with the exception of moderately-occurring *Phycosiphon incertum* fecal strings, is also indicative of high-stress, hypersaline conditions (Jaglarz and Uchman, 2010). In places where FA1 rocks are represented as clast-supported conglomerates comprised of pillow-shaped dolomite clasts associated with elongate sub-angular clay clasts in a clay-rich matrix, it is interpreted herein that shaking triggered by earthquakes led to the collapse of half-lithified, intercalated dolomite and mudstone beds. The abundant pillow-shaped clasts in FA1 reflect the reworking of half-lithified, “soft” sediment, in contrast to sub-angular to sub-rounded clasts that dominate FA3 which represent the breaking up of hard, lithified sediment. “Soft” clasts generally oriented parallel to bedding in a cohesive, water-saturated clay-rich matrix represent sediment transport under laminar flow processes in a sediment gravity flow (c.f. Marr et al., 2001; Haughton et al., 2009). Therefore,

these clast-supported conglomerates are likely the result of an initial disruption of “soft” or half-lithified intercalated dolomite and mudstone beds, followed by gravity mass flow transport and deposition.

4.4.3 Facies Association 2: Massive to Well Laminated Clay Clast-Bearing Silty Dolostone

The presence of predominantly ripple-cross-stratified silty dolostones, showing uni-directional and bi-directional downlapping lamina and laminasets with little to no siliciclastic mudstone intercalations suggests that these portions of the middle Three Forks Formation were deposited under both wave- and current-induced bedload transport processes, above fair weather wave base (Burchette and Wright, 1992; Demicco and Hardie, 1994). Abundant sub-rounded clay clasts that line basal scour surfaces of cross-stratified laminasets represent erosion of the seafloor and initial rounding of the grains by relatively high-energy currents. Overall, the complete lack of structures that are commonly characteristic of exposure such as dessication cracks, and fenestral fabrics such as birdseyes and root tubes, and gravitational meniscus cements (Shinn, 1983; Kendall and Warren, 1987; Demicco and Hardie, 1994), suggests deposition in a permanently submerged setting. Episodes of hypersaline conditions are reflected in locally-occurring dolomite-filled halite pseudomorphs. However, saline conditions similar to that of normal-marine seawater (~35 ‰) existed at times, as evidenced by localized abundant sub-vertical, diffuse bioturbation, as well as rarely-occurring discrete U-shaped *Diplocraterion* burrows that disrupt primary laminated fabrics (c.f. Buatois and Mángano, 2011). Nevertheless, salinities were likely elevated during deposition of FA2 rocks, evidenced by the overall small diversity of ichnofauna (c.f. Jaglarz and Uchman, 2010). In places where FA2 rocks are matrix- to- clast-supported conglomerates comprised of abundant elongate sub-angular clay clasts in a dolomite-rich matrix, it is interpreted that seismic shaking related to earthquakes caused unconsolidated,

water-saturated carbonate matrix to temporarily transform from a solid to a liquid state. The abundance of sedimentary injection dykes throughout these intervals further suggests that seismicity was active at the time that these sediments were being deposited (c.f. Levi et al., 2006). The orientation of elongate clay clasts roughly parallel to bedding indicates that the liquefied sediment acted as a somewhat cohesive matrix in which clay clasts were transported under gravity-driven laminar flow processes (c.f. Haughton et al., 2009).

4.4.4 Facies Association 3: Mud-Rich Conglomerate with Dolomite and Clay Clasts

The overall medium- to fine-grained matrix-supported nature of FA3, with a varying proportion of ungraded to inversely graded, and less frequently normally graded, dolomite and clay clasts, suggests that these rocks were deposited by non-turbulent, cohesive sediment gravity flows (Marr et al., 2001; Niedoroda et al., 2007; Talling et al., 2012). Orientation of elongate clasts roughly parallel to bedding is consistent with laminar transport processes that are characteristic of non-turbulent gravity mass flows (Haughton et al., 2009). Terminology applied to these deposits herein follows Einsele (2000) and Niedoroda et al. (2007), where mud-rich, clast-poor intervals are described as “mud flow deposits” and mud-rich, clast-rich units are termed “debrites.”

In places, inverse grading occurs within debrite intervals, and less commonly in mud flow deposits, as the result of relatively large clasts being forced upward due to dispersive pressures near the boundary of deposition (Fisher and Mattinson, 1968; Naylor 1980). When normal grading occurs, it is present exclusively toward the upper portions of clast-poor, mud flow deposits in the middle Three Forks Formation, and is likely the result of mixing and dilution with overlying seawater under waning flow conditions (Talling et al., 2012). In general, these

deposits are relatively thin (<1 m), have sharp contacts with adjacent beds. Mud flow deposits that occur as considerably thicker (>1 m), ungraded intervals in which no distinct internal boundaries define where one deposit terminates and the other begins are interpreted to represent amalgamated “compound” mud flow deposits based on their anomalous thickness and homogenized texture (c.f. Major, 1997).

5.0 FACIES ARCHITECTURE

The middle Three Forks Formation is approximately 10-25 m in thickness throughout the study area, and is subdivided into three to five well-defined stratigraphic units based on lithologies observed in twenty-two drill cores.

5.1 Middle Three Forks Formation Stratigraphy

The upper boundary of the middle Three Forks Formation is defined by a distinct green mudstone interval that is correlative on well logs and in core sample throughout the North Dakota portion of the Williston Basin (Bottjer et al., 2011; Egenhoff et al., 2011). This green mudstone is equivalent to unit 5 of Christopher (1961) and Nordeng and LeFever (2009) and Facies B of Berwick (2008). Underlying the green mudstone interval, the remainder of the middle Three Forks Formation corresponds to unit 4 of Christopher (1961) and Nordeng and LeFever (2009) and Facies B of Berwick (2008). The lower extent of the middle Three Forks Formation, which is equivalent to the boundary between units 3 and 4 of Christopher (1961) and Nordeng and LeFever (2009), is less obvious to discern on well logs and in core sample. Bottjer et al. (2011) define the lower limit of the middle Three Forks Formation based exclusively on a well log suite that shows a significant increase in gamma ray and resistivity responses. Contrarily, Egenhoff et al. (2011) delineate the base of the middle Three Forks Formation solely based on the transition from a mosaic to nodular anhydrite-rich unit at the lowermost part of the Three Forks succession, to an interval completely devoid of mosaic to nodular anhydrite toward the middle of the Three Forks succession. Based on a core-to-log comparison the relatively high gamma ray and resistivity responses noted by Bottjer et al. (2011) appear to reflect a massive red mudstone lithology, similar in composition to the green mudstone at the top of the middle Three

Forks succession. Therefore, this massive red mudstone unit is considered to be part of the middle Three Forks Formation. Following Egenhoff et al. (2011), the lower boundary of the formation applied herein is the lowermost part of the Three Forks Formation in which mosaic to nodular anhydrite is completely absent.

5.2 Facies Distribution and Stacking Patterns

Four transects across Williams, McKenzie, and Mountrail counties, North Dakota, illustrate a stratigraphic and areal distribution of facies within the middle Three Forks Formation (Appendices 1-4). These facies comprise coarsening-upward units, or “parasequences,” that are regionally correlative across distances several tens of kilometers (Figure 11; Appendices 1-4). Parasequences in the middle Three Forks Formation are represented by a basal mudstone unit with few dolomite intercalations that coarsens upward into a silty dolostone portion with few to no mudstone intercalations. Individual parasequences are arranged into four larger scale sediment packages, or intervals, within the middle Three Forks Formation.

Stratigraphic intervals have conventionally been described from base to top, where the lowermost unit is termed “Interval 1,” followed by an overlying “Interval 2,” etc. Nevertheless, because dolomitic intervals within the topmost portion of the middle Three Forks Formation are of the greatest economic interest, the uppermost unit is herein termed Interval 1, underlain by Interval 2, which has been deposited above Interval 3, which in turn rests on Interval 4 at the base of the middle Three Forks succession. The four intervals are described in detail below. However, as most cores do not penetrate the entire middle Three Forks succession, all four intervals are not present in all twenty-two cores. Similar to Christopher (1961) and Nordeng and LeFever (2009), the uppermost green mudstone portion of the middle Three Forks Formation has

been assigned its own subunit herein (Interval 0). Due to its complete lack of laminated mudstone and silty dolostone facies, a separate parasequence scheme is applied to Interval 0 based on size and arrangement of sub-angular to sub-rounded dolomite clasts in the unit.

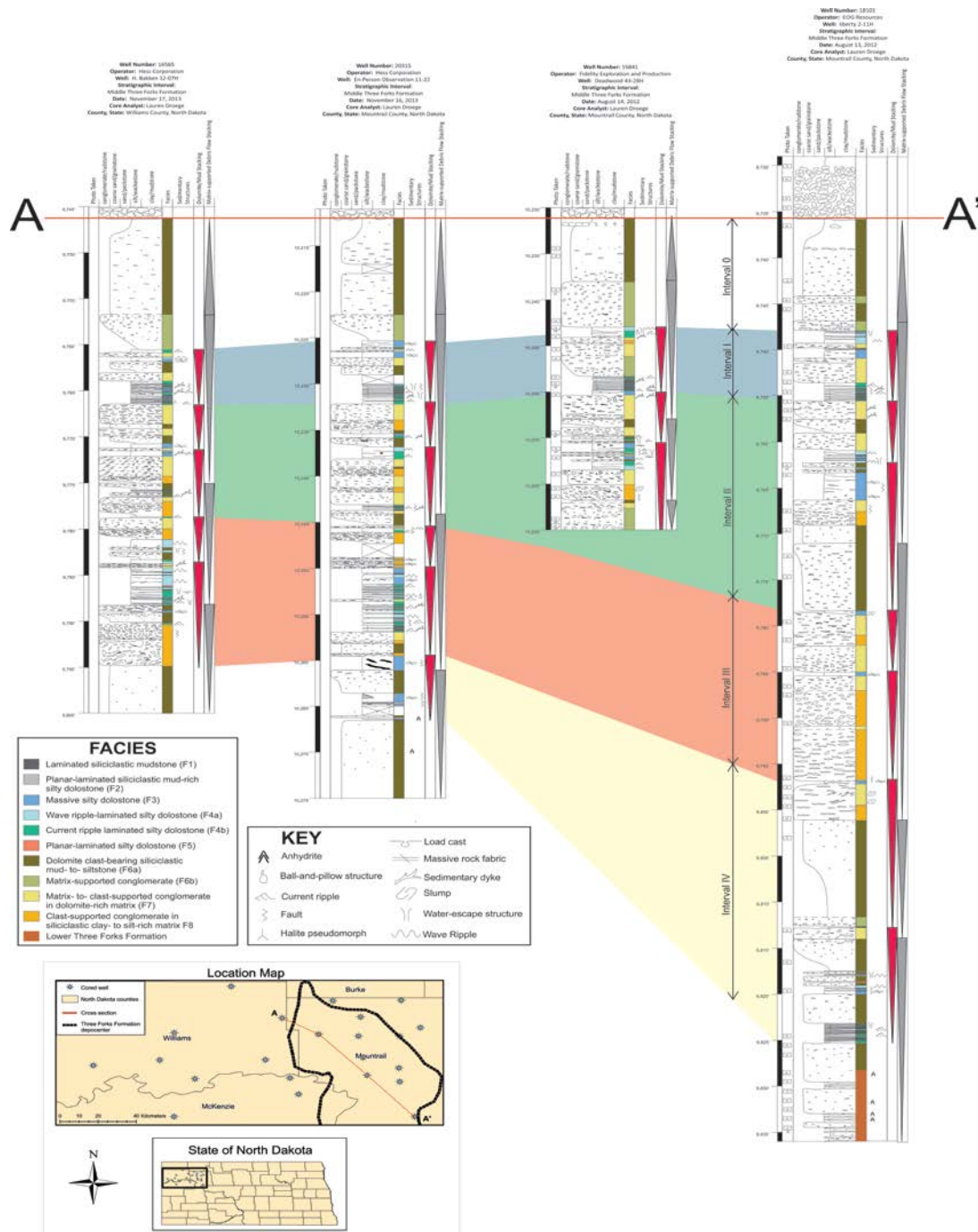


Figure 11. Cross-section of four cores through the middle Three Forks Formation showing detailed lithological core logs and correlation of Intervals 0, 1, 2, 3, and 4. Note all core depths are in feet.

5.2.1 Interval 0

The uppermost 3.0-4.5 m of the middle Three Forks Formation (Interval 0) is exclusively comprised of mud-rich matrix-supported conglomerates with dolomite and clay clasts (FA3). The base of Interval 0 is characterized by a regionally occurring coarsening-upward unit, 0.7-1.5 m in thickness, consisting of abundant, relatively large sub-angular to sub-rounded dolomite clasts (2-30 mm) and sub-angular clay clasts (5-25 mm) in a green siliciclastic mud- to- siltstone matrix. This coarsening-upward, clast-rich unit is present regionally and occurs in all twenty-two cores documented herein. Overlying the basal coarsening-upward portion of Interval 0, dolomite and clay clasts exhibit an overall fining-upward trend, decreasing in size and abundance toward the top of the interval. Clast-rich intercalations, similar in composition to the lower coarsening-upward unit, occur sporadically throughout the overall clast-poor fine-grained part of Interval 0. Toward the top of the stratigraphic interval, sub-mm pyrite crystals form locally occurring 1-5 mm concentrated clusters, commonly associated with elongate clay stringers. Oval-shaped 2-10 mm pyrite concretions also occur locally in the upper portion of the interval. The contact of Interval 0 with the overlying upper Three Forks Formation is sharp and irregular throughout the study area.

5.2.2 Interval 1

The uppermost stratigraphic unit (Interval 1) occurs in all cores described in this project. It is readily identified within every core by one laterally correlative coarsening-upward parasequence, approximately 1.5-2.0 m in thickness (Appendices 1-4). The lower part of the parasequence is generally comprised of laminated siliciclastic mudstones with silty dolostone intercalations (FA1), which grade upward into massive to well laminated clay clast-bearing silty dolostones

(FA2) with little to no clay intercalations. Mud-rich matrix-supported conglomerates with sparse dolomite and clay clasts (FA3) occur as 150-900 mm intercalations between basal laminated siliciclastic mudstones with silty dolostone intercalations (FA1) and upper massive to well laminated clay clast-bearing silty dolostones (FA2). The frequency of mud-rich matrix-supported conglomerates with dolomite and clay clasts (FA3) decreases toward the middle Three Forks Formation depocenter situated in Mountrail County, North Dakota. In contrast, the upper massive to well laminated clay clast-bearing silty dolostone (FA2) unit generally increases in thickness toward the depocenter, incorporating some 1-2 mm thick mudstone intercalations. The basal laminated siliciclastic mudstone with silty dolostone intercalations (FA1) unit also increases in overall thickness toward the depocenter, from approximately 130 mm at the basin margin to roughly 600 mm at the depocenter. Mud-rich matrix-supported conglomerates with dolomite and clay clasts (FA3) increase in abundance toward the basin margins, commonly intercalated into massive to well laminated clay clast-bearing silty dolostones (FA2).

5.2.3 Interval 2

Interval 2 underlies Interval 1 and is present in all twenty-two cores documented herein. Overall, gross thickness of Interval 2 increases from roughly 4.5 m near the basin margin to a maximum thickness of 7.0 m at the depocenter. Interval 2 is dominated by abundant mud-rich matrix-supported conglomerates with dolomite and clay clasts (FA3) intercalated into matrix- to- clast-supported conglomerates in a dolomite-rich matrix and massive silty dolostones (FA2), as well as clast-supported conglomerates in a siliciclastic silt- to- mudstone matrix (FA1). It consists of two laterally correlative parasequences, 1-5 m in thickness. In general, parasequences increase in thickness where intercalations of mud-rich matrix-supported conglomerates with dolomite and clay clasts (FA3) occur more frequently. The lower portion of each parasequence is

characterized by a relatively thin unit (50-600 mm) comprised of laminated siliciclastic mudstones with silty dolostone intercalations (FA1) (Appendices 1-4). The central part of each parasequence consists predominantly of matrix- to- clast-supported conglomerates that contain abundant elongate sub-angular clay clasts in a dolomite-rich matrix (FA2), clast-supported conglomerates comprised of pillow-shaped dolomite clasts in a siliciclastic silt- to- mudstone matrix (FA1), and mud-rich matrix-supported conglomerates with dolomite and clay clasts (FA3). Each parasequence is capped by a massive to well laminated clay clast-bearing silty dolostone (FA2) unit with little to no clay content, approximately 100-900 mm in thickness.

5.2.4 Interval 3

Interval 3 is situated directly under Interval 2 and is exclusively present in eight of the twenty-two cores documented in this study. In general, Interval 3 is dominated by FA 1 and FA2 rocks, whereas mud-rich matrix-supported conglomerates with dolomite and clay clasts (FA3) are rare to completely absent. This stratigraphic unit is thickest in the basin depocenter where it is comprised of two laterally correlative coarsening-upward parasequences, reaching a maximum thickness of 5.5 m. Toward the basin margin, the two parasequences amalgamate into one coarsening-upward parasequence, approximately 1.5 m in thickness (SM Energy Jaynes 16-12H; North Plains Energy LLC. Scanlan 3-5H, Burlington Resources Oil and Gas Company Washburn 44-36H). Each parasequence is 1.0-3.5 m in thickness and characterized by a basal unit comprised of FA1 rocks. In places where two parasequences occur in Interval 3, a laminated siliciclastic mudstone intercalated with silty dolostone (FA1) unit characterizes the base of the upper parasequence, whereas the basal portion of the lower parasequence is comprised of pillow-shaped dolomite clasts in a siliciclastic silt- to- mudstone matrix (FA1). Nevertheless, both parasequences are capped by a 50-300 mm thick massive to well laminated clay clast-bearing

silty dolostone (FA2) unit with no mudstone intercalations that generally thickens toward the basin depocenter. In places where Interval 3 is comprised of one parasequence, the resulting amalgamated parasequence is characterized by a lower clast-supported conglomerate unit comprised of pillow-shaped dolomite clasts in a siliciclastic silt- to- mudstone matrix (FA1) that grades upward into a well laminated silty dolostone (FA2). When present, mud-rich matrix-supported conglomerates with dolomite and clay clasts (FA3) occur as 100-300 mm thick intercalations at the base of the stratigraphic interval in two cores located near the basin margin (Hess Corporation H. Bakken 12-07H; Hess Corporation EN-Person Observation 11-22 (Figure 11)).

5.2.5 Interval 4

Interval 4 is the lowermost stratigraphic unit in the middle Three Forks Formation and only present in five of the twenty-two cores documented in this study. It is dominated by abundant mud-rich matrix-supported conglomerate with dolomite and clay clasts (FA3) intervals, 0.3-3.5 m in thickness, that are similar in composition to the uppermost portion of Interval 0. The entire interval, which is only observed in one core, consists of two coarsening-upward parasequences, 3-5 m in thickness (EOG Resources Inc. Liberty 2-11H, Figure 11). When present, the base of the upper parasequence is characterized by a relatively thin (< 100 mm) laminated siliciclastic mudstone intercalated with silty dolostone (FA1) unit. It is generally capped by a relatively thin (< 300 mm) massive to laminated silty dolostone unit or matrix- to clast-supported conglomerate in a dolomite-rich matrix (FA2) unit with little to no mudstone intercalations. The lower parasequence is only present in two cores (EOG Resources Inc. Liberty 2-11H and Burlington Resources Oil and Gas Company Washburn 44-36H), where it is capped by matrix- to- clast-supported conglomerates in a dolomite-rich matrix (FA2). The central portion of each

parasequence is dominated by mud-rich matrix-supported conglomerate with dolomite and clay clasts (FA3). In places, these mud-rich matrix-supported conglomerates with dolomite and clay clasts (FA3) show both fining- and- coarsening-upward trends, but generally consist of very few clasts (< 10%) with an overall structureless fabric.

6.0 DEPOSITIONAL MODEL

Within the study area, the middle Three Forks Formation represents a transect that encompasses facies deposited on a low-angle carbonate ramp in a restricted epeiric sea. Overall, the middle Three Forks Formation is comprised of mostly intrabasinal sediments and some extrabasinal matrix material. Units that show bedding and primary sedimentary structures are predominantly composed of authigenic dolomite crystals and basin-derived intraclasts. In contrast, sediment gravity flow deposits largely consist of clay and dolomite intraclasts in a largely terrigenous, clay-rich matrix. Nevertheless, the abundance of both wave- and- current-induced bedforms and stratifications in the middle Three Forks succession suggests that overall deposition occurred in a relatively shallow subtidal setting (Demicco and Hardie, 1994). Based on the facies identified herein, this shallow subtidal setting is further subdivided into two environments following Burchette and Wright's (1992) subdivision of carbonate ramps: (1) inner ramp above fair weather wave base (FWWB), and (2) mid-ramp just below FWWB, above storm wave base (SWB) (Figure 12).

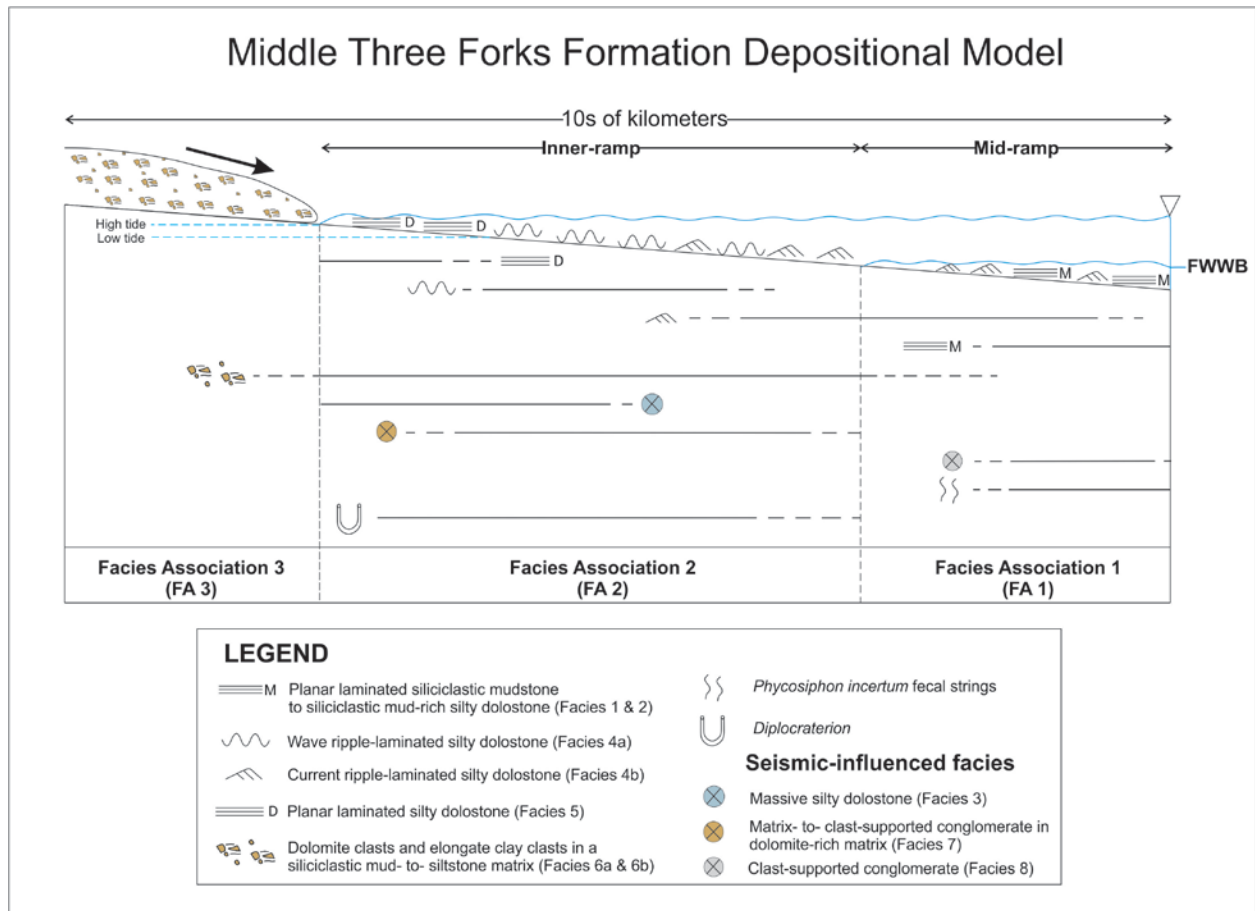


Figure 12. Depositional model for the middle Three Forks Formation.

6.1 Inner-ramp and Mid-ramp Depositional Environments

Sediments representing deposition in the mid-ramp environment just below FWFB and above SWB are dominated by laminated siliciclastic mudstones intercalated with cross-laminated silty dolostones. The intercalation of current ripple-laminated, relatively coarse-grained material into overall very fine-grained sediment is typical of deposition in an environment that experienced fluctuating energy conditions between FWFB and SWB (Zentmyer et al., 2011). Relatively low-energy conditions are reflected in planar- to undulating lamina and laminasets comprised predominantly of clay- to fine silt-size detritus that was transported and deposited by weak bottom currents. Although mid-ramp sediments generally experience frequent storm reworking,

very-fine grained mudstones that were deposited under tranquil conditions between storm events may have allowed the organism producing *Phycosiphon incertum* fecal strings to disrupt much of the laminated fabric of the mid-ramp setting. In contrast, ripple cross-laminated silty dolostones that are intercalated into laminated siliciclastic mudstones reflect episodic high-energy storm events (Tucker, 1982; Zentmyer et al., 2011) strong enough to transport coarse silt- to very fine sand-size sediments from the inner-ramp to the mid-ramp setting. Cross-laminated silty dolostones frequently have basal scour surfaces that are in places lined with clay rip-up clasts, which are evidence of seafloor reworking caused by high-energy currents (e.g. Schieber, 1998).

The overall coarser grain-size of detrital grains in clay-poor, “clean” silty dolostones relative to mid-ramp siliclastic mudstones suggests that these sediments were deposited in an overall shallower, higher-energy setting. Deposition of silty dolostones likely occurred in a shallow subtidal inner-ramp setting with almost constant wave agitation as evidenced by abundant bi-directional downlapping foresets comprised of abundant coarse silt- to fine sand-size detrital grains, with very little to no clay content (Burchette and Wright, 1992; Demicco and Hardie, 1994; Durringer and Vecsei, 1998). The occurrence of ripples comprised of uni-directional downlapping foresets with bi-directional ripple foresets suggests that uni-directional bottom currents were also active in the wave-dominated inner-ramp setting. Rarely occurring, planar-laminated silty dolostones reflect deposition under upper-flow regime conditions in the foreshore portion of the inner-ramp setting (Reineck and Singh, 1973). Here, supercritical flow velocities forced sediment to be transported and deposited in a sheet flow across the overall planar beach surface (Clifton et al., 1971).

6.2 Sediment Gravity Flows

Based on the overall increase in abundance of debrites and mud flow deposits toward the basin margins, it is likely that the clay and silt matrix components of these intervals are largely, if not fully, terrigenous (c.f. Talling et al., 2012). Dolomite and elongate clay rip-up clasts, however, represent intrabasinal reworking, where erosion of the seafloor produced dolomite and clay clasts which were incorporated into the clay-rich “slurry” as it entered the basin. During upper Devonian times, paleo-highs that served as sediment sources for the Williston Basin include the Transcontinental Arch to the south-southeast and the North American craton to the east-northeast (Peterson and MacCary 1987; LeFever, 1992). While debrites and mud flow deposits occur extensively throughout the basin, the positions of these sediment sources are consistent with more frequently-occurring debrite and mud flow intercalations in the southern to northeastern portions of the basin. Furthermore, submarine sediment gravity flows can continue to move on slopes as low as 0.25° (Talling et al., 2007), so it is no surprise that debrites and mud flow deposits are so widespread throughout the basin, occurring even in the middle Three Forks Formation depocenter in Mountrail, County, North Dakota.

Although sediment gravity flow deposits are present throughout the basin, they are more abundant in some stratigraphic intervals than others. The alternating character between intervals rich in these deposits and those that lack them suggests a fluctuating climate control on deposition (Egenhoff et al., 2011). Debrite- and mud flow-dominated Intervals 0, II, and IV may be attributed to overall wetter conditions, in which relatively cohesive, water-saturated terrigenous sediment masses would readily enter the basin due to gravitational forces. Whereas, a generally arid climate lacking water-saturated terrigenous sediment gravity flows is represented by Intervals I and III.

7.0 DIAGENESIS

The middle Three Forks Formation shows a number of diagenetic phases and events that have altered the original depositional fabric of the rock and as a result have greatly influenced reservoir characteristics. A detailed analysis into the diagenetic overprint of the middle Three Forks Formation is based predominantly on thin section observations due to the relatively small scale of diagenetic features such as cements and porosity types. Diagenetic phases observed in the middle Three Forks Formation are described in detail below.

7.1 Dolomite

The middle Three Forks Formation consists of approximately 90% authigenic dolomite. Crystal sizes and textures are generally consistent throughout each facies. The types of dolomite textures described in the middle Three Forks Formation are based on the nomenclature and classification established by Randazzo and Zachos (1983) (see 3.0 Methodology).

Laminasets that comprise planar- to cross-laminated silty dolostone facies typically consist of a basal, quartz-rich inequigranular dolosparstone with contact-rhomb texture (Figure 13A) that grade into a quartz-poor, equigranular sutured dolomicrosparstone (Figure 13B). In contrast, massive silty dolostones are generally composed of dolomicrosparstones with floating rhomb texture (Figure 13C) and equigranular sutured dolomicrosparstones to dolosparstones (Figure 13B, 13D).

The middle Three Forks Formation is comprised of eight distinct types of dolomite that are described in detail below.

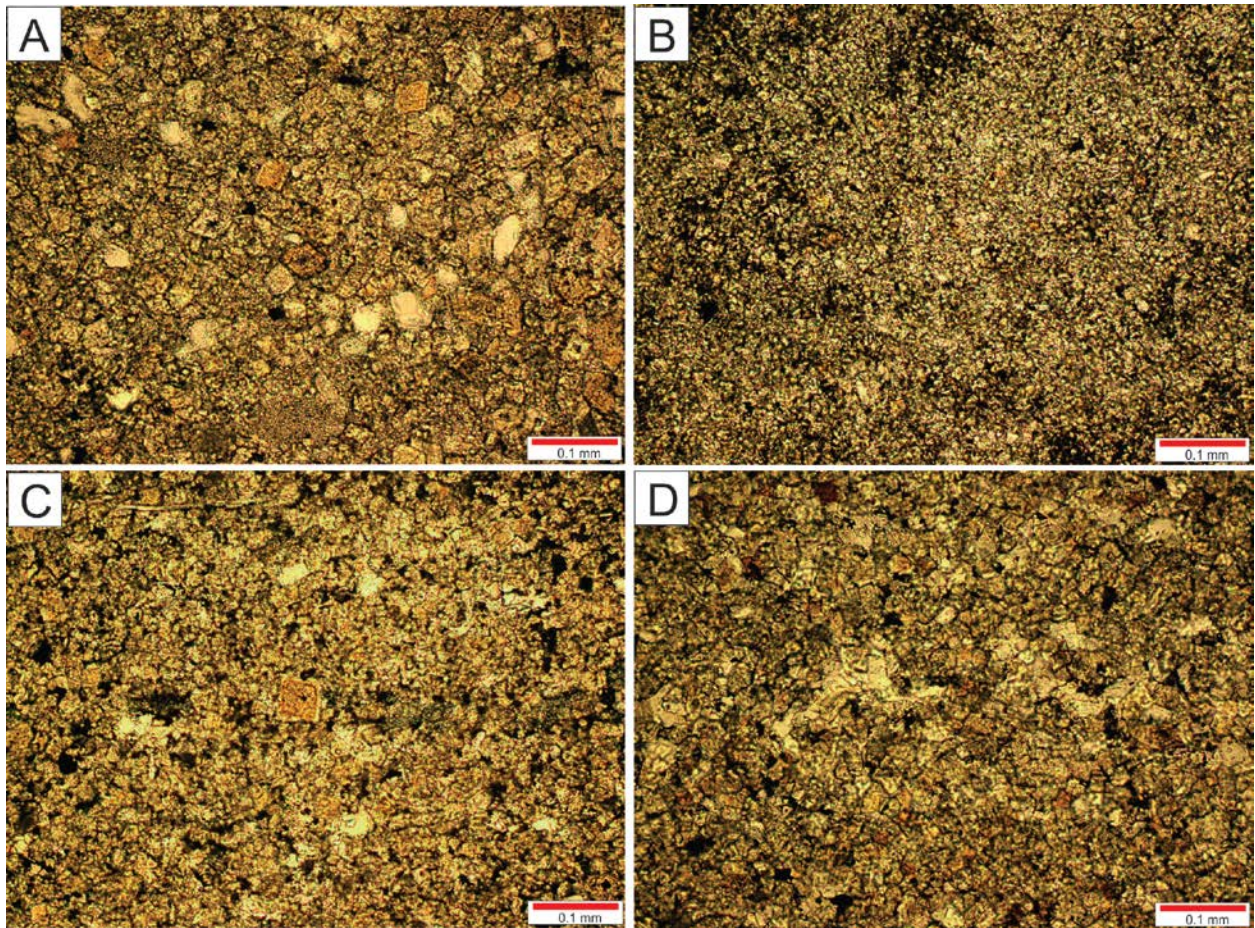


Figure 13. Types of dolomite textures present in the middle Three Forks Formation. **(A)** Quartz-rich inequigranular dolosparstone with contact-rhomb texture (SM Energy Company Jaynes 16-12H, 11186.9 ft). **(B)** Quartz-poor equigranular dolomicrosparstone with sutured texture (Hess Corporation H. Bakken 12-07H, 9763.9 ft). **(C)** Inequigranular dolosparstone with floating rhomb texture (Brigham Oil and Gas L.P. State 26-1 2H, 10873.2 ft). **(D)** Equigranular sutured dolosparstone (Hess Corporation EN-Person Observation 11-22, 10230.1 ft).

7.1.1 Dolomite I

Dolomite I is the most abundant type of dolomite in the middle Three Forks Formation (Figure 14A, 14C, 14F). It comprises the majority of the matrix throughout the succession, occurring as mostly sutured planar-euhedral to subhedral, fine- to medium-size, “dusty” dolomite crystals (0.004-0.01 mm). As a result of its overall fine-crystalline character, boundaries of Dolomite I crystals are sometimes not well-defined, therefore giving it an anhedral crystal texture. Relatively fine Dolomite I crystals frequently occur as inclusions in bladed anhydrite crystals as well as in coarse, euhedral dolomite crystals (Figure 14A).

7.1.2 Dolomite II

Dolomite II is relatively common throughout the middle Three Forks Formation, and consists of colorless to cloudy, planar-euhedral to subhedral dolomite crystals approximately 0.01-0.5 mm in size (Figure 14A-F). It has a “dusty,” inclusion-rich appearance and occurs as the core of zoned dolomite crystals that have one or more dolomite cement overgrowths.

7.1.3 Dolomites III through VIII

Dolomite II crystals are frequently rimmed with several sub-mm overgrowths (up to six in places), that generally alternate between clear and inclusion-rich dolomite, referred to herein as Dolomite III to VIII. Dolomites III, V, and VII occur as relatively thin (< 0.002 mm) rims that are colorless and generally inclusion-poor. Due to their overall thin character, the presence of Dolomite generations III, V, and VII may not always be apparent. In places where they occur as the outermost rim of zoned dolomite crystals, their crystal boundaries are mostly diffuse, but overall appear to have a planar-subhedral texture. Due to their similar overall colorless thin character, distinguishing among Dolomites III, V, and VII is only possible in zoned dolomite

crystals comprised of five or more overgrowth generations (Figure 14D). Dolomite IV is orange to brown in color when viewed in plane polarized light (Figure 14C, 14D). It occurs in zoned dolomite crystals as a 0.005-0.01 mm thick, inclusion-rich rim. In places where Dolomite IV is the outermost rim of zoned dolomite crystals, its crystal boundaries are well-defined with a planar-euhedral texture. Dolomite VI has an inclusion-rich, “dusty” appearance (Figure 14D). It occurs as a poorly-defined diffuse rim less than 0.002 mm thick that is not always apparent, likely because it is so thin and has no distinct crystal boundaries. Dolomite VIII consists of a thin overgrowth (< 0.001 mm) that is only discernible under relatively high magnifications, such as those applied in a scanning electron microscope (SEM) (Figure 14E). In contrast to all of the preceding dolomite types, Dolomite VIII is iron-rich and completely devoid of inclusions (Appendix 7). Dolomite VIII also occurs as planar-euhedral crystals, approximately 0.004-0.05 mm in size, that frequently occur as crystal “clusters” on detrital quartz grain surfaces, as well as planar-euhedral quartz rhombs, and appear to be partially to completely replacing the quartz (Figure 14F). In places, relatively coarse Dolomite VIII crystals (0.03-0.05 mm) occur as inclusions in blocky to bladed anhydrite crystals, as well as along the periphery of anhydrite aggregate clusters.

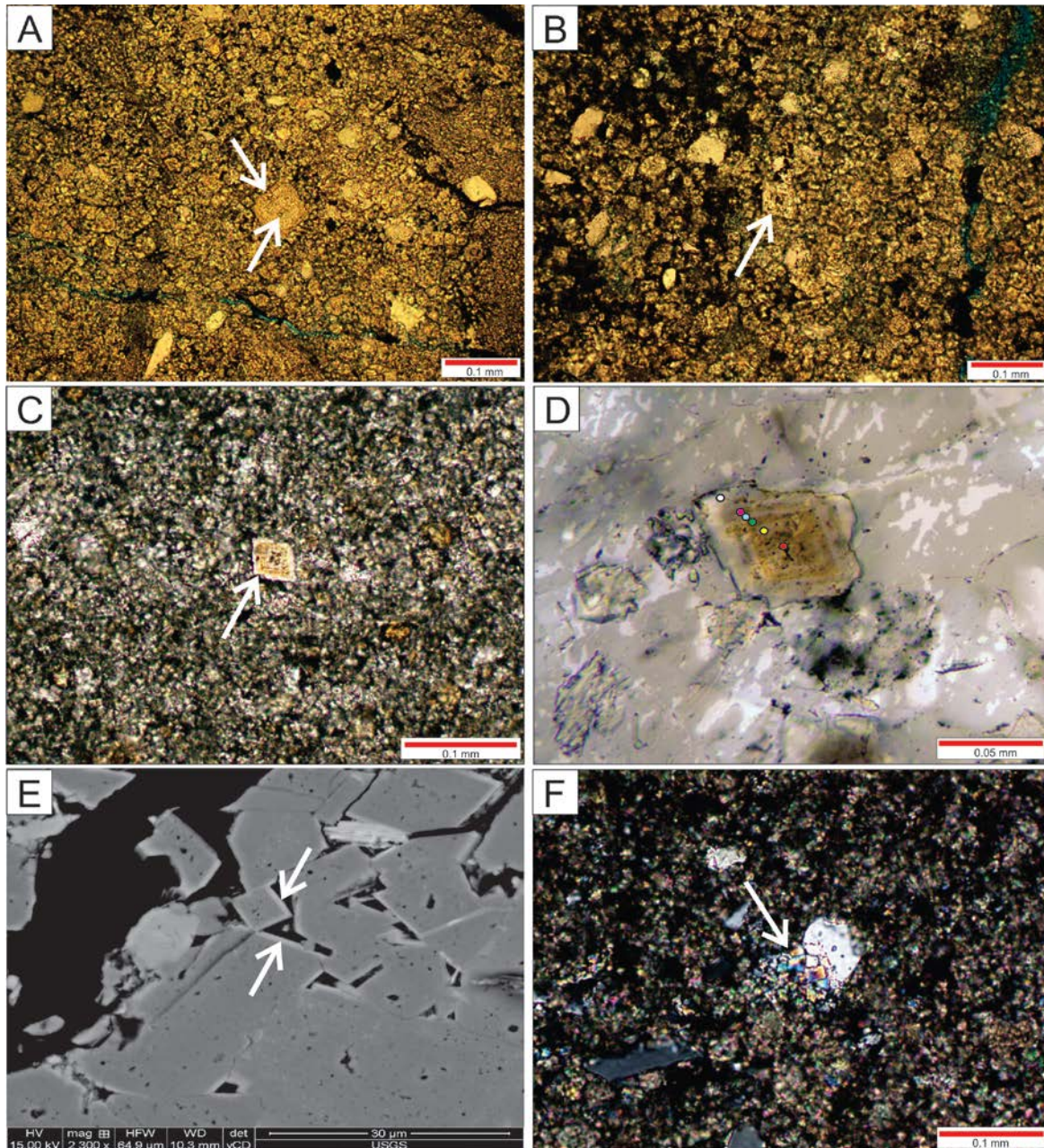


Figure 14. Types of dolomite present in the middle Three Forks Formation. **(A)** Fine-crystalline Dolomite I crystals included in a coarse dolomite crystal (arrows). Dolomite I comprises the majority of matrix material (Brigham Oil and Gas L.P. State 26-1 2H, 10873.2 ft). **(B)** Inclusion-rich, dusty planar-euhedral Dolomite II crystal, indicated by arrow (Hess Corporation EN-Person Observation 11-22, 10237.3 ft). **(C)** Zoned dolomite crystal (arrow) comprised of inclusion-rich Dolomite II core, thin, colorless, inclusion-poor Dolomite III overgrowth, brown Dolomite IV rim, and thin, colorless, inclusion-poor Dolomite V outermost rim (EOG Resources Liberty 2-11H, 9750.1 ft). **(D)** Zoned dolomite crystal comprised of: inclusion-rich Dolomite II core (red dot); thin, colorless, inclusion-poor Dolomite III overgrowth (yellow dot); brown Dolomite IV rim (green dot); thin, colorless, inclusion-poor Dolomite V rim (blue dot); inclusion-rich, poorly-defined Dolomite VI rim (pink dot); limpid, colorless Dolomite VII outermost rim (white dot) (SM Energy Jaynes 16-12H, 11180.9 ft). **(E)** SEM backscatter micrograph showing iron-poor dolomite crystals (dark grey) with thin, iron-rich Dolomite VIII overgrowths (light grey, arrows). Scalebar is 30 microns (Hess Corporation EN-Person Observation 11-22, 10237.3 ft). **(F)** Limpid, Dolomite VIII crystals (arrow) associated with a detrital quartz grain in cross-polarized light (Brigham Oil and Gas L.P. Richardson 30 No. 1, 8418.7 ft).

7.1.4 Dolomite Iron Concentrations

A quantitative electron microprobe analysis of two zoned dolomite crystals comprised of Dolomite II, a thin colorless rim directly overgrowing Dolomite II (Dolomite III, V, or VII), and an inclusion-bearing rim (Dolomite IV or VI) yielded the following iron mass percentages: 0.4-3.6 wt% at the Dolomite II core; 6.0-6.7 wt% in the thin colorless overgrowth; 5.2 wt% in the inclusion-bearing rim (Figure 15, Appendix 8). Although this dataset is very limited, it does reveal that iron content overall increases from the Dolomite II core to outer dolomite rims. This trend is consistent with observations made based on qualitative SEM analyses, in which the results yielded that only the outermost Dolomite VIII rim consisted of dolomite with high iron concentrations, while little to no iron content was recorded throughout the remainder of dolomite crystals (Appendix 7 – SEM report).

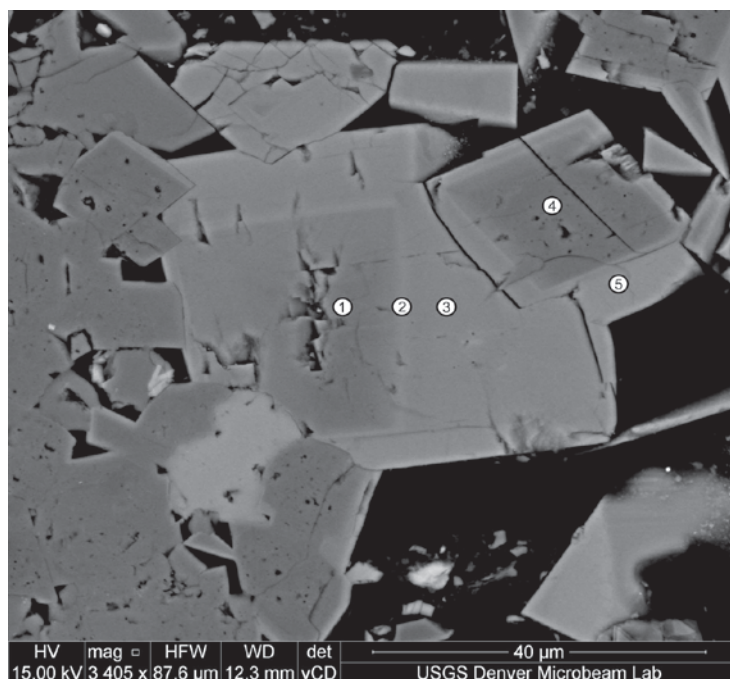


Figure 15. Electron microprobe backscatter micrograph of two zoned dolomite crystals comprised of Dolomite II (points 1 & 4), thin colorless overgrowth (Dolomite III, V, or VII) (point 2), and inclusion-bearing rim (Dolomite IV or IV) (points 3 & 5). Numbered points are positioned in areas where quantitative elemental data was collected and numbered according to their corresponding dataset in Appendix 8. Note because of the relative thinness of the colorless overgrowth, data was only compiled for the thin colorless overgrowth of the large dolomite crystal.

7.2 Quartz

In places, quartz occurs as colorless 0.05-0.1 mm size inclusion-rich to inclusion-poor planar-euhedral rhombs. Quartz rhombs are randomly distributed throughout different facies of the middle Three Forks Formation, occurring in both clay-rich horizons as well as areas rich in coarse silt-size detrital quartz grains and dolomicrosparstone to dolosparstone. They are relatively rare, accounting for less than 1% of the bulk rock volume throughout the study area. In places where quartz rhombs contain abundant inclusions, they appear similar to inclusion-rich Dolomite II crystals in plane-polarized light (Figure 16A). However, in cross-polarized light the rhombs exhibit the same first order birefringence as surrounding detrital quartz grains (Figure 16B). Inclusion-poor quartz rhombs have similar optical properties as surrounding detrital quartz grains in both plane-polarized light and cross-polarized light, and they are frequently lined with fine- to medium-crystalline planar-euhedral Dolomite VIII crystals (Figure 16C).

7.3 Anhydrite

Anhydrite mostly occurs as subhedral to euhedral individual bladed to blocky crystals approximately 0.05-0.8 mm in size that typically form 0.2-1.0 mm aggregate clusters (Figure 16D, 16E). It comprises 1% or less of the bulk rock volume throughout the study area. The aggregate clusters typically have an overall sub-rounded to angular shape and appear to be filling vug-like openings in the rock. In places, fine crystalline Dolomite I, zoned Dolomite II crystals with varying amounts of overgrowths, as well as late-stage medium- to coarse-crystalline Dolomite VIII crystals occur as disseminated inclusions throughout anhydrite crystals (Figure 16D). In places, planar-euhedral coarse-crystalline dolomite crystals also occur along the edges of anhydrite aggregate clusters. Rarely, blocky anhydrite crystals appear to fill once-open sub-vertical fractures (Figure 16F).

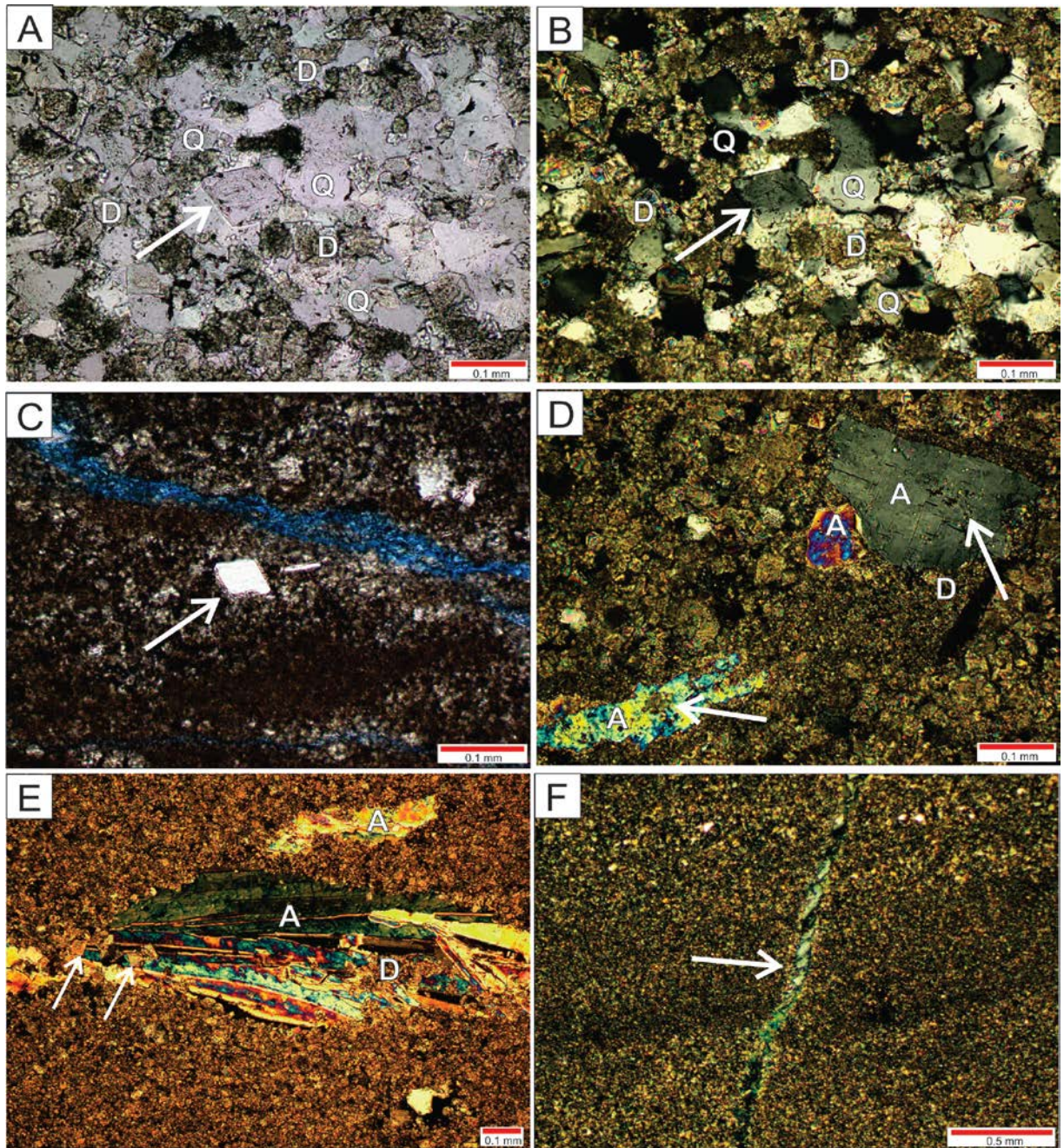


Figure 16. Diagenetic anhydrite and quartz textures present in the middle Three Forks Formation. (A) and (B) Inclusion-rich quartz rhomb (arrow) surrounded by coarse silt-size detrital quartz grains (Q) and fine- to medium-crystalline Dolomite I matrix (D) in plane-polarized light (PPL) (A) and cross-polarized light (CPL) (B) (SM Energy Jaynes 16-12H, 11180.9 ft). (C) Inclusion-poor quartz rhomb (arrow) lined with fine-crystalline Dolomite VIII crystals in PPL (Amerada Hess Corporation State ND 1-11H, 9569.9 ft). (D) Aggregate clusters comprised of poorly- to well-defined blocky anhydrite crystals (A) that appear to be lined with abundant very fine crystalline Dolomite I crystals (D) in CPL. Note abundant disseminated very fine Dolomite I inclusions throughout anhydrite crystals (arrows) (SM Energy Jaynes 16-12H, 11186.9 ft). (E) Aggregate cluster comprised of euhedral bladed anhydrite crystals (A) with fine-crystalline Dolomite I (D) inclusions, coarse-crystalline Dolomite VIII inclusions, and planar-euhedral crystals at the edge of the aggregate cluster (arrows) in CPL (Brigham Oil and Gas L.P. State 26-1 2H, 10873.2 ft). (F) Sub-vertical fracture completely filled with blocky anhydrite crystals (arrow) in CPL (SM Energy Jaynes 16-12H, 11186.9 ft).

7.4 Pyrite

Pyrite generally comprises 1% or less of the bulk rock volume throughout the study area. In thin section it predominantly occurs as disseminated euhedral angular to subhedral sub-rounded crystals approximately 0.01-0.05 mm in size (Figure 17A). In places, it forms linear “bands” or rounded aggregates comprised of angular 0.05-0.4 mm euhedral crystals (Figure 17B, 17C). When present in core sample, pyrite typically occurs as 1-3 mm clusters comprised of sub-mm to 1 mm euhedral pyrite crystals either concentrated in distinct linear horizons or randomly distributed in a clay-rich matrix (Figure 17D). Rounded pyrite concretions 2-8 mm in size also occur locally in clay-rich intervals (Figure 17E).

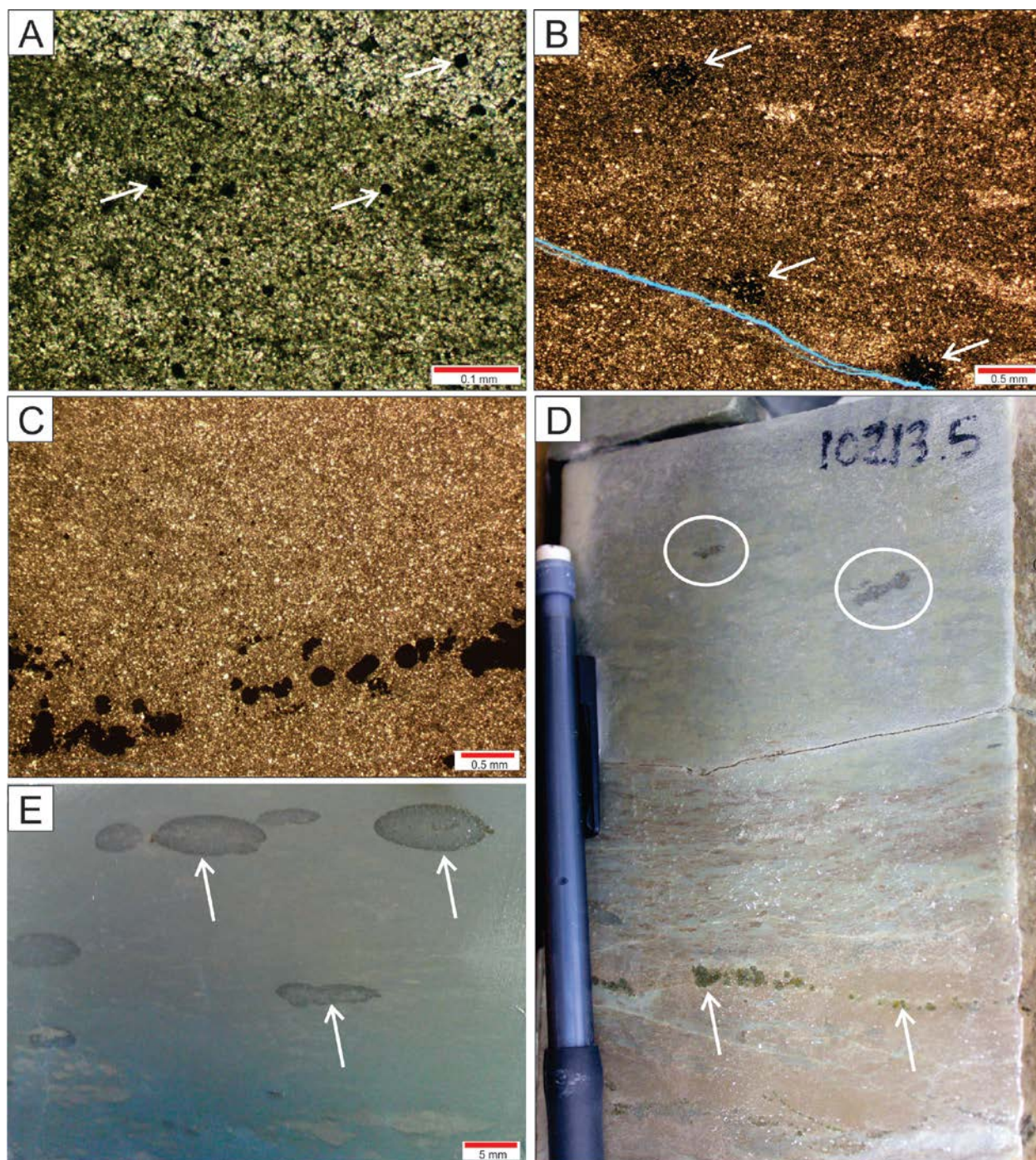


Figure 17. Pyrite textures present in the middle Three Forks Formation. **(A)** Optical photomicrograph of disseminated subhedral pyrite crystals (arrows) in a clay-rich dolomicrosparstone matrix (Brigham Oil and Gas L.P. Anderson 28 1-H, 10219.4 ft). **(B)** Optical photomicrograph showing rounded aggregates comprised of subhedral pyrite crystals (arrows) in a clay-rich dolomicrosparstone matrix (Fidelity Exploration and Production Company Farhart 11-11H, 9791.0 ft). **(C)** Optical photomicrograph of a linear band of concentrated euhedral pyrite crystals (Fidelity Exploration and Production Company Farhart 11-11H, 9791.0 ft). **(D)** Core photograph of clusters of pyrite crystals concentrated along a distinct horizon (arrows) as well as randomly distributed (circles) in a clay-rich matrix (Hess Corporation EN-Person Observation 11-22, 10213.5 ft). **(E)** Core photograph illustrating rounded pyrite concretions (arrows) in a clay-rich matrix (Amerada Hess Corporation State ND 1-11H, 9573.5 ft).

7.5 Porosity

Open pore spaces in the middle Three Forks Formation are predominantly less than 0.05 mm in diameter, but may reach up to 0.1 mm in places. Connectivity among pore spaces is very low, and as a result isolated areas of porosity occur randomly distributed throughout dolomicrosparstones and dolosparstones. Following a modified version of Choquette and Pray's (1970) classification for porosity in carbonate rocks (see 3.0 Methodology), five types of porosity are present throughout the middle Three Forks succession: micro-intercrystalline porosity, intercrystalline porosity, intracrystalline porosity, moldic porosity and linear dissolution porosity. These porosity types are described in detail below.

7.5.1 Micro-Intercrystalline Porosity

Micro-intercrystalline porosity is the most common type of porosity in the middle Three Forks Formation. It is characterized by micron-scale porosity associated with fine-crystalline dolomite matrix crystals. As a result of their relatively small size, these pores are only detected in thin sections that are impregnated with blue epoxy (Figure 18A, 18B). Nevertheless, micro-intercrystalline porosity occurs as irregular patches that are randomly distributed throughout dolomicrosparstones, commonly associated with clay-rich areas. These pore spaces appear to be moderately connected, however due to its irregular, patchy distribution overall connectivity of the pore networks throughout the middle Three Forks Formation is low.

7.5.2 Intracrystalline Porosity

Intracrystalline pore types are only distinguishable under high magnifications, such as those applied in a SEM (Figure 15). Pores are generally around 1 micron in diameter, but in places may be up to 5 microns across, and have a round to elongate angular shape. Intracrystalline

porosity is present in all dolomite types based on SEM analyses, with the exception of very thin, Fe-rich Dolomite VIII rims.

7.5.3 Intercrystalline Porosity

Intercrystalline pores occur along the margins of individual dolomite crystals and typically have diffuse, poorly-defined pore walls (Figure 18C,18D). These pore types are irregularly shaped to sub-rounded areas that are approximately 0.02-0.1 mm across. Intercrystalline porosity is present most frequently in detrital quartz-rich dolosparstones, but may occur in places where detrital quartz grains are scarce. Connectivity among intercrystalline pores is moderate to high, however, these pore networks generally occur as sporadically distributed areas throughout the middle Three Forks Formation.

7.5.4 Moldic Porosity

Moldic porosity is characterized by pore spaces approximately 0.04-0.05 mm in size. These pores typically occur in quartz-rich dolosparstones and typically are rhomb-shaped (Figure 18E). Moldic porosity is uncommon in the middle Three Forks Formation and when present it occurs as isolated pore spaces with no connectivity.

7.5.5 Linear Dissolution Porosity

Linear dissolution pore types occur as horizontal to sub-vertical “bands” of porosity that are 0.008-0.01 mm wide (Figure 18F). Clay minerals and very fine dolomite crystals (< 0.004 mm) frequently line the walls of these pore spaces. Overall, this type of porosity is rare throughout the middle Three Forks Formation. When present, it mostly occurs in clay-rich dolomicrosparstones, but may also be present in clay-rich dolosparstones.

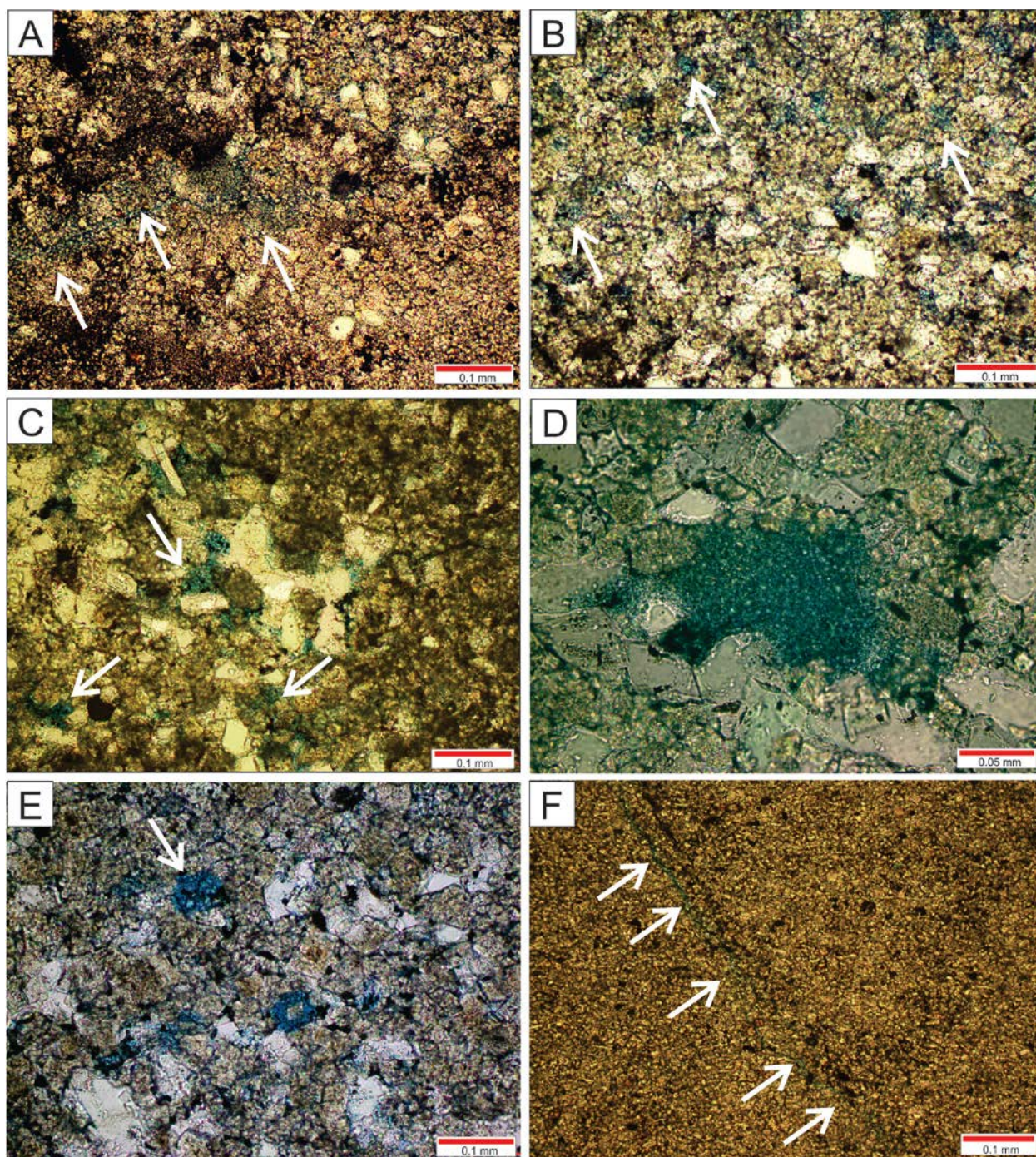


Figure 18. Porosity types present in the middle Three Forks Formation. **(A)** and **(B)** Micro-intercrystalline porosity randomly distributed in dolomicrosparstone (arrows) (Hess Corporation H. Bakken 12-07H, 9763.9 ft; Amerada Hess Corporation State ND 1-11H, 9581.5 ft). **(C)** Patchy distribution of irregularly shaped intercrystalline pore spaces between individual dolomite crystals (arrows) (Whiting Oil and Gas Corporation Braaflat 11-11H, 10020.6 ft). **(D)** Intercrystalline porosity with an overall sub-rounded shape with diffuse pore walls between individual dolomite crystals (Hess Corporation H. Bakken 12-07H, 9760.3 ft). **(E)** Rhomb-shaped moldic porosity (arrow) (EOG Resources Sidonia 1-06H, 8855.9 ft). **(F)** Linear dissolution porosity (arrows) (Hess Corporation EN-Person Observation 11-22, 10230.1 ft).

7.5.6 Porosity Distribution

Point-counting of forty-eight thin sections taken from twenty drill cores yield average visible porosities ranging from 0-5% throughout the study area (Figure 19, Appendix 6). Porosities in the middle Three Forks Formation show a general trend in which relatively lower porosities in the western portion of the study area increase slightly to the east. The highest porosities occur in the northern and eastern parts of Mountrail County, whereas several areas throughout McKenzie County and southeastern Williams County yield less than 1% porosity based on the point-counted dataset. Well control throughout the study area is highly variable, with high cored well density in Mountrail County, and relatively lower cored well density in Williams and McKenzie counties. Although a coarse trend is observed in the current dataset, porosity distribution would likely be better constrained with a more evenly populated dataset.

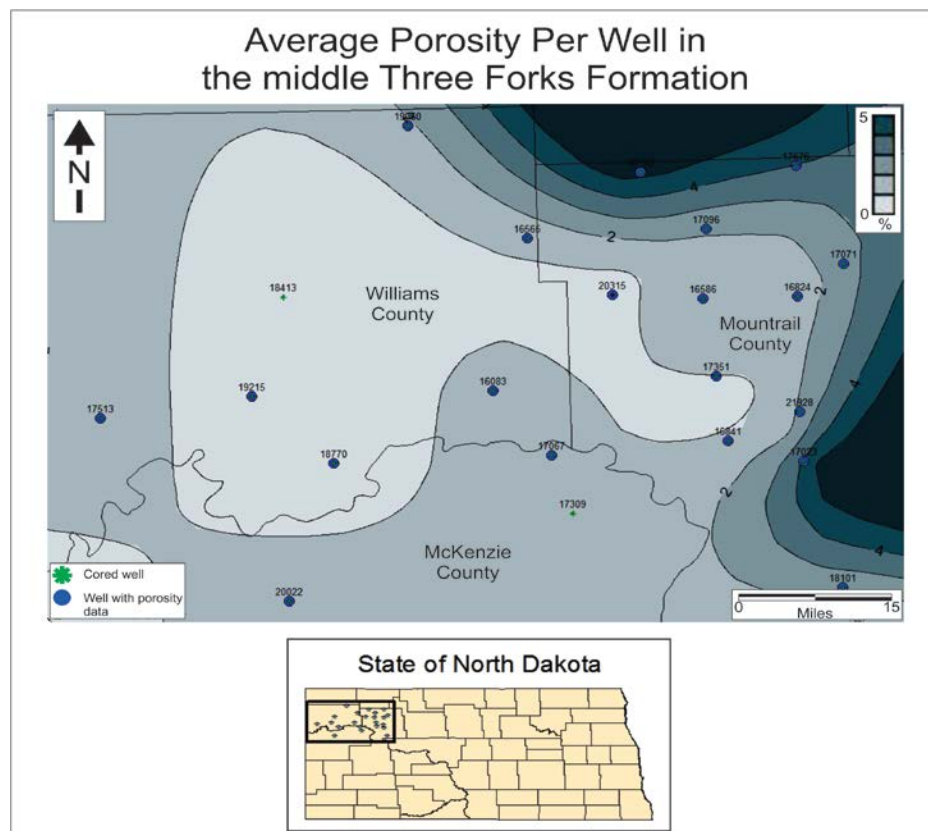


Figure 19. Map showing the distribution of average porosity per core in the middle Three Forks Formation.

7.6 Diagenetic History

Relative timing of diagenetic events that have affected the middle Three Forks Formation is determined based on textural relationships among diagenetic phases (Figure 20). Interpretations of these diagenetic attributes are explained in detail below.

7.6.1 Dolomite

All eight types of dolomite described above are interpreted herein to be “secondary,” or post-depositional in origin. Based on textural characteristics, such as size, shape and distribution of the dolomite types identified in the middle Three Forks Formation, a relative diagenetic history is constructed in which each dolomite type represents a distinct episode of dolomite formation.

Planar-euhedral to subhedral “dusty” Dolomite I crystals reflect the first stage of dolomite formation that occurred throughout the middle Three Forks Formation. Overall fine-crystalline Dolomite I matrix crystals are interpreted herein to have replaced a fine-crystalline calcitic matrix, or micrite, penecontemporaneously or during shallow burial (c.f. Al-Aasm and Packard, 2000; Rott and Qing, 2013). This interpretation is consistent with previous empirical studies which revealed that dolomitization is commonly matrix-selective at low temperatures (< 50-80°C), typical of relatively shallow-burial depths (Machel, 2005).

Following the initial matrix-selective dolomitization episode from which Dolomite I formed, a second stage of dolomitization occurred from which a relatively smaller population of cloudy, inclusion-rich replacement Dolomite II crystals developed. The pre-cursor of Dolomite II is likely low-Mg calcite, which contains nucleation sites that are far apart because it is more resistant to dolomitization than high-Mg calcite (c.f. Sibley, 1982). Therefore, the overall widely-spaced nucleation sites on the low-Mg calcite pre-cursor ultimately resulted in relatively

coarse replacement Dolomite II crystals. Dolomite II crystals were subsequently overgrown by alternating inclusion-poor and inclusion-rich dolomite rims (Dolomites III-VIII). These overgrowths are considered to reflect relatively late-stage cements that precipitated directly from an aqueous solution, instead of replacing a precursor (c.f. Machel, 2005). In places where all six cements envelope a Dolomite II core, the relative timing of dolomite growth episodes, or “stages,” is deduced as follows: Dolomite III cements overgrew Dolomite II during a third stage, succeeded by a later fourth episode from which Dolomite IV cements enveloped Dolomite III, and so on through an eighth stage from which iron-rich Dolomite VIII overgrew Dolomite VII cements. Planar-euhedral, medium- to coarse-crystalline Dolomite VIII cements likely formed due to a decreased number of nucleation sites on pre-cursor calcite crystals where dolomite could form, as well as decreasing fluid saturation with respect to dolomite, over time (c.f. Sibley and Gregg, 1987). In places where Dolomite VIII is closely associated with detrital quartz grains, pressure exerted by growing dolomite crystals likely selectively dissolved adjacent quartz grains (c.f. Maliva and Siever, 1990).

7.6.2 Quartz

In places where quartz occurs as planar-euhedral rhombs, an episode of silicification likely caused planar-euhedral, medium- to coarse-crystalline dolomite crystals to be replaced by quartz. The silicification episode may have been the result of Si^{4+} and O^{2-} ions that were released during the pressure dissolution of quartz grains by Dolomite VIII crystals. Nevertheless, the generally coarse size of quartz rhombs suggests that relatively coarse Dolomite II crystals with variable cement overgrowths are the likely precursor that has been replaced by quartz. Quartz rhombs seem to have formed more or less contemporaneously based on their overall similar crystal shapes and sizes.

7.6.3 Anhydrite

In places where dolomite inclusions appear dispersed throughout anhydrite crystals, it is likely that anhydrite replaced both Dolomite I matrix crystals, as well as euhedral rimmed Dolomite II and limpid Dolomite VIII crystals. Aggregate clusters that in places have an overall vug-shape likely represent precipitation of anhydrite crystals that occurred in once-open vuggy porespace. The presence of coarse-crystalline planar-euhedral dolomite crystals that occur along the edges of aggregate cluster boundaries further suggests that the crystals were growing into open space, resulting in a planar-euhedral crystal shape. Nevertheless, anhydrite aggregate clusters in the middle Three Forks Formation are interpreted to represent late-burial anhydritization that occurred after dolomitization. This interpretation is based on abundant inclusions of early-stage fine-crystalline Dolomite I, Dolomite II crystals with varying amounts of overgrowths, as well as late-stage medium- to coarse-crystalline Dolomite VIII, disseminated throughout anhydrite crystals.

7.6.4 Pyrite

At least two episodes of pyritization took place through the diagenetic history of the middle Three Forks Formation. Rounded pyrite aggregates are interpreted herein to be pyrite framboids, which are indicative of early diagenetic pyrite formation at shallow burial depths where temperatures and pressures are relatively low (Rickard, 1970). Following the formation of framboidal pyrite, pyrite concretions as well as disseminated euhedral pyrite crystals precipitated (c.f. Raiswell and Plant, 1980).

7.6.5 Porosity

All pore types that occur throughout the middle Three Forks Formation are interpreted herein to represent secondary porosity that was created in the rock after final deposition (c.f. Choquette and Pray, 1970). Intercrystalline porosity that occurs between individual dolomite crystals, generally fine Dolomite I (“micro-intercrystalline”) and coarse Dolomite II crystals with varying amounts of cement overgrowths (“intercrystalline”), is likely the result of pore space generated due to the mole per mole dolomite replacement of calcite, as dolomite replacement of calcite generally produces up to 13% of porosity (Machel, 2005). The replacement of very fine-crystalline micritic calcite crystals by Dolomite I resulted in small, micro-intercrystalline pores. In contrast, intercrystalline pores that are associated with rimmed Dolomite II crystals are generally larger than micro-intercrystalline pores due to the overall coarse nature of Dolomite II crystals relative to matrix-selective Dolomite I crystals. Intracrystalline porosity that occurs within dolomite crystals formed as a result of dissolution of inclusions, likely low-Mg calcite (c.f. Sibley, 1982). These pores initially formed relatively early in the diagenetic history of the middle Three Forks Formation and continued to develop through the formation of Dolomite VII, as it occurs in all dolomite types except late Dolomite VIII. Moldic pore space is the result of complete dissolution of dolomite crystals due to acidification of pore waters (c.f. Machel, 2004). Based on the overall coarse size of the moldic pores, this porosity type likely formed from the dissolution of relatively coarse dolomite crystals comprised of two or more overgrowth cements. Linear dissolution pore space likely formed along linear zones of weakness that allowed acidic fluids to flow and partially dissolve adjacent dolomite crystals. This pore type formed post-compaction in the late-burial stages of the middle Three Forks Formation, as these pores have an overall undisrupted, unfolded, linear appearance.

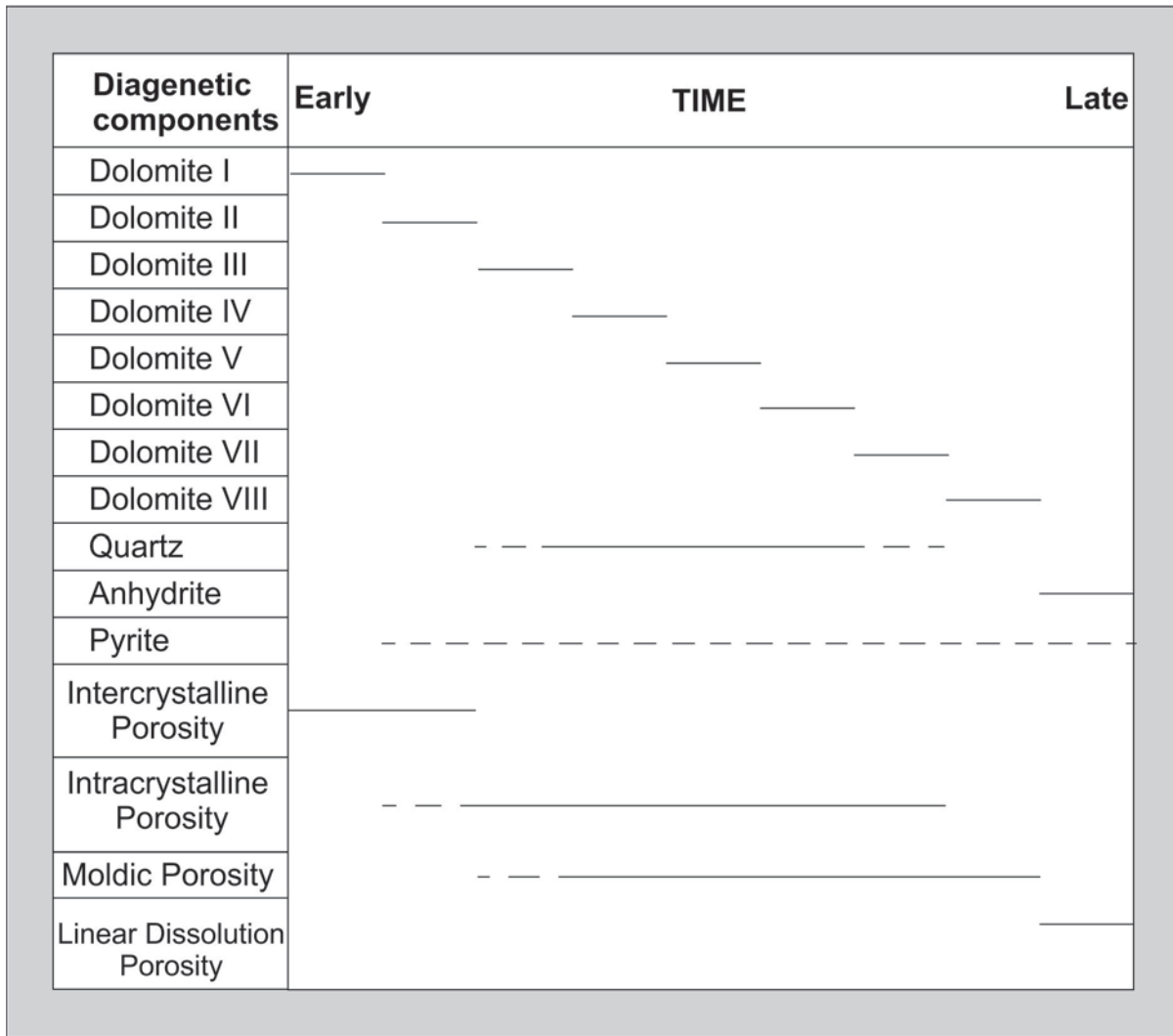


Figure 20. Relative timing of diagenetic components in the middle Three Forks Formation.

8.0 DISCUSSION

8.1 Middle Three Forks Formation Depositional Environment

In this study, the middle Three Forks Formation is interpreted as having been deposited in a permanently submerged shallow subtidal setting on a low-angle epeiric ramp, where laminated siliciclastic mudstones with silty dolostone intercalations (FA1) represent deposition in a distal mid-ramp environment, and massive to well laminated clay clast-bearing silty dolostones (FA2) reflect deposition in a proximal inner-ramp setting. In contrast, previous workers have described the Three Forks Formation as being deposited in a predominantly supratidal to intertidal setting largely based on the presence of anhydrite nodules, dissolution breccias and silt- and dolomite-filled injection dykes (c.f. Chen and Lee, 2013) that have previously been interpreted to be desiccation cracks (e.g. Dumonceaux, 1984; Berwick, 2008; Gantyno, 2010). Although supra- to intertidal features, such as evaporite beds and desiccation cracks, may be present in places in the lower Three Forks Formation, they are completely absent throughout the middle Three Forks Formation within the limits of the study area. It is assumed that the facies and facies associations identified herein represent the most distal sediments present in the middle Three Forks Formation sedimentary system based on the location of the study area approximately in its depocenter. Therefore, in order for exclusively supra- to intertidal sedimentation to occur at this location, the entire Williston Basin would have had to be drained once (diurnal) or, more likely two times (semi-diurnal) daily. However, using Hudson Bay, Canada, as a modern analog for ancient, relatively shallow epicontinental seas (c.f. Pawlak et al., 2011), the Williston basin was likely affected by semi-diurnal tide cycles where tidal range did not exceed 1 m. The possibility of flooding and draining the basin two times daily, thus depositing mostly inter- to supratidal

facies, would only have been viable if the maximum depth of the basin never exceeded 1 m. However, water depths were considerably more than 1 m, as indicated by mid-ramp clay-rich facies that represent deposition between FWWB and SWB, likely at water depths between 10-30 m (c.f. Immenhauser, 2009). Also, in order to flood and drain the entire area of the basin ($\sim 250,000 \text{ km}^2$) two times per day, the velocity of diurnal tidal waves would have needed to be exceptionally fast. Therefore, deposition of the middle Three Forks Formation within the limits of the study area most likely occurred in a permanently submerged setting, not one that was intermittently sub-aerially exposed during low- to high-tide cycles.

8.2 Halite Pseudomorphs as Indicators of Basinwide Hypersaline Conditions

The occurrence of dolomite-filled halite pseudomorphs on the interfaces of laminated mudstones with silty dolostone intercalations (FA1) suggests that salinities of the basin were significantly elevated at times during middle Three Forks Formation deposition. The halite casts, however, are exclusive to these intervals, and do not occur in units that consist only of massive to well laminated clay clast-bearing silty dolostones (FA2). It is likely that halite crystals also precipitated in these “clean” dolomite intervals without mudstone intercalations, yet the pseudomorphs are not preserved because (1) dolomite-filled casts of halite in silty dolostone beds are less likely to be recognized and not as profound as in mudstones, and (2) halite crystals were likely more prone to being reworked under relatively high-energy inner-ramp conditions, than those typical in an overall low-energy mid-ramp setting. Nevertheless, the formation of halite pseudomorphs, such as those observed in the middle Three Forks Formation, has traditionally been interpreted as occurring in playa lakes and restricted lagoons protected by carbonate rims or barriers, where rapid evaporation rates result in the formation of dense supersaturated brines (c.f. Rouchy et al., 2001; Martill et al., 2007). Despite the fact that the

middle Three Forks Formation is herein interpreted to have been deposited on a shallow-dipping epeiric ramp where no evidence of a carbonate rim or barrier exists that may have restricted the basin, it must have been partly cut off from the open ocean by a barrier-like feature in order to precipitate halite (c.f. Gornitz and Schreiber, 1981; Rouchy et al., 2001). It is therefore most likely that the enclosure of the Williston basin during late Devonian times may be attributed to a tectonic influence, likely flexural deformation of the lithosphere related to the late Devonian Antler Orogeny. Although the effects of the Antler Orogeny on the foreland areas to the east of the Antler allochthon are poorly understood (Dorobek et al., 1991), it is possible that flexural deformation associated with compressional forces related to the advancement of the Antler orogenic wedge led to areas of uplift to the east of the allochthon adjacent to the eastern portion of the foredeep. A relative sea-level drop concurrent with the uplifted swell between the Williston basin and the Antler foredeep may have resulted in isolation of the basin, and therewith to the transition from a normal marine to restricted marine environment. Abundant unconformities throughout the Three Forks Formation in Montana further suggests that this area was intermittently subaerially exposed during times of uplift and contemporaneous relative sea-level fall (c.f. Dorobek et al., 1991). A similar interpretation has been applied to the middle Devonian-aged Prairie Formation: slight regional uplift coupled with accelerated downwarping of the basin led to restriction of the basin, resulting in anhydrite and halite precipitation at the center, or most distal parts, of the basin (Sandberg, 1961).

8.3 Middle Three Forks Formation Dolomitization Model

The middle Three Forks Formation is exclusively comprised of secondary dolomite, both replacement dolomite and dolomite cement, that likely formed during relatively shallow burial at or just below the sediment-water interface in an overall shallow subtidal setting. The

conventional interpretation of relatively shallow-burial dolomitization processes is based largely on the comparison of ancient dolomites with modern evaporative and sabkha dolomites formed in supratidal settings, such as the Persian Gulf, the Bahamas and Florida (e.g. Illing et al., 1965; Shinn et al., 1965; Carballo et al., 1986). In these types of settings evaporation is the driving mechanism, where Mg-rich brines form over time as the Ca/Mg ratio decreases as a result of sulphates (e.g. gypsum) and other evaporite minerals (e.g. halite) precipitating out of solution (Folk and Land, 1975). Based on the close relationship of dolomite and evaporites observed in these dolomitization models, Friedman (1980) proposed that dolomite be considered an evaporite mineral. Nevertheless, no evidence exists throughout the middle Three Forks Formation in the study area that suggests that deposition occurred in a supratidal sabkha setting. Therefore, shallow-burial dolomitization of the middle Three Forks Formation is envisioned to have occurred by the reflux of hypersaline marine waters driven by dense brines that penetrated through shallow carbonate strata (c.f. Vandeginste et al., 2006, 2009; Qing et al., 2001; Rott and Qing, 2013). Based on the presence of halite pseudomorphs, as well as the overall low diversity of ichnofauna throughout the middle Three Forks Formation, seawater salinities must have been elevated frequently during deposition of the unit. Following the reflux model, the dense Mg-rich brine seeped through underlying carbonate strata, moving along the regional slope down-dip, while displacing marine pore waters of lower density. As a result of the relatively high amounts of Mg^{2+} ions in the brine solution, dolomite began to replace thermodynamically metastable fine-crystalline calcite matrix (c.f. Machel, 2004; Rott and Qing, 2013). Nevertheless, this process was likely followed by multiple episodes of dolomite formation via burial processes such as compaction flow or thermal convection (c.f. Machel, 2004), based on the eight stages of

dolomite observed in this study, as well as the complete lack of calcite throughout the middle Three Forks Formation succession.

8.4 Debris and Mud-Flow Deposits as Indicators of Variations in Climate During Deposition of the Middle Three Forks Formation

As shown in this study, matrix-supported conglomerates with dolomite and clay clasts (FA3) tend to occur more frequently in stratigraphic Intervals 0, 2, and 4 than they do in Intervals 1 and 3 of the middle Three Forks Formation. The fact that the frequency of debris flow deposits fluctuates between stratigraphic intervals in the succession suggests a triggering mechanism that acted in a recurring manner over time. Based on previous studies that involve a positive correlation between debris flow frequency and rainfall duration and intensity (e.g. Anderson and Sitar, 1995; Guzzetti et al., 2007), fluctuating humid versus arid climate conditions are the likely driving mechanism behind the occurrence and non-occurrence of debris flow deposits throughout the middle Three Forks Formation. These so-called “rainfall-induced debris flows” are essentially slope failures that initiate due to a reduction of confining stress as a result of increased pore-water pressures during or after periods of intense rainfall (Anderson and Sitar, 1995). Initiation of slope failures is envisioned to have occurred in places with relatively steep gradients adjacent to the basin in areas either associated with the forebulge where slumps likely formed, or toward the southeast of the basin where the Transcontinental Arch was active in late Devonian times (c.f. Peterson and MacCary 1987; LeFever, 1992). Based on the frequency of these rainfall-induced debris flows, stratigraphic intervals that are dominated by FA3 rocks (Intervals 0, 2, and 4) likely represent periods of time in which climate was overall humid with frequently-occurring, intense episodes of rainfall that resulted in shallow slope failures (c.f. Anderson and Sitar, 1995). In contrast, the rare occurrence of FA3 rocks throughout Intervals 1

and 3 suggests that these stratigraphic intervals reflect times of generally arid climate conditions with little precipitation. The presence of halite pseudomorphs in Interval 1 further supports this interpretation, because the precipitation of halite requires high evaporation rates coupled with an overall arid climate where influx of meteoric waters is relatively low (c.f. Rouchy et al, 2011). However, reworking of previously broken-up dolomite and clay horizons may also have occurred on slightly elevated zones within the basin itself, as evidenced by the distribution of FA3 deposits throughout the basin, rather than exclusively adjacent to the Antler forebulge and Transcontinental Arch to the west and southeast. The occurrence of abundant slumps in the middle member of the Bakken Formation, the unit directly overlying the Three Forks Formation, suggests that local highs were present throughout the basin during deposition of the middle Bakken member (c.f. Egenhoff et al., 2011; Simenson et al., 2011). The fact that the Three Forks Formation exhibits similar lateral thickness trends as the overlying Bakken Formation (c.f. LeFever, 2008; Simenson et al., 2011), indicates that areas of relief that existed at the time the middle Bakken member was deposited were also present during middle Three Forks Formation deposition. In this case, debris flows may not only have originated from two distinct areas to the west and the southeast of the basin, but also within the basin itself in places of topographic relief, resulting in a basinwide distribution of these deposits throughout the middle Three Forks Formation.

8.5 Lateral Distribution of Dolomitic Pay Zones: Implications for Petroleum Exploration

Based on high recovery factors of wells drilled into the upper Three Forks Formation in the North Dakota portion of the Williston Basin, an evaluation of the potential reservoir quality of the middle Three Forks Formation adds to the understanding of the Bakken-Three Forks petroleum system in this area. Maps showing the spatial distribution of average visible

porosities for twenty cored wells in the study area, combined with thickness maps of net pay intervals illustrate reservoir areas, or “sweet spots,” to potentially target in the middle Three Forks Formation in Mountrail, McKenzie, and Williams counties, North Dakota.

Traditionally, dolomite successions have been associated with overall good reservoir qualities because of enhanced permeabilities and improved porosities that develop during dolomitization of pre-existing limestones (Sun, 1995). In fact, dolomite reservoirs account for approximately 80% of recoverable oil and gas volumes in carbonate plays in North America (Zenger et al., 1980). Therefore, pay intervals in the middle Three Forks Formation are defined herein as clay-poor massive to well laminated clay clast-bearing silty dolostones (FA2). These rock types generally have higher porosities than laminated siliciclastic mudstones with silty dolostone intercalations (FA1) and mud-rich conglomerates with dolomite and clay clasts (FA3). Based on detailed core-logging of twenty-two drill cores, pay intervals are less than one foot thick in places, therefore a thickness cutoff is not applied in the definition of pay. Three distinct stratigraphic net pay zones that are laterally correlative are identified in the middle Three Forks succession (Figure 21). Isopach maps of net pay intervals throughout the middle Three Forks Formation within the study area are presented herein based on well logs from ninety-nine wells across Williams, McKenzie, and Mountrail counties, North Dakota, including the twenty-two wells from which core data is available (Figures 22, 23, 24).

Well Number: 17096
 Operator: Fidelity Exploration Company
 Well: Farhart 11-11H
 County, State: Mountrail County, North Dakota

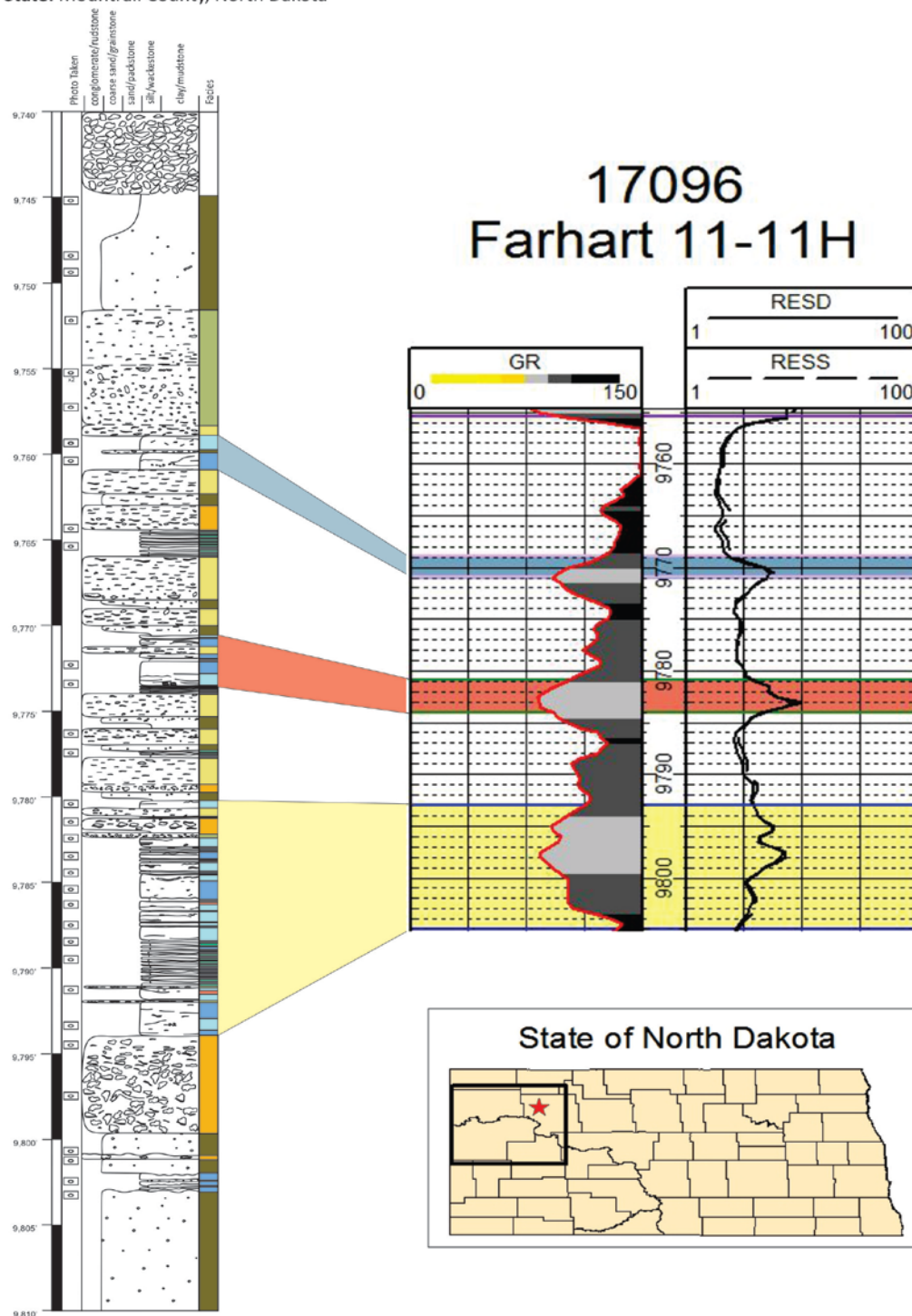


Figure 21. Type core (left) and corresponding gamma ray and resistivity logs (right) showing three distinct pay zones throughout the middle Three Forks Formation. Pay zone 1 is shown in blue, pay zone 2 in red, and pay zone 3 in yellow. Well location is shown on the index map (red star) in the study area (black box). Depths of core and well log are both in feet.

Pay Zone 1 Isopach

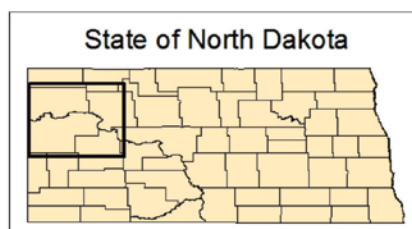
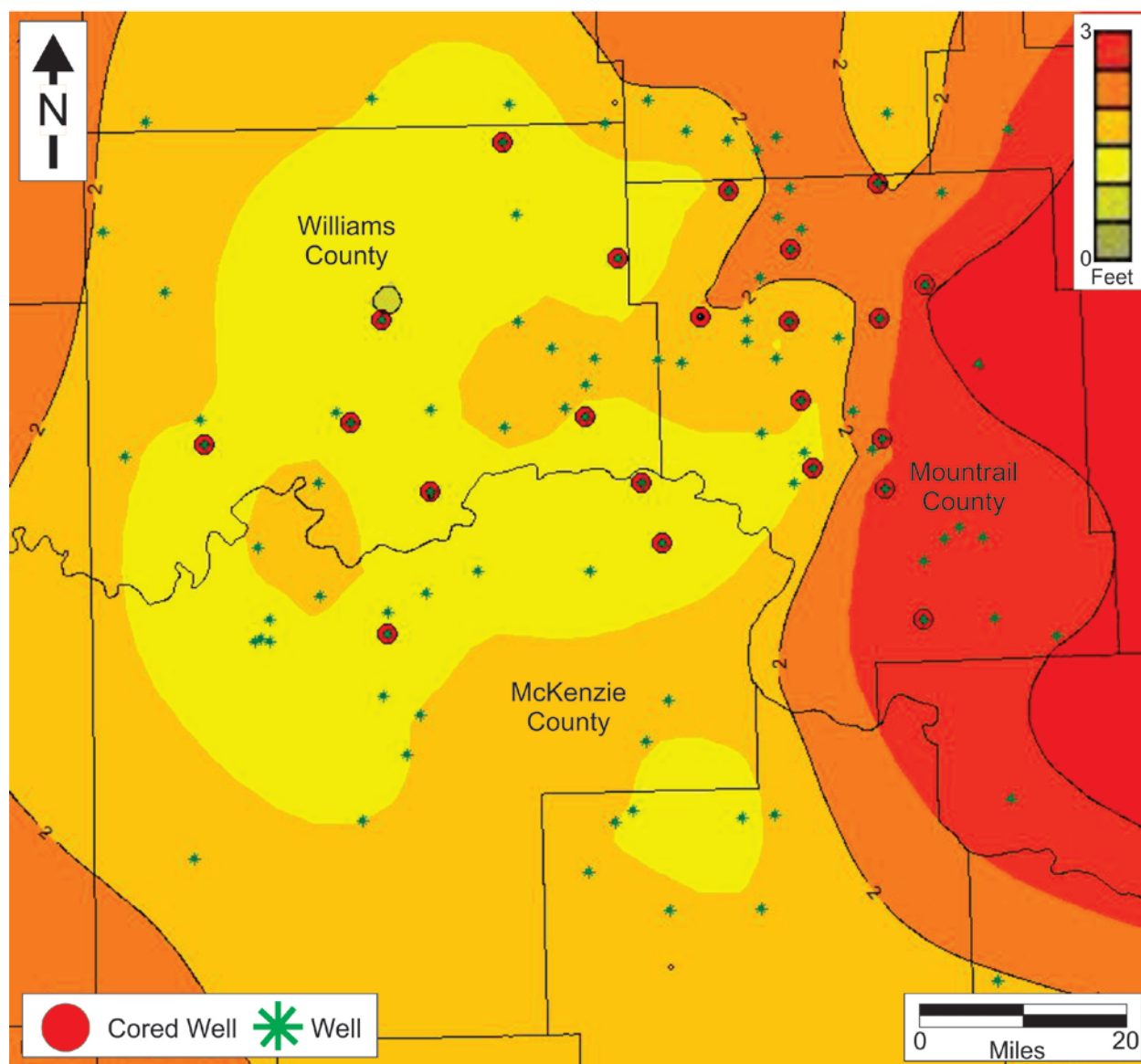


Figure 22. Isopach map of pay zone 1 throughout the study area (black box on index map).

Pay Zone 2 Isopach

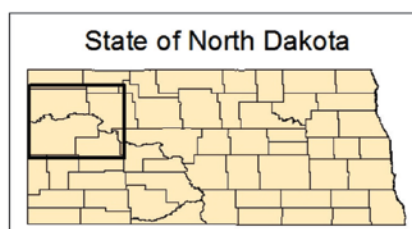
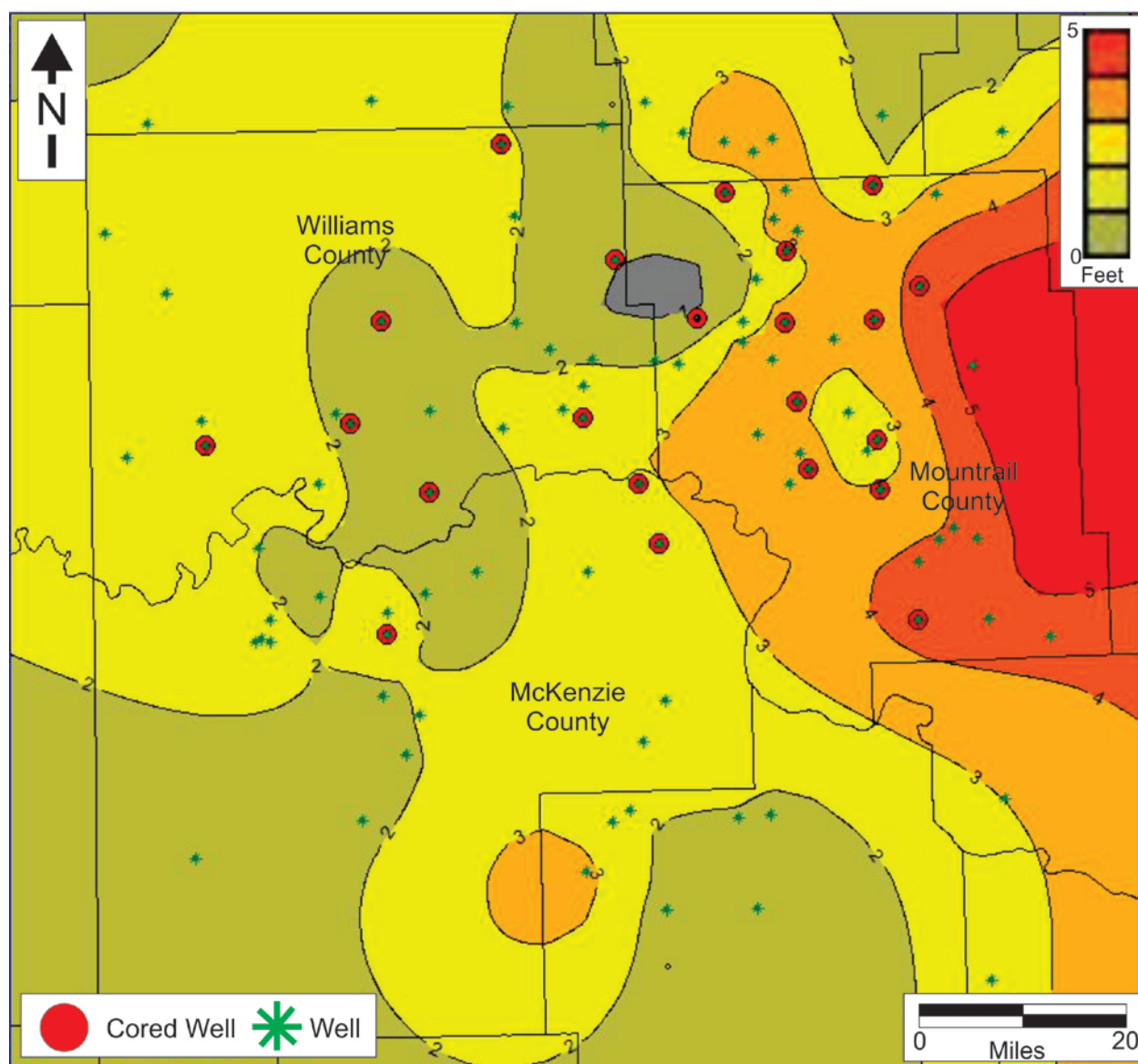


Figure 23. Isopach map of pay zone 2 throughout the study area.

Pay Zone 3 Isopach

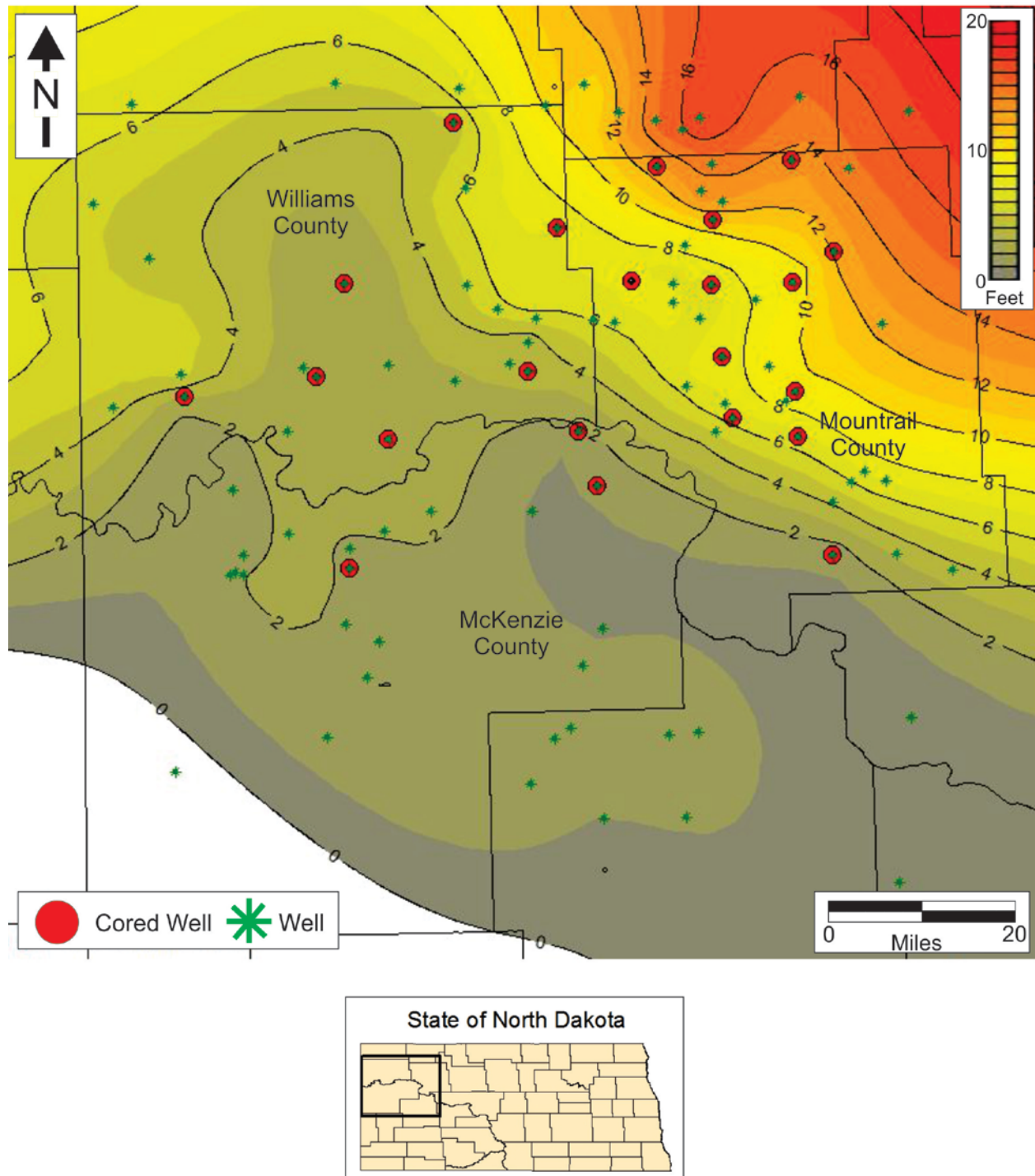


Figure 24. Isopach map of pay zone 3 throughout the study area.

Net pay zones in the middle Three Forks Formation range from less than one foot to approximately 18 ft. For this reason, an isopach map showing the cumulative thickness of these units, or gross thickness, is likely the best indicator of where the highest amounts of FA2 pay zones are located within the limits of the study area. Although many FA2 rocks represent areas of moderate reservoir quality because of their overall low clay content, high amounts of pore-occluding dolomite cement has heavily affected both porosity and permeability of these rock types. Therefore, combining gross pay thickness with average porosity data compiled from point-counting of representative thin sections provides a more accurate spatial distribution of reservoir quality throughout the middle Three Forks Formation. These data are presented as a gross pay isopach map overlain by average porosity values (Figure 25).

The gross pay isopach with average porosity map illustrates the spatial distribution of a somewhat localized “sweet spot,” or area with the most favorable reservoir characteristics and highest potential to produce economically, in central to northern Mountrail County, toward the northeast portion of the study area. Core data are consistent with these results, as this area appears to contain fewer amounts of clay-rich debris flow deposits that would act as barriers to the flow of hydrocarbons, if in fact hydrocarbons are present. Nevertheless, average visible porosity values of the middle Three Forks Formation are relatively low, rarely exceeding 3%, and pore connectivity is generally poor. Therefore, caution in interpreting these data as a “sweet spot” is necessary due to the overall poor reservoir characteristics, as well as the complete lack of evidence of hydrocarbons (i.e. dead oil) throughout the middle Three Forks succession.

Gross Pay Isopach With Average Porosity

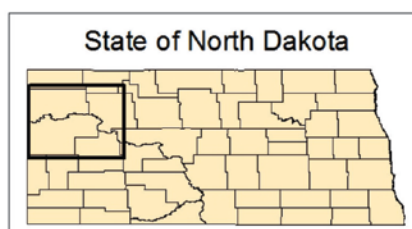
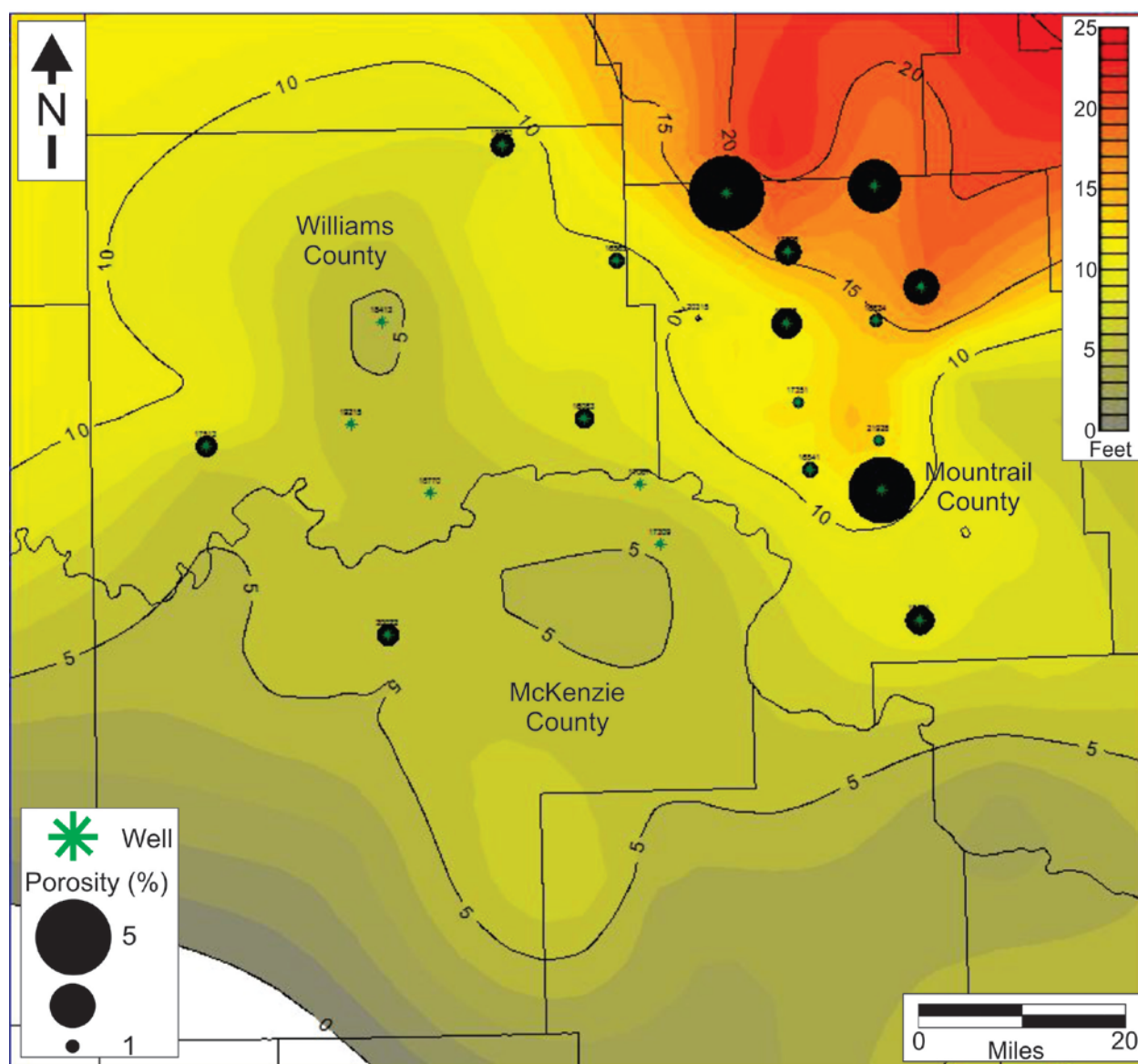


Figure 25. Isopach map of gross pay overlain with average porosity values represented by relatively-sized bubbles throughout the study area.

9.0 CONCLUSIONS

1. The middle Three Forks Formation consists of ten mixed carbonate-siliciclastic facies that are grouped into the following three facies associations: laminated siliciclastic mudstone with silty dolostone intercalations (FA1), massive to well laminated clay clast-bearing silty dolostone (FA2), and mud-rich conglomerate with dolomite and clay clasts (FA3).
2. The middle Three Forks Formation succession is comprised of up to six coarsening-upward sequences characterized by laminated siliciclastic mudstones with silty dolostone intercalations (FA1) at the base that grade into massive to well laminated clay clast-bearing silty dolostones (FA2) at the top. Each of these coarsening-upward sequences defines one shallowing-upward parasequence. Throughout the study area, varying amounts of mud-rich conglomerates with dolomite and clay clasts (FA3) are intercalated into coarsening-upward units.
3. The middle Three Forks Formation can be subdivided into five distinct stratigraphic zones termed Intervals 0-4. These intervals mark regional facies changes from units dominated by mud-rich conglomerates with dolomite and clay clasts (FA3) (Intervals 0, 2 and 4) to intervals comprised of mostly laminated siliciclastic mudstones with silty dolostone intercalations (FA1) and massive to well laminated clay clast-bearing silty dolostone (FA2) with little to no FA3 deposits (Intervals 1 and 3).
4. Coarsening-upward units in the middle Three Forks Formation represent parasequences that show a distinct fine-grained facies architecture, which can be correlated for up to 200 km across the study area. Intervals 0, 2, and 4 were deposited in an overall humid climate in which delivery of mud-rich conglomerates with dolomite and clay clasts (FA3) to the basin was

frequent due to high amounts of rainfall. In contrast, deposition of Intervals 1 and 3 occurred under arid climate conditions in which evaporation rates were high, resulting in precipitation of halite pseudomorphs throughout the basin and little to no mud-rich conglomerates with dolomite and clay clasts (FA3).

5. The middle Three Forks Formation consists of wide facies belts deposited on a mixed carbonate-siliciclastic ramp. Laminated siliciclastic mudstones intercalated with silty dolostones reflect deposition in an overall low-energy mid-ramp environment just below FWFB and above SWB that experienced frequent reworking by storms. In contrast, clay-poor laminated to massive silty dolostones represent deposition in a relatively high-energy inner-ramp setting above FWFB. Debrites and mud-flow deposits occur in both inner-ramp and mid-ramp settings throughout the basin, but overall increase in abundance toward proximal inner ramp areas toward the basin margins.

6. Diagenetic phases of the middle Three Forks Formation include: at least eight stages of dolomite, anhydrite precipitation and replacement of dolomite, silicification resulting in diagenetic quartz rhombs, pyrite framboids, concretions and disseminated euhedral pyrite crystals, as well as micro-intercrystalline, intercrystalline, intracrystalline, moldic, and linear dissolution porosity.

7. A potential sweet spot is located in the northeast portion of the study area, where gross pay thickness is approximately 10-20 feet and average porosities per well ranges from 3-5%. Economic potential of this area should be further evaluated, as pore connectivity is overall low and pore-occluding dolomite and anhydrite cements are ubiquitous throughout the middle Three Forks succession.

REFERENCES

- Al-Aasm, I.S., and Packard, J.J., 2000, Stabilization of early-formed dolomite: A tale of divergence from two Mississippian dolomites: *Sedimentary Geology*, v. 131, p. 97-108.
- Anderson, S.A., and Sitar, N., 1995, Analysis of rainfall-induced debris flows: *Journal of Geotechnical Engineering*, v. 121, p. 544-552.
- Anna, L.O., 2011, Assessment of undiscovered oil and gas resources of the Williston Basin Province of North Dakota, Montana, and South Dakota, 2010: U.S. Geological Survey Digital Data Series 69-W, 76 p.
- Baillie, A.D., 1955, Devonian system of Williston basin: *American Association of Petroleum Geologists Bulletin*, v. 39, p. 575-629.
- Berwick, B., 2008, Depositional environments, mineralogy, and sequence stratigraphy of the late Devonian Sanish member (upper Three Forks Formation), Williston Basin, North Dakota: Master's thesis, Colorado School of Mines, 262 p.
- Bottjer, R.J., Sterling, R., Grau, A., Dea, P., 2011, Stratigraphic relationships and reservoir quality at the Three Forks-Bakken unconformity, Williston Basin, North Dakota, *in* L. Robinson, J. LeFever, and S. Gaswirth, eds., *Bakken-Three Forks Petroleum System in the Williston Basin: Rocky Mountain Association of Geologists guidebook*, p. 173-228.
- Buatois, L.A., and Mángano, M.G., 2011, *Ichnology: Organism-substrate interactions in space and time*: Cambridge University Press, 358 p.
- Burchette, T.P., and Wright, V.P., 1992, Carbonate ramp depositional systems: *Sedimentary Geology*, v. 79, p. 3-57.
- Carballo, J.D., Land, L.S., and Miser, D.E., 1986, Holocene dolomitization of supratidal sediments by active tidal pumping, Sugarloaf Key, Florida: *Journal of Sedimentary Petrology*, v. 52, p. 153-165.
- Christopher, J.E., 1961, Transitional Devonian-Mississippian formations of southern Saskatchewan: Saskatchewan Department of Mineral Resources, Report No. 66, 103 p.
- Chen, J., and Lee, H.S., 2013, Soft-sediment deformation structures in Cambrian siliciclastic and carbonate storm deposits (Shandong Province, China): Differential liquefaction and fluidization triggered by storm-wave loading: *Sedimentary Geology*, v. 288, p. 81-94.
- Choquette, P.W., and Pray, L.C., 1970, Geologic nomenclature and classification of porosity in sedimentary carbonates: *American Association of Petroleum Geologists Bulletin*, v. 54, p. 207-250.

- Clifton H.E., Hunter, R.E., and Phillips, R.L., 1971, Depositional structures and processes in the non-barred high-energy nearshore: *Journal of Sedimentary Petrology*, v. 41, p. 651-670.
- Cornish, F.G., 1986, The trace-fossil *Diplocraterion*: Evidence of animal-sediment interactions in Cambrian tidal deposits: *Society of Economic Paleontologists and Mineralogists Research Report*, v. 1, p. 478-491.
- Decima, A., McKenzie, J.A., and Schreiber, B.C., 1988, The origin of “evaporative” limestones: An example from the Messinian of Sicily (Italy): *Journal of Sedimentary Geology*, v. 58, p. 256-272.
- Demicco, R.V., and Hardie, L.A., 1994, Sedimentary structures and early diagenetic features of shallow marine carbonate deposits: *Society of Economic Paleontologists and Mineralogists Atlas Series 1*, 265 p.
- Dorobek, S.L., Reid, S.K., Elrick, M., Bond, G.C., and Kominz, M.A., 1991, Subsidence across the Antler foreland of Montana and Idaho: Tectonic versus eustatic effects: *Kansas Geological Survey Bulletin*, v. 233, p. 231-251.
- Dumonceaux, G. M., 1984, Stratigraphy and depositional environments of the Three Forks Formation (upper Devonian), Williston Basin, North Dakota: Master’s thesis, The University of North Dakota, 114 p.
- Duringer, P., and Vecsei, A., 1998, Middle Triassic shallow-water limestones from the upper Muschelkalk of eastern France: The origin and depositional environment of some early Mesozoic fine-grained limestones: *Sedimentary Geology*, v. 121, p. 57-70.
- Einsele, G., 2000, Sedimentary basins: Evolution, facies and sediment budget, 2nd edition: Springer-Verlag, Berlin, Heidelberg, New York, 628 p.
- Egenhoff, S.O., Jaffri, A., Medlock, P., 2011, Climate control on reservoir distribution in the Upper Devonian Three Forks Formation, North Dakota and Montana: *American Association of Petroleum Geologists Bulletin Search and Discovery (Abstract) #90124*. <http://www.searchanddiscovery.com/abstracts/html/2011/annual/abstracts/Egenhoff2>
- Egenhoff, S.O., and Fishman, N.S., 2013, Sedimentology of the upper Bakken shale member, North Dakota, USA, *Journal of Sedimentary Research*, v. 83, p. 803-824.
- Fisher, R.V., and Mattinson, J.M., 1968, Wheeler gorge turbidite-conglomerate series, California; inverse grading: *Journal of Sedimentary Petrology*, v. 38, p. 1013-1023.
- Flügel, E., 2004, Microfacies of carbonate rocks: Analysis, interpretation, and application: Springer, Heidelberg, 976 p.
- Folk, R.L., and Land, L.S., 1975, Mg/Ca ratio and salinity: Two controls over crystallization of dolomite: *American Association of Petroleum Geologists Bulletin*, v. 59, p. 60-68.

- Friedman, G.M., 1965, Terminology of crystallization textures and fabrics in sedimentary rocks: *Journal of Sedimentary Petrology*, v. 35, p. 643-655.
- Friedman, G.M., 1980, Dolomite is an evaporite mineral: Evidence from the rock record and from sea-marginal ponds of the Red Sea: *Society of Economic Paleontologists and Mineralogists Special Publication*, v. 28, p. 69-80.
- Gantyno, A., 2010, Sequence stratigraphy and microfacies analysis of the late Devonian Three Forks Formation, Williston Basin, North Dakota and Montana, U.S.A: Master's thesis, Colorado School of Mines, 201 p.
- Gerhard, L.C., Anderson, S.B., and Fischer D.W., 1990, Petroleum geology of the Williston Basin: *American Association of Petroleum Geologists Memoir* 51, v. 51, p. 507-559.
- Gornitz, V.M., and Schreiber, B.C., 1981, Displacive halite hoppers from the Dead Sea: Some implications for ancient evaporite deposits: *Journal of Sedimentary Petrology*, v. 51, p. 787-794.
- Guzzetti, F., Peruccacci, S., Rossi, M., and Stark, C.P., 2007, The rainfall intensity-duration control of shallow landslides and debris flows: An update: *Landslides*, v. 5, p. 3-17.
- Harms, J.C., Southard, J., Spearing, D.R., Walker, R.G., 1975, Depositional environments as interpreted from primary sedimentary and stratification sequences: *Society of Economic Paleontologists and Mineralogists short course notes* 2, 161 p.
- Houghton, P., Davis, C., McCaffrey, W., and Barker, S., 2009, Hybrid sediment gravity flow deposits – Classification, origin and significance: *Marine and Petroleum Geology*, v. 26, p. 1900-1918.
- Heck, T.J., LeFever, R.D., Fischer, D.W., LeFever, J., 2002, Overview of the petroleum geology of the North Dakota Williston Basin, Bismarck: *North Dakota Geological Survey*. <https://www.dmr.nd.gov/ndgs/Resources/>
- Illing, L.V., Wells, A.J., and Taylor, J.C.M., 1965, Penecontemporary dolomite in the Persian Gulf: *Society of Economic Paleontologists and Mineralogists Special Publication*, v. 13, p. 89-111.
- Immenhauser, A., 2009, Estimating palaeo-water depth from the physical rock record: *Earth-Science Reviews*, v. 96, p. 107-139.
- Jaglarz, P., and Uchman, A., 2010, A hypersaline ichnoassemblage from the middle Triassic carbonate ramp of the Tatricum domain in the Tatra Mountains, Southern Poland: *Palaeogeography, Palaeoclimatology, Palaeoecology*, v. 292, p. 71-81.
- Kendall, C.G.S.T., and Warren, J., 1987, A review of the origin and setting of tepees and their associated fabrics: *Sedimentology*, v. 34, p. 1007-1027.

- Kent, D.M., and Christopher, J.E., 1994, Geological history of the Williston Basin and the Sweetgrass Arch, *in* Geological Atlas of Western Canada. Mossop, G.D. and Shetson, I. (comps.): Canadian Society of Petroleum Geologists and Alberta Research Council, p. 421-430.
- LeFever, J. A., 2008, Isopach of the Three Forks Formation: North Dakota Geological Survey, Geologic Investigations no. 64, scale 1:1,000,000.
- LeFever, J.A., Martiniuk, C.D., Dancsok, E.F.R., Mahnic, P.A., 1991, Petroleum potential of the middle member, Bakken Formation, Williston Basin, *in* W.B. Hansen, ed., 1991 Guidebook to Geology and Horizontal Drilling of the Bakken Formation: Montana Geological Society, Billings, Montana, p. 74-94.
- Levi, T., Weinberger, R., Aïfa, T., Eyal, Y., Marco, S., 2006, Earthquake-induced clastic dikes detected by anisotropy of magnetic susceptibility: *Geology*, v. 34, p. 69-72.
- Machel, H.G., 2004, Concepts and models of dolomitization: A critical reappraisal: Geological Society of London, Special Publication, v. 235, p. 7-63.
- Machel, H.G., 2005, Dolomites, *in* R.C. Selley, R. Cocks, and I.R. Pilmer, eds., *Encyclopedia of Geology*, p. 79-94.
- Major, J.T., 1997, Depositional processes in large-scale debris-flow-experiments: *The Journal of Geology*, v. 105, p. 345-366.
- Maliva, R.G., and Siever, R., 1990, Influences of dolomite precipitation on quartz surface textures: *Journal of Sedimentary Petrology*, v. 60, p. 820-826.
- Marr, J.G., Harff, P.A., Shanmugam, G., and Parker, G., 2001, Experiments on subaqueous sandy gravity flows: The role of clay and water content in flow dynamics and depositional structures: *Geological Society of America Bulletin*, v. 113, p. 1377-1386.
- Martill, D.M., Loveridge, R., and Heimhofer, U., 2007, Halite pseudomorphs in the Crato Formation (early Cretaceous, late Aptian-early Albian), Araripe Basin, northeast Brazil: Further evidence for hypersalinity: *Cretaceous Research*, v. 28, p. 613-620.
- Mount, J.F., 1984, Mixing of siliciclastic and carbonate sediments in shallow shelf environments: *Geology*, v. 12, p. 432-435.
- Mount, J.F., 1985, Mixed siliciclastic and carbonate sediments: A proposed first-order textural and compositional classification: *Sedimentology*, v. 32, p. 435-442.
- Naylor, M.A., 1980, The origin of inverse grading in muddy debris flow deposits – A review: *Journal of Sedimentary Petrology*, v. 50, p. 1111-1116.
- Nekhorosheva, V., 2011, Stratigraphy, diagenesis and fracture characterization of the upper

- Devonian Three Forks Formation in Montana, Wyoming and South Dakota: Master's thesis, Colorado School of Mines, 102 p.
- Niedoroda, A.W., Reed, C.W., Das, H., Hatchett, L., 2007, The general behavior of mass gravity flows in the marine environment, *in* V. Lykousis, D. Sakellariou, and J. Locat, eds., *Submarine Mass Movements and Their Consequences*, p. 111-118.
- Nordeng, S. H., and Helms, L.D., 2010, Bakken Source System Three Forks Formation Assessment: North Dakota Department of Mineral Resources, 22 p.
- Nordeng, S.H., and LeFever, J.A., 2009, Three Forks Formation log to core correlation: North Dakota Geological Survey Geologic Investigations No. 75, 1 plate.
- North Dakota Department of Mineral Resources, 2013, Bakken Horizontal Wells by Zone: <https://www.dmr.nd.gov/oilgas/bakkenwells.asp>
- Pawlak, A., Eaton, D.W., Bastow, I.D., Kendall, J.M., Helffrich, G.G., Wookey, J., and Snyder, D., 2011, Crustal structure beneath Hudson Bay from ambient-noise tomography: implications for basin formation: *Geophysical Journal International*, v. 184, p. 65-82.
- Peterson, J. A., and MacCary, L.M., 1987, Regional Stratigraphy and General Petroleum Geology of the U.S. Portion of the Williston Basin and Adjacent Areas, *in* M.W. Longman, ed., *Williston Basin: Anatomy of a Cratonic Oil Province: Rocky Mountain Association of Geologists Symposium*, Denver, Colorado, p. 9-43.
- Pitman, J.K., Price, L.C., LeFever, J.A., 2001, Diagenesis and fracture development in the Bakken Formation, Williston Basin: Implications for reservoir quality in the middle member: *United States Geological Survey Professional Paper* 1653, 19 p.
- Qing, H., Bosence, D.W.J., and Rose, E.P.F., 2001, Dolomitization by penesaline sea water in early Jurassic peritidal platform carbonates, Gibraltar, western Mediterranean: *Sedimentology*, v. 48, p. 153-163.
- Raiswell, R., and Plant, J., 1980, The incorporation of trace elements into pyrite during diagenesis of black shales, Yorkshire, England: *Economic Geology*, v. 75, p. 684-699.
- Randazzo, A.F., and Zachos, L.G., 1983, Classification and description of dolomitic fabrics of rocks from the Floridan aquifer, U.S.A.: *Sedimentary Geology*, v. 37, p. 151-162.
- Reineck, H.-E., and Singh, I.B., 1973, *Depositional sedimentary environments*: Springer-Verlag, Berlin, 439 p.
- Rickard, D.T., 1970, The origin of framboids: *Lithos*, v. 3, p. 269-293.
- Rott, C.M., and Qing, H., 2013, Early dolomitization and recrystallization in shallow marine carbonates, Mississippian Alida beds, Williston Basin (Canada): Evidence from

- petrography and isotope geochemistry: *Journal of Sedimentary Research*, v. 83, p. 928-941.
- Rouchy, J.M., Taberner, C., and Peryt, T.M., 2001, Sedimentary and diagenetic transitions between carbonates and evaporates: *Sedimentary Geology*, v. 140, p. 1-8.
- Sandberg, C. A., and Hammond, C.R., 1958, Devonian system in Williston basin and central Montana: *American Association of Petroleum Geologists Bulletin*, v. 42, p. 2293-2333.
- Sandberg, C.A., 1961, Distribution and thickness of Devonian rocks in Williston basin and in central Montana and north-central Wyoming: *Geological Survey Bulletin* 1112-D, p. 105-127.
- Schieber, J., 1998, Sedimentary features indicating erosion, condensation, and hiatuses in the Chattanooga shale of central Tennessee: Relevance for sedimentary and stratigraphic evolution, *in* J. Scheiber, W. Zimmerle, and P. Sethi, eds., *Shales and Mudstones* (v. 1): Basin Studies, Sedimentology and Paleontology, Schweizerbart'sche Verlagsbuchhandlung, Stuttgart, p. 187-215.
- Shinn, E.A., Ginsburg, R.N., and Lloyd, R.M., 1965, Recent supratidal dolomite from Andros Island, Bahamas, *in* L.C. Pray and R.C. Murray eds., *Dolomitization and limestone diagenesis*: Society of Economic Paleontologists and Mineralogists Special Publication, v. 13, p. 112-123.
- Shinn, E.A., 1983, Birdseyes, fenestrae, shrinkage pores, and loferites: A reevaluation: *Journal of Sedimentary Petrology*, v. 53, p. 619-628.
- Sibley, D.F., 1982, The origin of common dolomite fabrics: Clues from the Pliocene: *Journal of Sedimentary Petrology*, v. 52, p. 1087-1100.
- Sibley, D.F., and Gregg, J.M., 1987, Classification of dolomite rock textures: *Journal of Sedimentary Petrology*, v. 57, p. 967-975.
- Sims, J.D., 2012, Earthquake-induced load casts, pseudonodules, ball-and-pillow structures, and convolute lamination: Additional deformation structures for paleoseismic studies, *in* R.T. Cox, M.P. Tuttle, O.S. Boyd, J. and Locat, eds., *Recent Advances in North American Paleoseismology and Neotectonics East of the Rockies*: Geological Society of America Special Paper 493, p. 191-201.
- Smith, M.G., and Bustin, R.M., 2000, Late Devonian and Early Mississippian Bakken and Exshaw black shale source rocks, Western Canada sedimentary basin; a sequence stratigraphic interpretation: *American Association of Petroleum Geologists Bulletin*, v. 84, p. 940-960.
- Sonnenberg, S.A., and Pramudito, 2009, Petroleum geology of the giant Elm Coulee field, Williston Basin: *American Association of Petroleum Geologists Bulletin*, v. 93, p. 1127-1153.

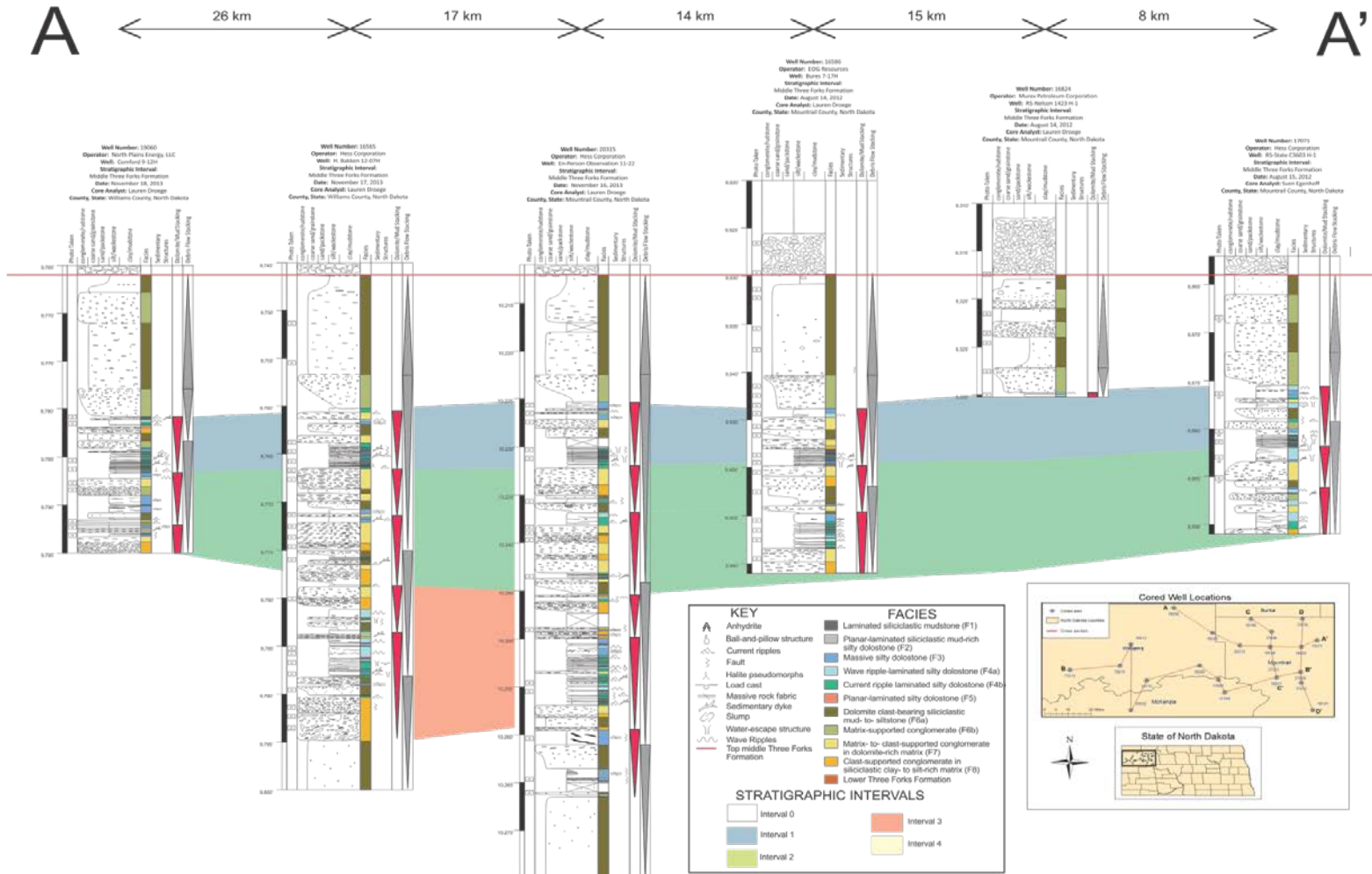
- Sun, S.Q., 1995, Dolomite reservoirs: Porosity evolution and reservoir characteristics: American Association of Petroleum Geologists Bulletin, v. 79, p. 186-204.
- Talling, P.J., Wynn, R.B., Masson, D.G., Frenz, M., Cronin, B.T., Schiebel, R., Akhmetzhanov, A.M., Dallmeier-Tiessen, S., Benetti, S., Weaver, P.P.E., Georgeiopolou, A., Zuhlsdorff, C., and Amy, L.A., 2007, Onset of submarine debris flow deposition far from original giant landslide: *Nature*, v. 450, p. 541-544.
- Talling, P.J., Malgesini, G., Sumner, E.J., Amy, L.A., Felletti, F., Blackbourn, G., Nutt, C., Wilcox, C., Harding, I.C., and Akbari, S., 2012, Planform geometry, stacking pattern, and extrabasinal origin of low strength and intermediate strength cohesive debris flow deposits in the Marnoso-arenacea Formation, Italy: *Geosphere*, v. 8, p. 1207-1230.
- Tucker, M., 1982, Storm-surge sandstones and the deposition of interbedded limestone; late Precambrian, southern Norway, *in* G. Einsele and A. Seilacher, eds., *Cyclic and Event Stratification*, Berlin, Springer-Verlag, p. 363-370.
- Webster, R.L., 1984, Petroleum source rocks and stratigraphy of Bakken Formation in North Dakota: American Association of Petroleum Geologists Bulletin, v. 68, p. 953.
- Wilson, E.J., and Lokier, S.W., 2002, Siliciclastic and volcanoclastic influences on equatorial carbonates: Insights from the Neogene of Indonesia: *Sedimentology*, v. 49, p. 583-601.
- Woolfe, K.J., and Larcombe, P., 1998, Terrigenous sediment accumulation as a regional control on the distribution of reef carbonates, *in* G.F. Camoin and P.J. Davies, eds., *Reefs and Carbonate Platforms in the Pacific and Indian Oceans: International Association of Sedimentologists Special Publication*, v. 25, p. 295-310.
- Wright, V.P., 1992, A revised classification of limestones: *Sedimentary Geology*, v. 76, p. 177-185.
- Van Buchem, F.S.P., Razin, P., Homewood, P.W., Oterdoom, W.H., Philip, J., 2002, Stratigraphic organization of carbonate ramps and organic-rich intrashelf basins: Natih Formation (middle Cretaceous) of northern Oman: American Association of Petroleum Geologists Bulletin, v. 86, p. 21-53.
- Vandeginste, V., Swennen, R., Gleeson, S.A., Ellam, R.M., Osadetz, K., and Roure, F., 2006, Development of secondary porosity in the Fairholme carbonate complex (southwest Alberta, Canada): *Journal of Geochemical Exploration*, v. 89, p. 394-397.
- Vandeginste, V., Swennen, R., Reed, M.H., Ellam, R.M., Osadetz, K., and Roure, F., 2009, Host rock dolomitization and secondary porosity development in the upper Devonian Cairn Formation of the Fairholme carbonate complex (South-west Alberta, Canadian Rockies): Diagenesis and geochemical modeling: *Sedimentology*, v. 56, p. 2044-2060.
- Zenger, D.H., Dunham, J.B., and Ethington, R.L., eds., 1980, *Concepts and models of*

dolomitization: Society of Economic Paleontologists and Mineralogists Special Publication, v. 28, 320 p.

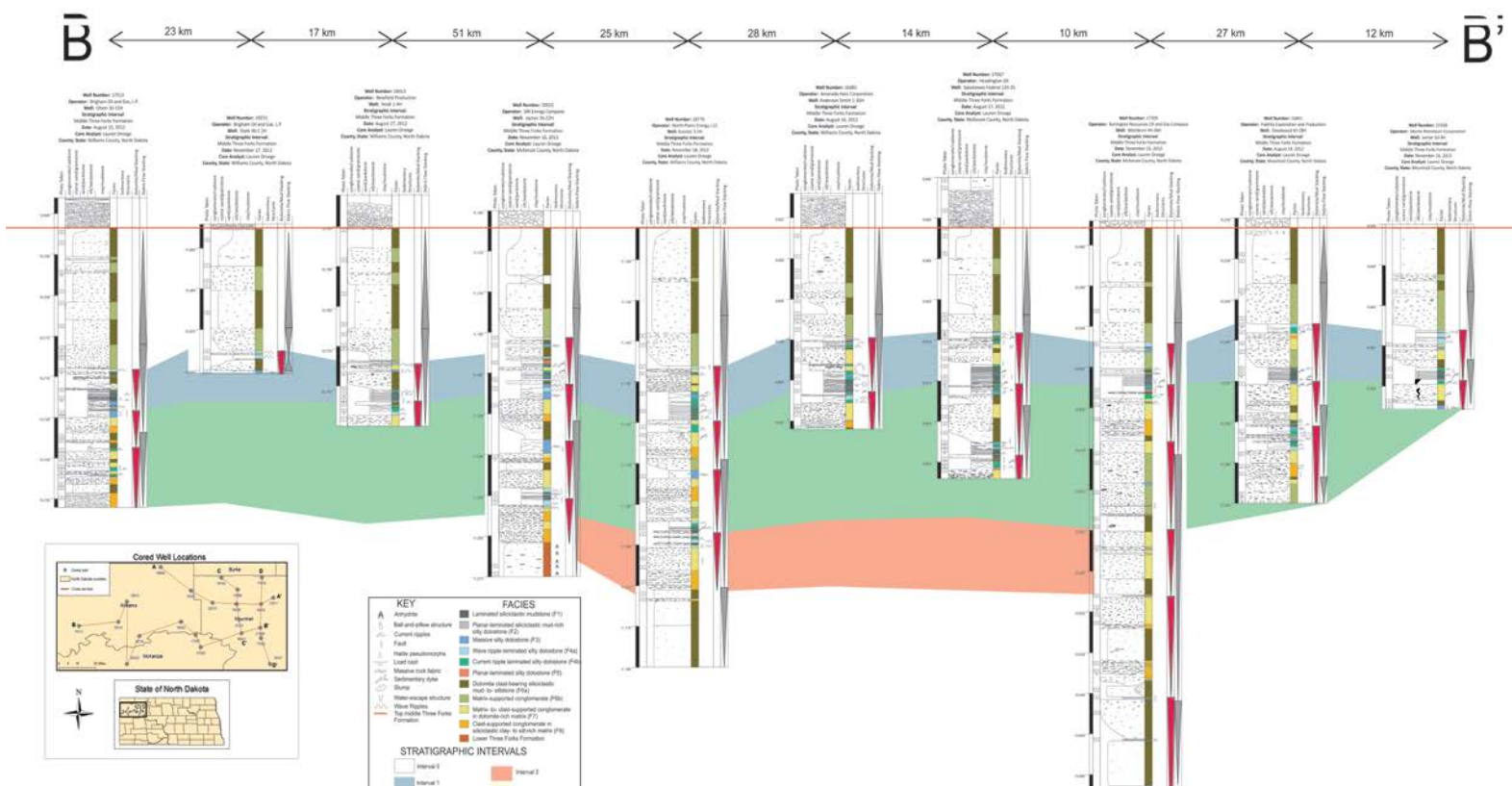
Zentmeyer, R.A., Pufahl, P.K., James, N.P., and Hiatt, E.E., 2011, Dolomitization on an evaporitic Paleoproterozoic ramp: Widespread syndimentary dolomite in the Denault Formation, Labrador Trough, Canada: *Sedimentary Geology*, v. 238, p. 116-131.

APPENDICES

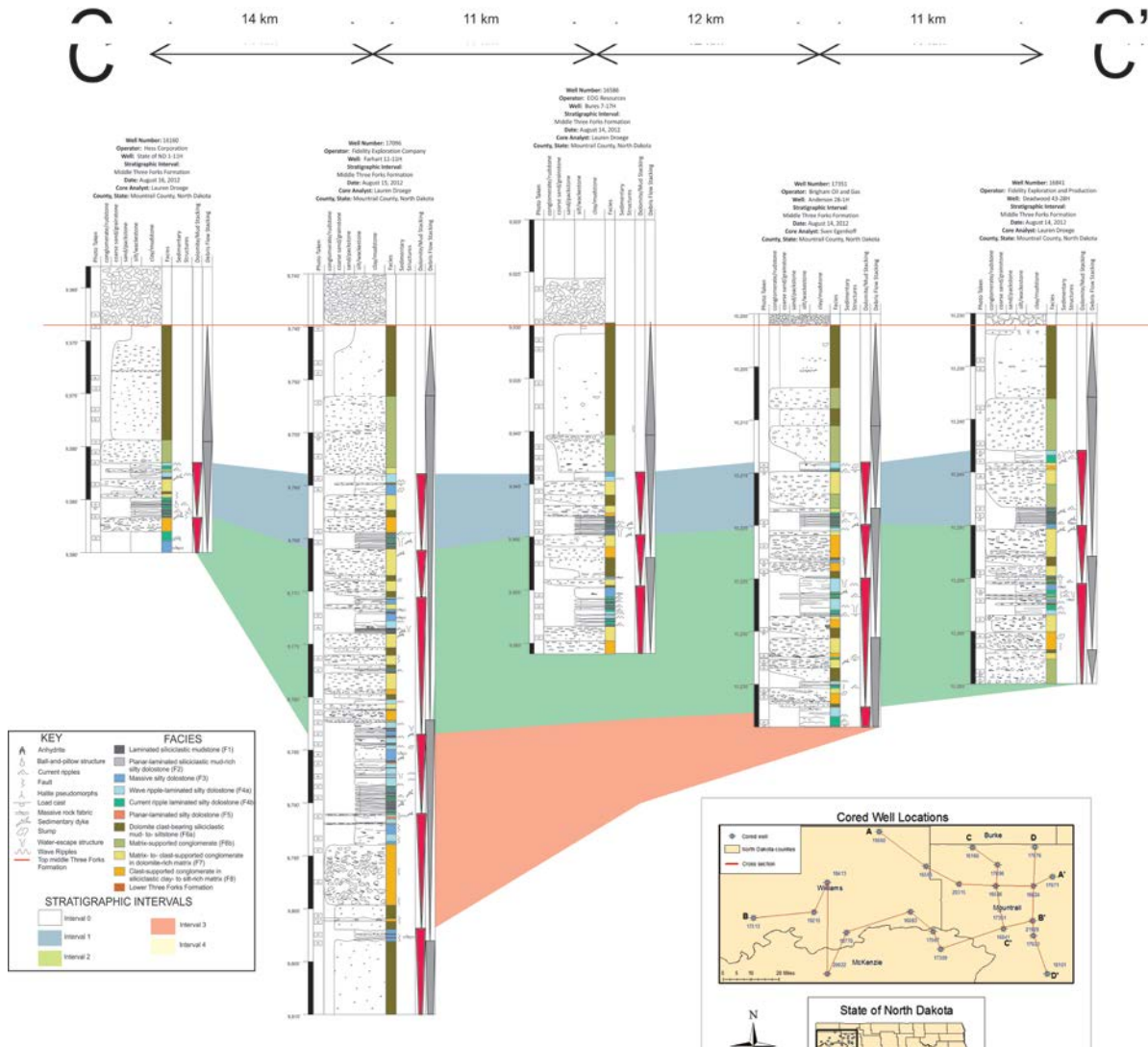
Appendix 1: West-East Transect A-A' from western Williams County, North Dakota to eastern Mountrail County, North Dakota through the middle Three Forks Formation, Williston Basin



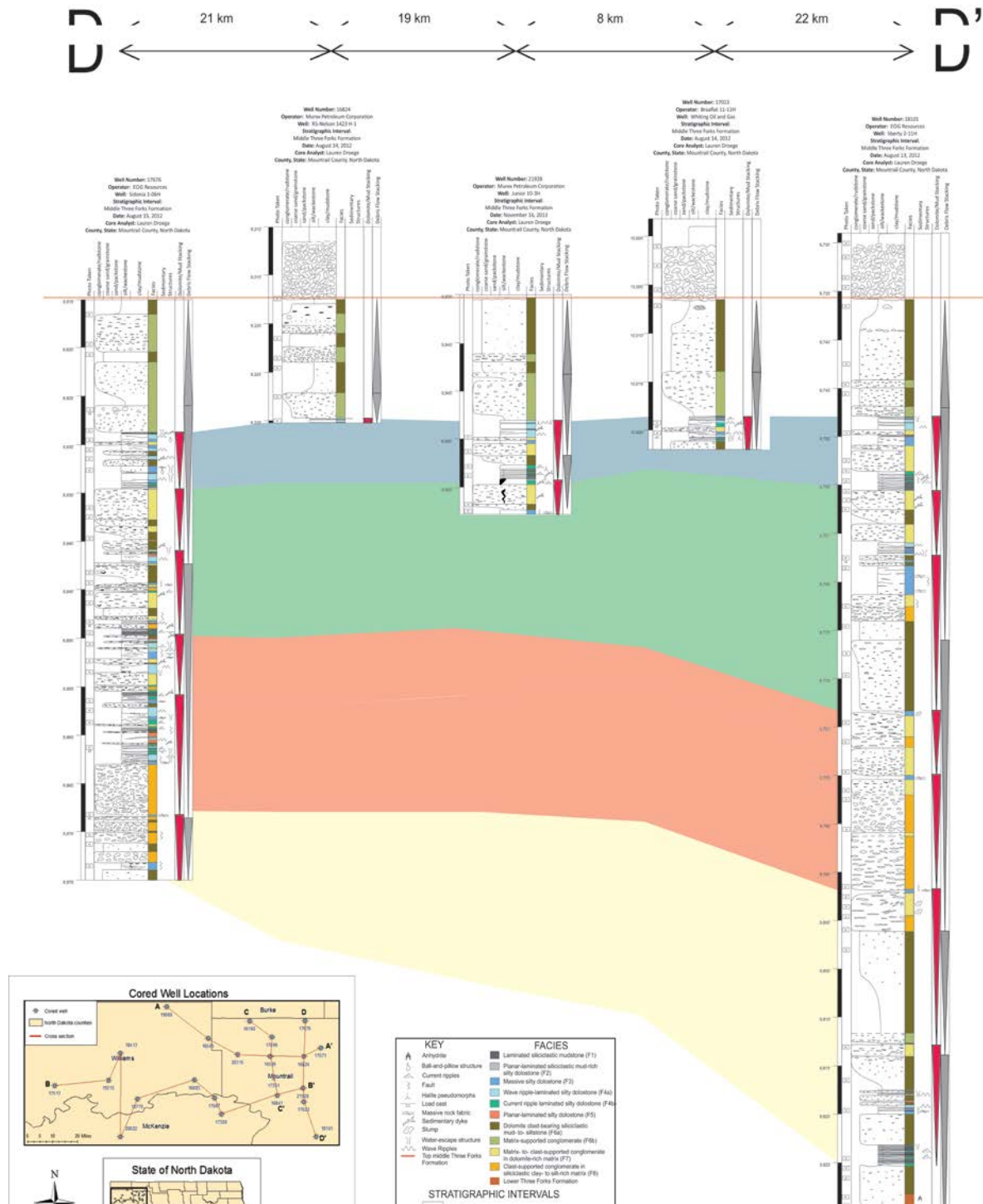
Appendix 2: West-East Transect B-B' from western Williams County and northern McKenzie County, North Dakota to eastern Mountrail County, North Dakota through the middle Three Forks Formation, Williston Basin




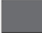





















Appendix 3: North-South Transect C-C' from northern Mountrail County, North Dakota to central Mountrail County, North Dakota through the middle Three Forks Formation, Williston Basin



Appendix 4: North-South Transect D-D' from northern Mountrail County, North Dakota to southern Mountrail County, North Dakota through the middle Three Forks Formation, Williston Basin

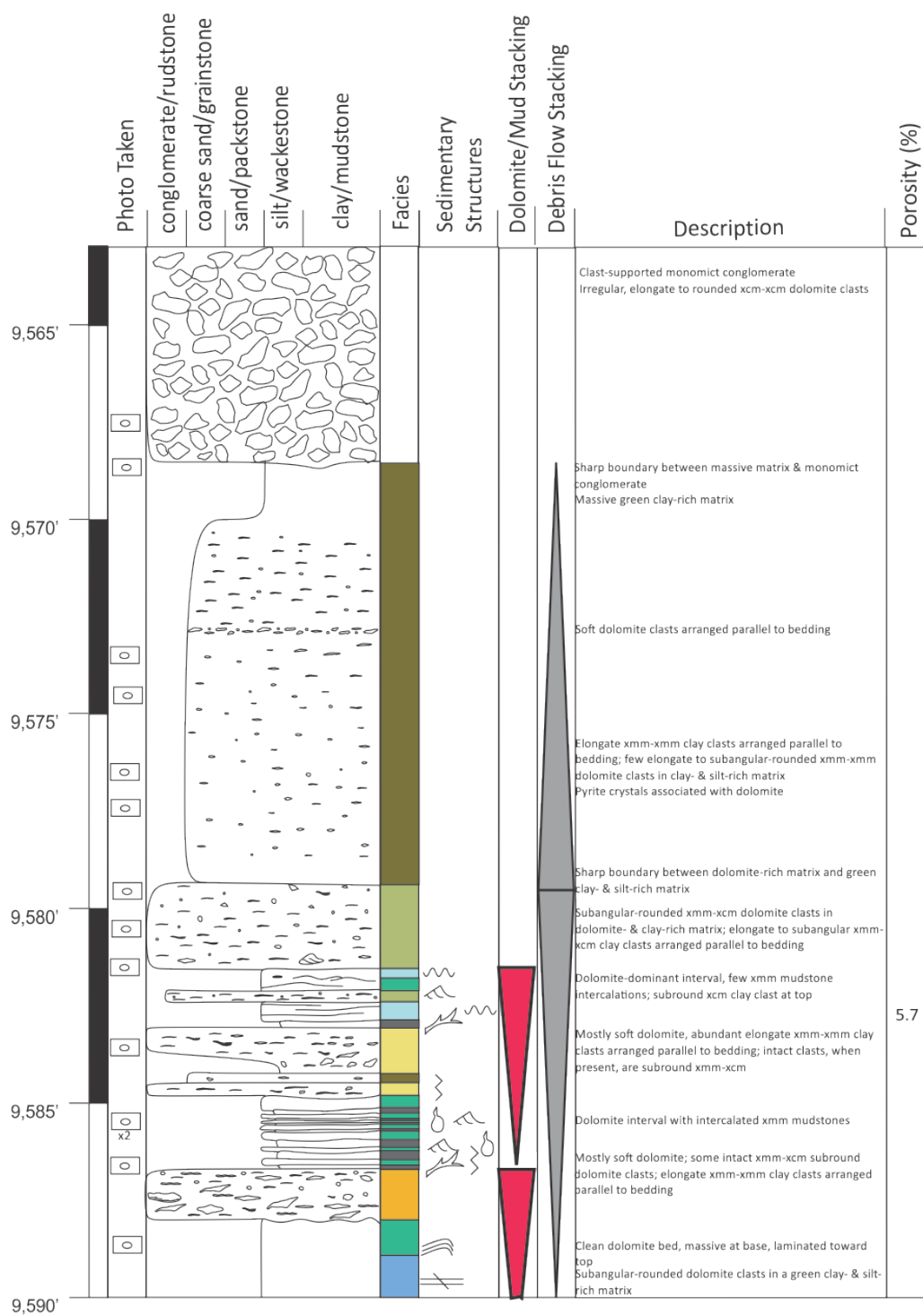


Appendix 5: Core logs

KEY		FACIES	
	Anhydrite		Laminated siliciclastic mudstone (F1)
	Ball-and-pillow structure		Planar-laminated siliciclastic mud-rich silty dolostone (F2)
	Current ripples		Massive silty dolostone (F3)
	Fault		Wave ripple-laminated silty dolostone (F4a)
	Halite pseudomorphs		Current ripple laminated silty dolostone (F4b)
	Load cast		Planar-laminated silty dolostone (F5)
	Massive rock fabric		Dolomite clast-bearing siliciclastic mud- to- siltstone (F6a)
	Sedimentary dyke		Matrix-supported conglomerate (F6b)
	Slump		Matrix- to- clast-supported conglomerate in dolomite-rich matrix (F7)
	Water-escape structure		Clast-supported conglomerate in siliciclastic clay- to silt-rich matrix (F8)
	Wave Ripples		Lower Three Forks Formation
	Top middle Three Forks Formation		

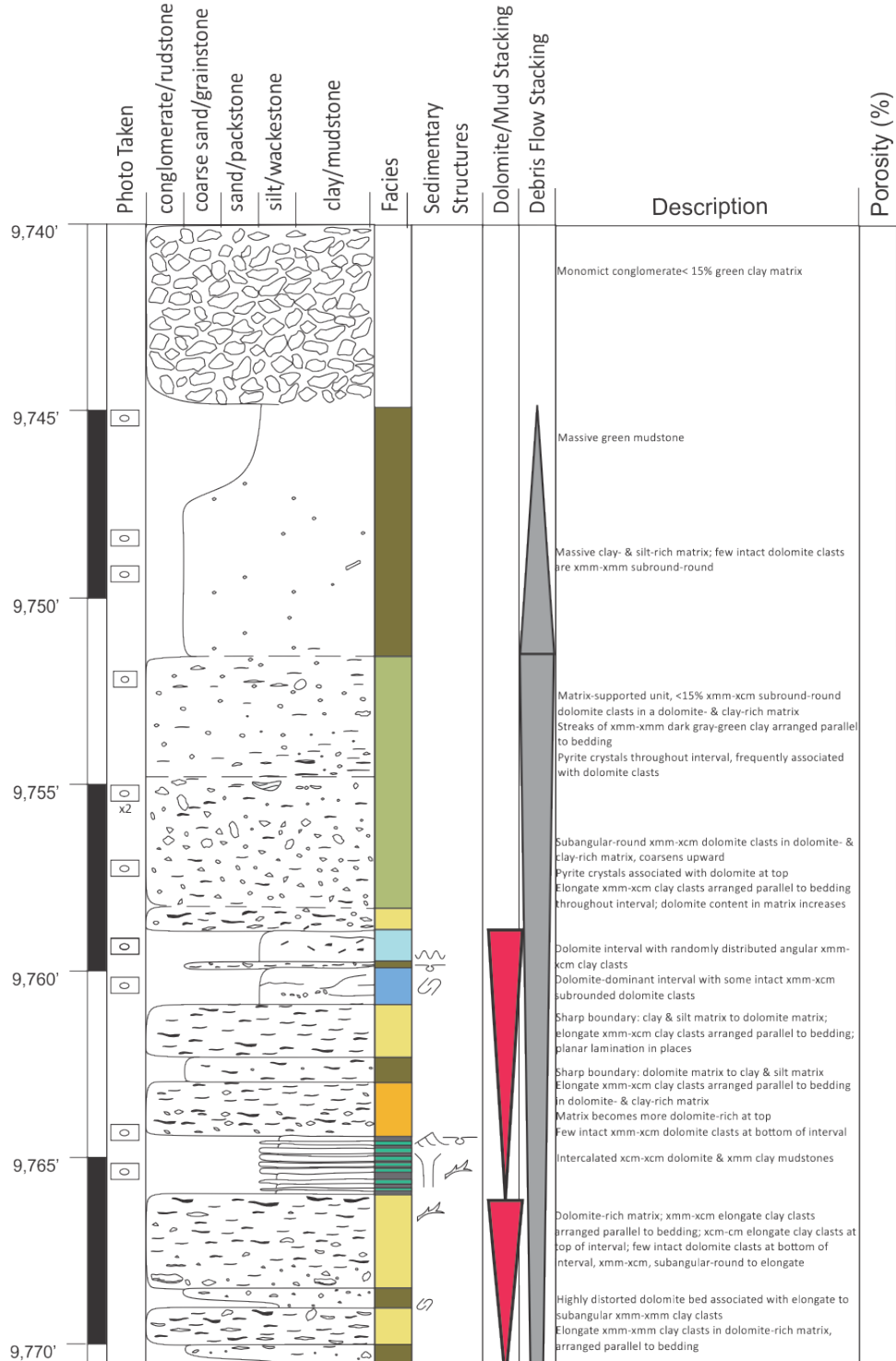
Operator: Hess Corporation
Well: State of ND 1-11H
Stratigraphic Interval: Middle Three Forks Formation

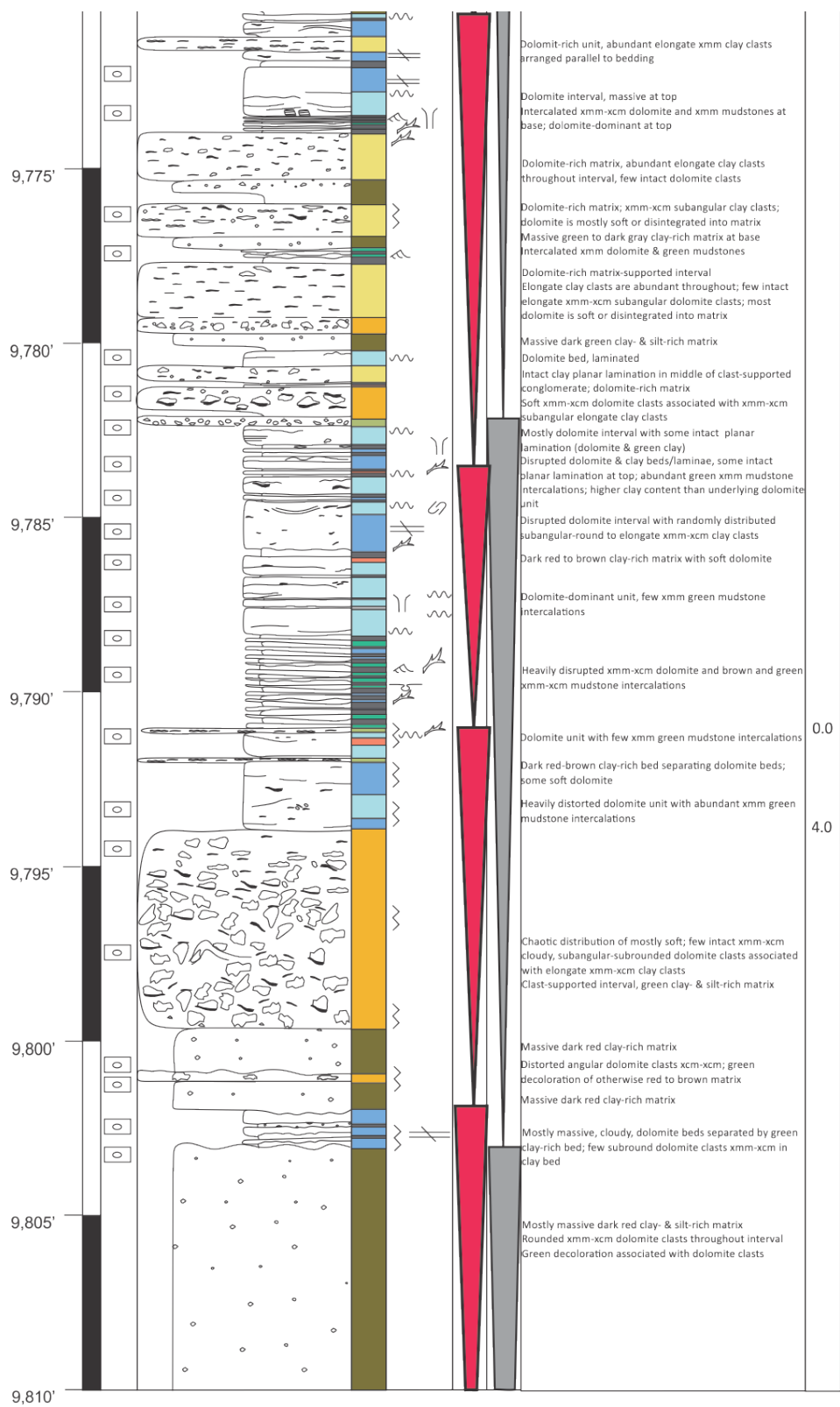
Date: August 16, 2012
Core Analyst: Lauren Droege
County, State: Mountrail Co., North Dakota



Operator: Fidelity Exploration Company
Well: Farhart 11-11H
Stratigraphic Interval: Middle Three Forks Formation

Date: August 15, 2012
Core Analyst: Lauren Droege
County, State: Mountrail Co., North Dakota





Operator: EOG Resources

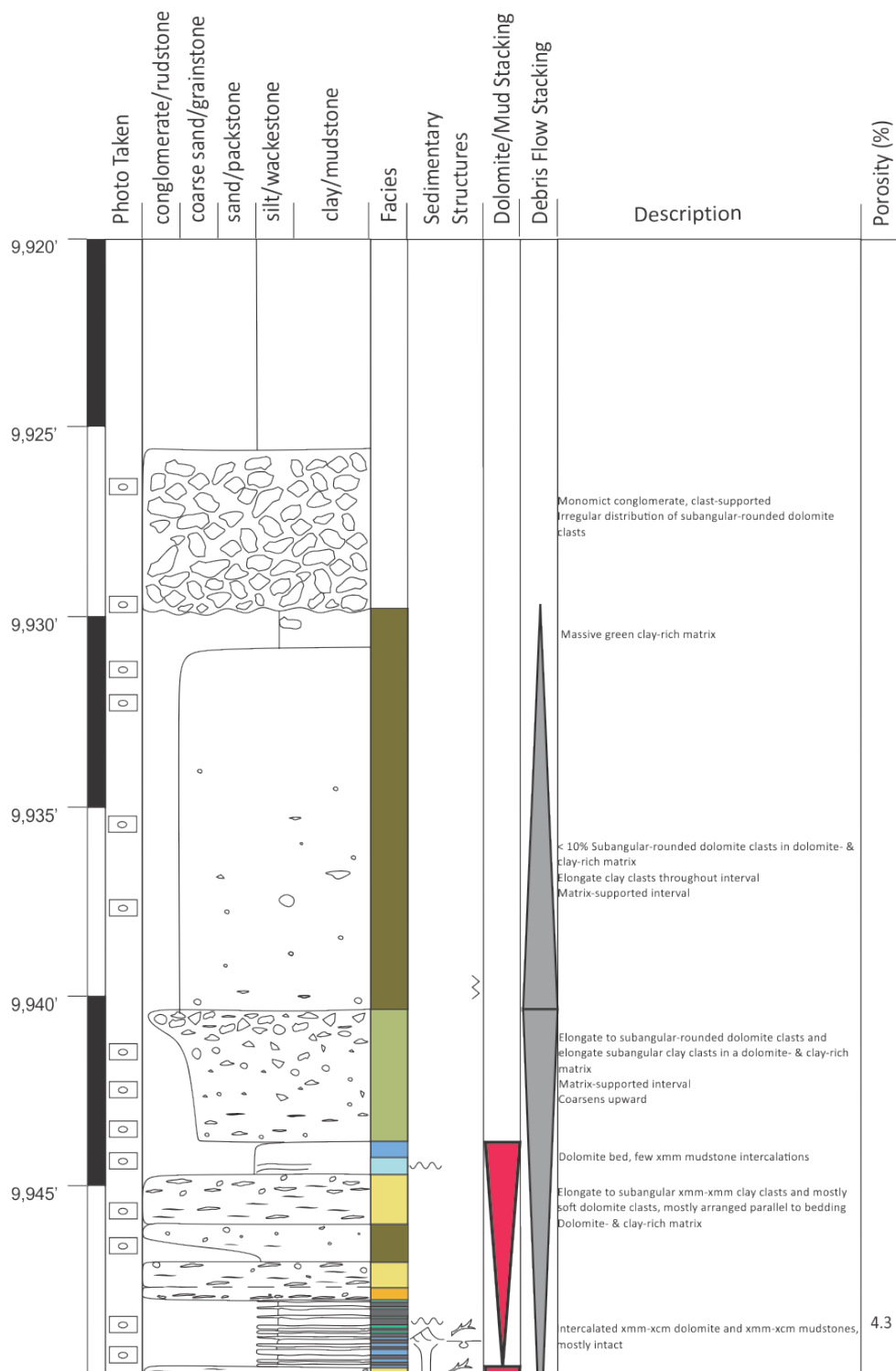
Well: Bures 1-17H

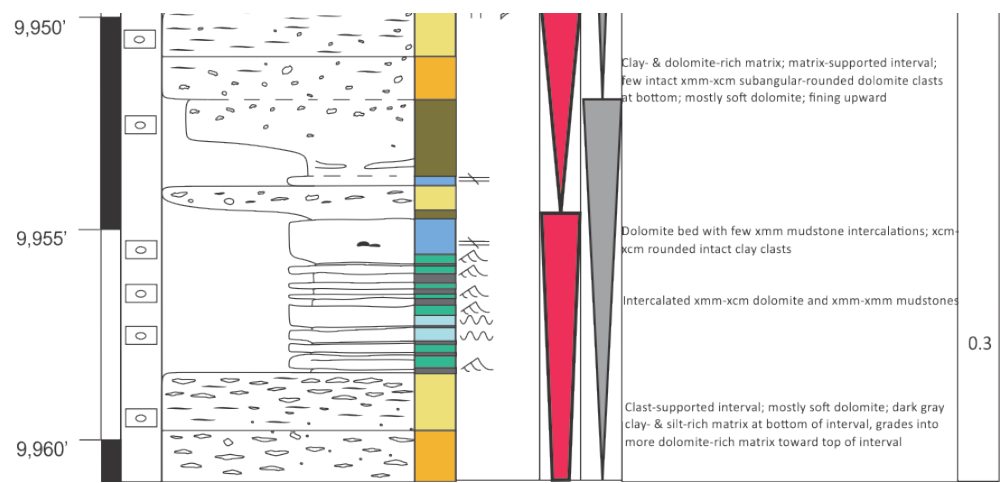
Stratigraphic Interval: Middle Three Forks Formation

Date: August 14, 2012

Core Analyst: Lauren Droege

County, State: Mountrail Co., North Dakota





Operator: Brigham Exploration

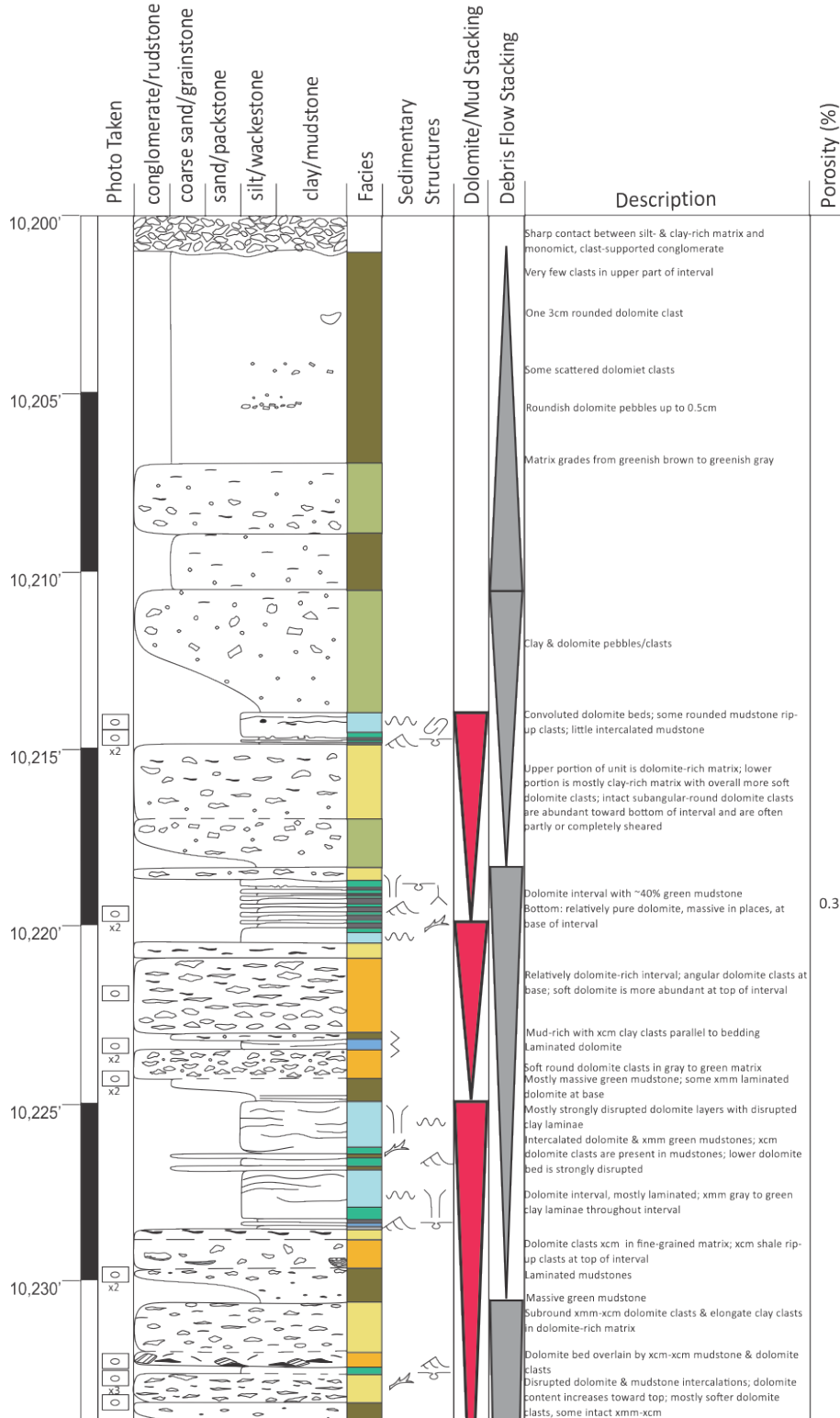
Well: Anderson 28-1H

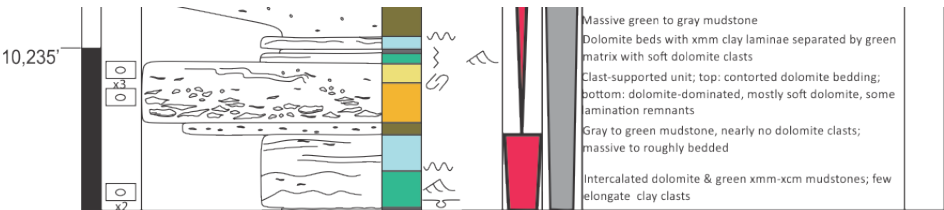
Stratigraphic Interval: Middle Three Forks Formation

Date: August 14, 2012

Core Analyst: Sven Egenhoff

County, State: Williams Co., North Dakota





Operator: Fidelity Exploration

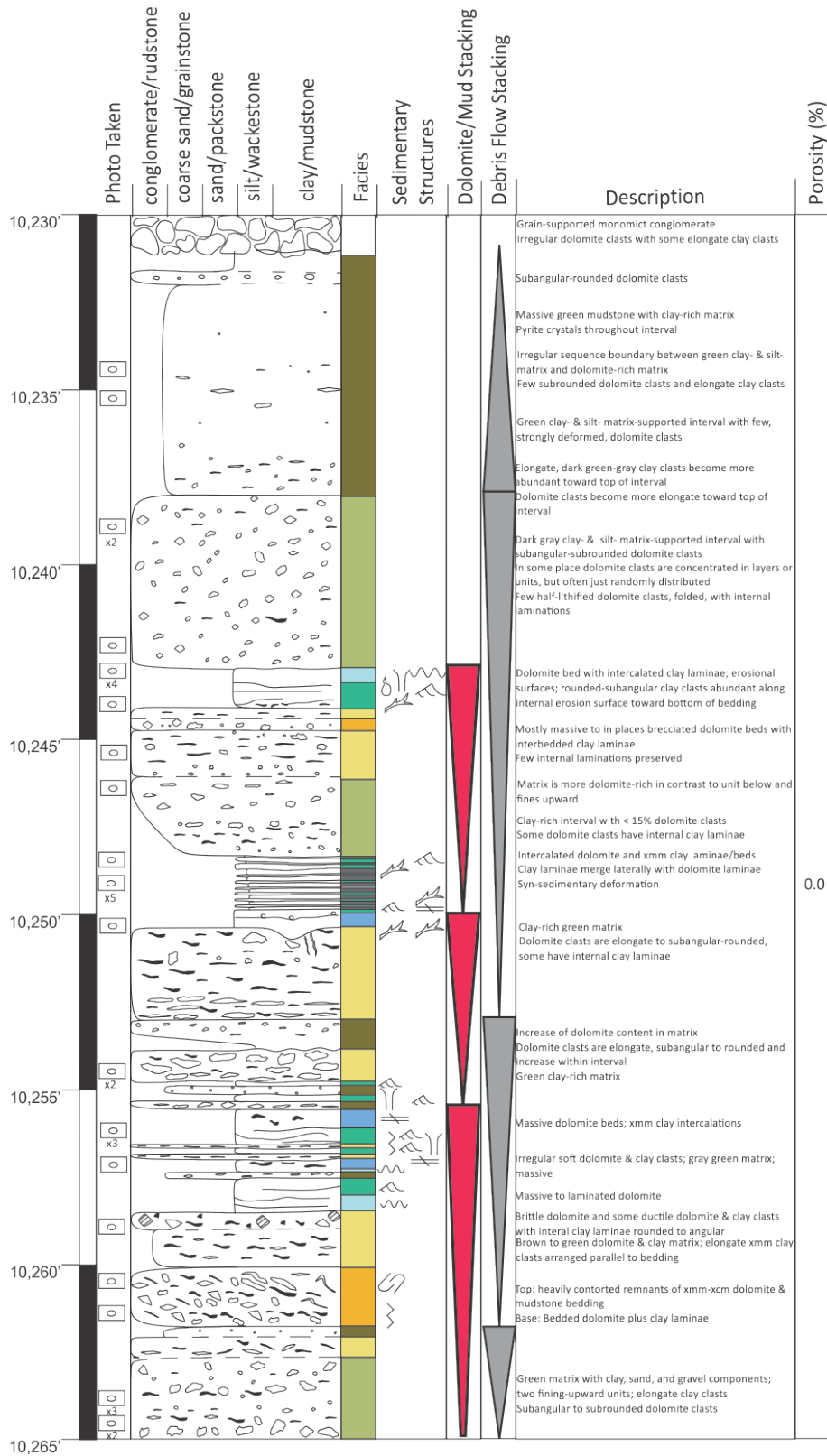
Well: Deadwood 43-28H

Stratigraphic Interval: Middle Three Forks Formation

Date: August 14, 2012

Core Analyst: Sven Egenhoff

County, State: Mountrail Co., North Dakota



Operator: EOG Resources

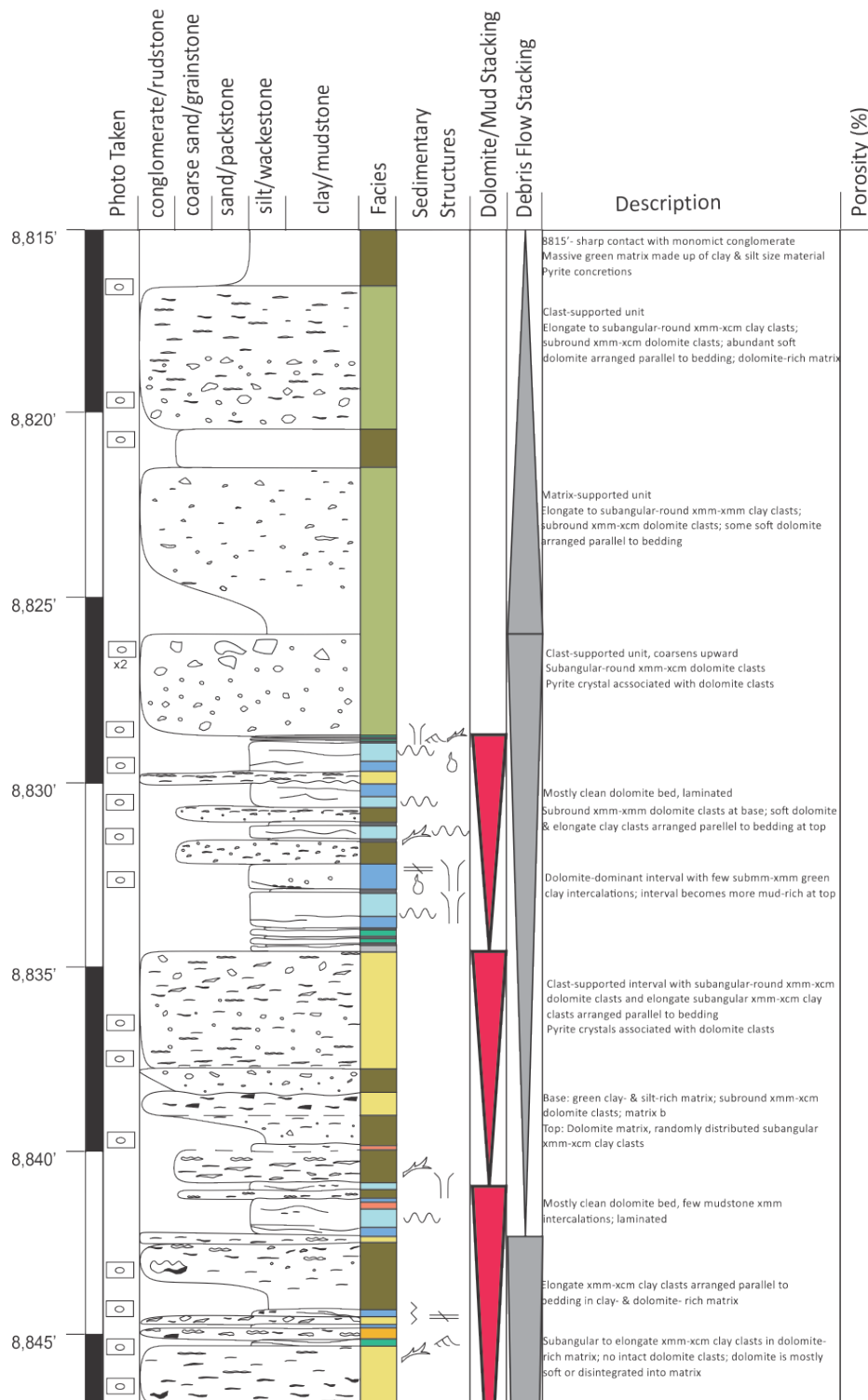
Well: Sidonia 1-06H

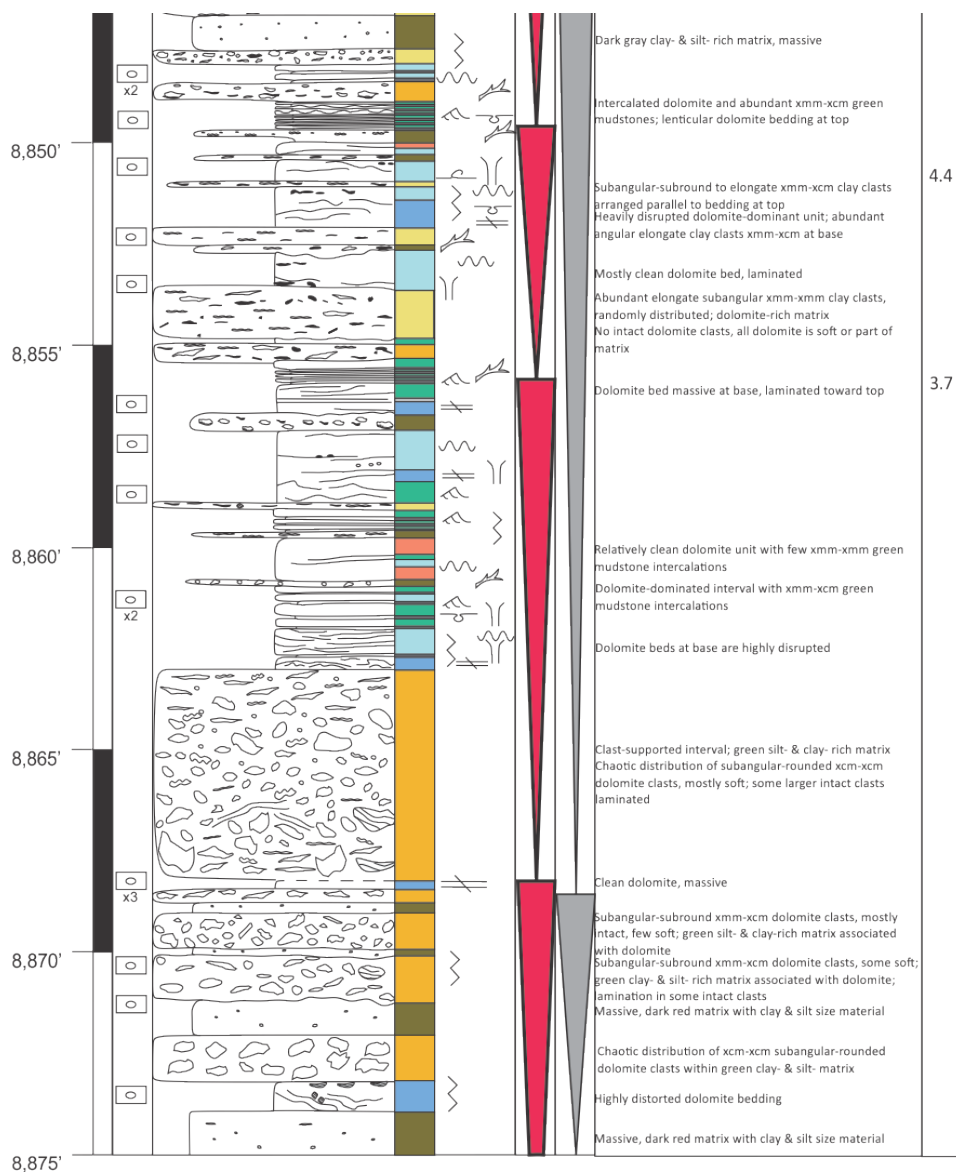
Stratigraphic Interval: Middle Three Forks Formation

Date: August 15, 2012

Core Analyst: Lauren Droegge

County, State: Mountrail Co., North Dakota





Operator: Hess Corporation

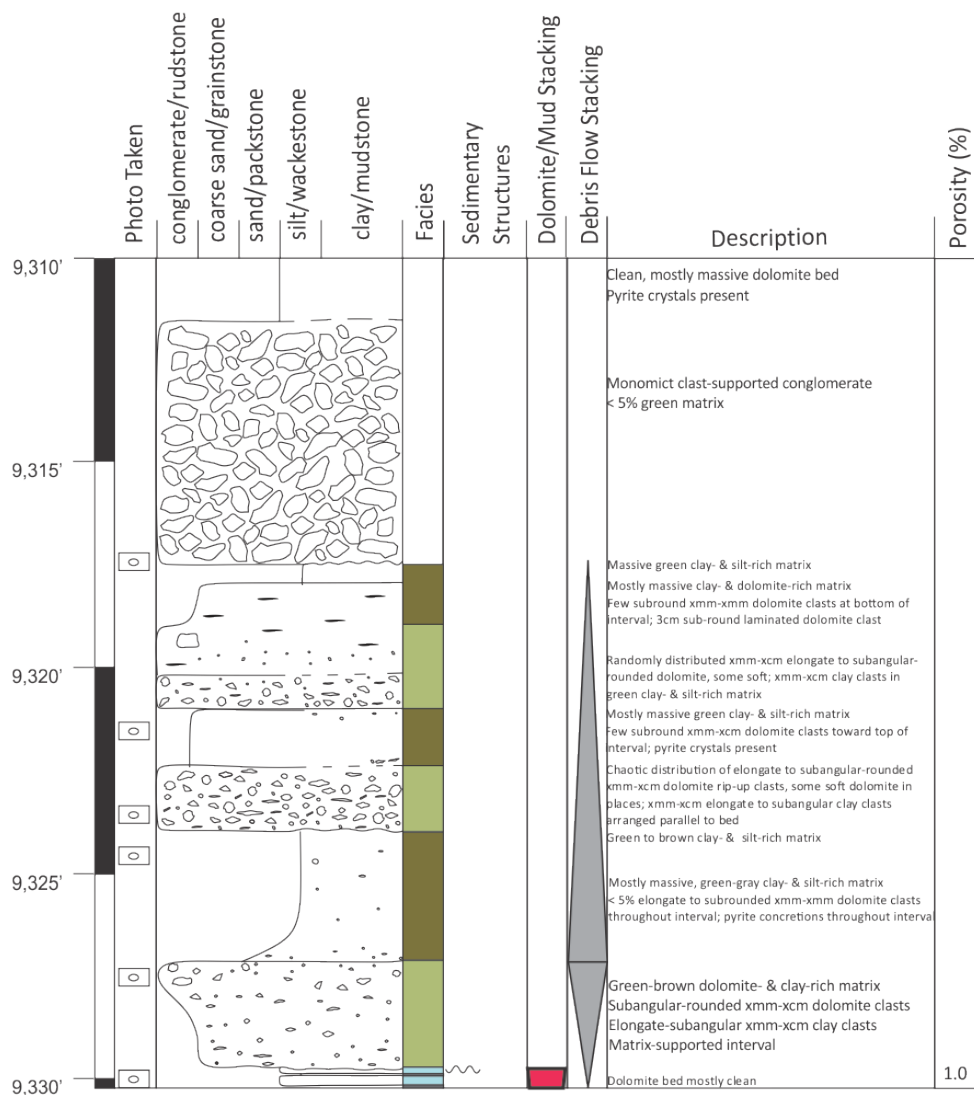
Well: RS-Nelson 1423 H-1

Stratigraphic Interval: Middle Three Forks Formation

Date: August 14, 2012

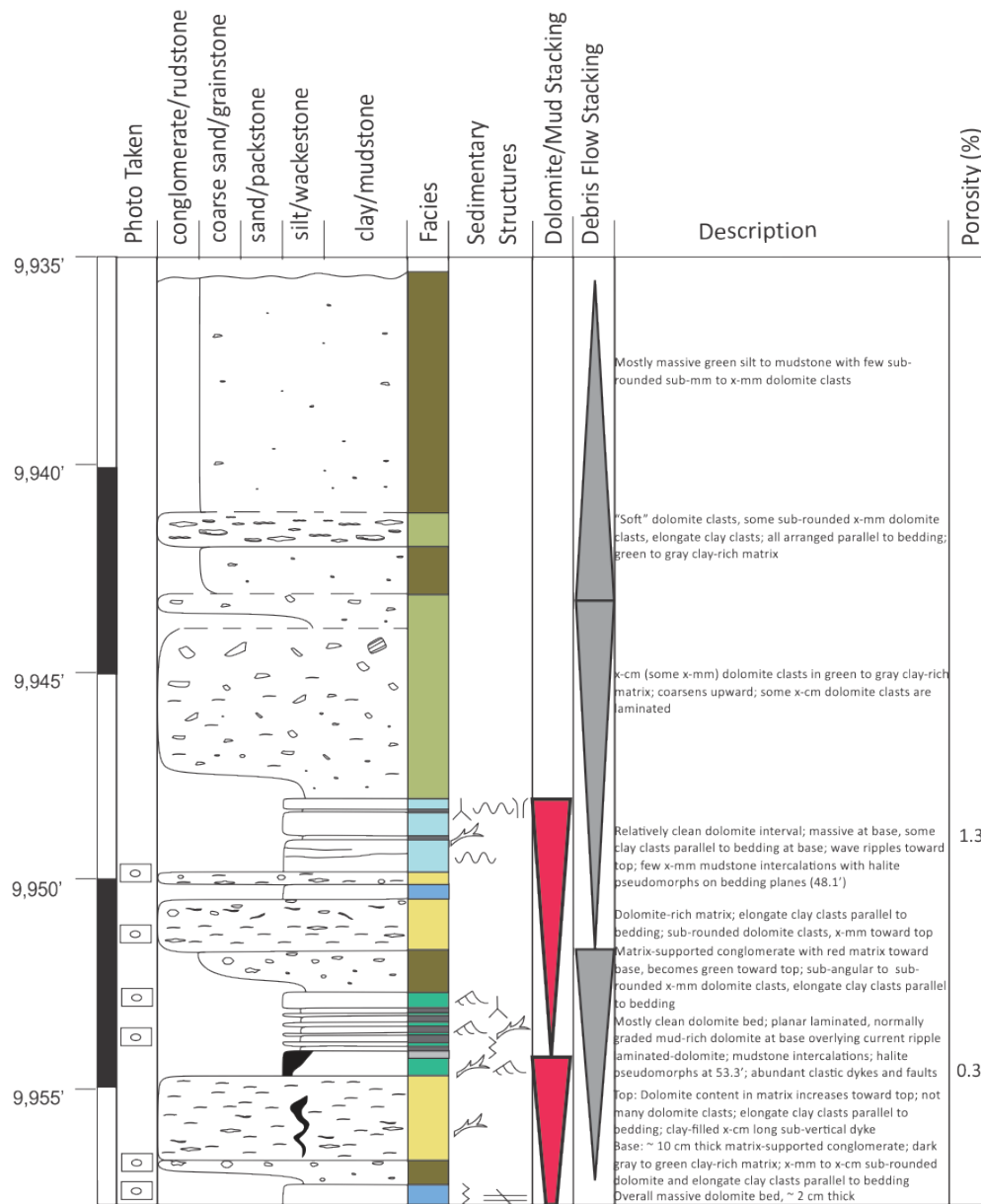
Core Analyst: Lauren Droege

County, State: Mountrail Co., North Dakota



Operator: Murex Petroleum Corporation
Well: Junior 10-3H
Stratigraphic Interval: Middle Three Forks Formation

Date:
Core Analyst: Lauren Droege
County, State: Mountrail County, North Dakota



Operator: Whiting Oil and Gas

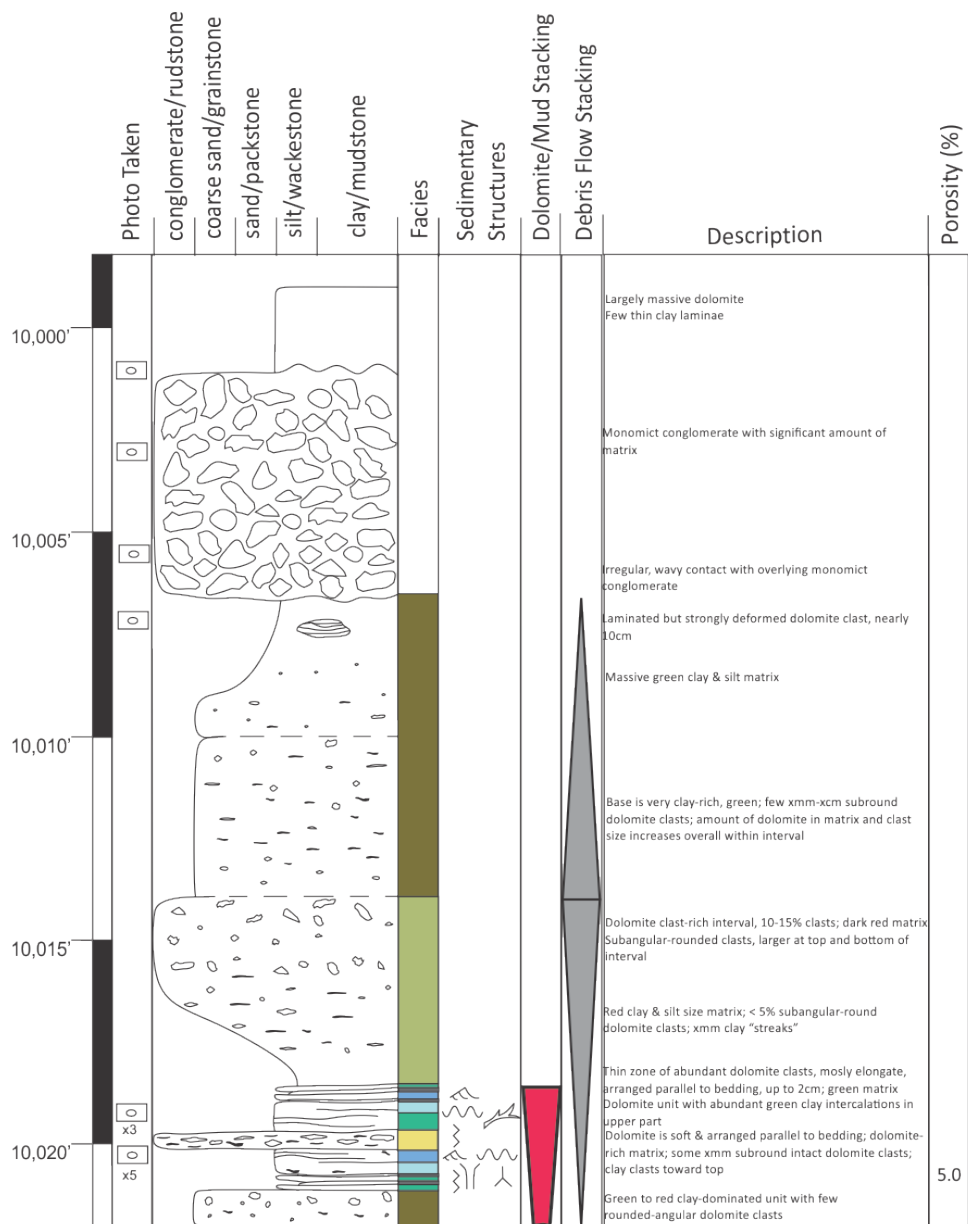
Well: Braaflat 11-11H

Stratigraphic Interval: Middle Three Forks Formation

Date: August 14, 2012

Core Analyst: Sven Egenhoff

County, State: Mountrail Co., North Dakota



Operator: EOG Resources

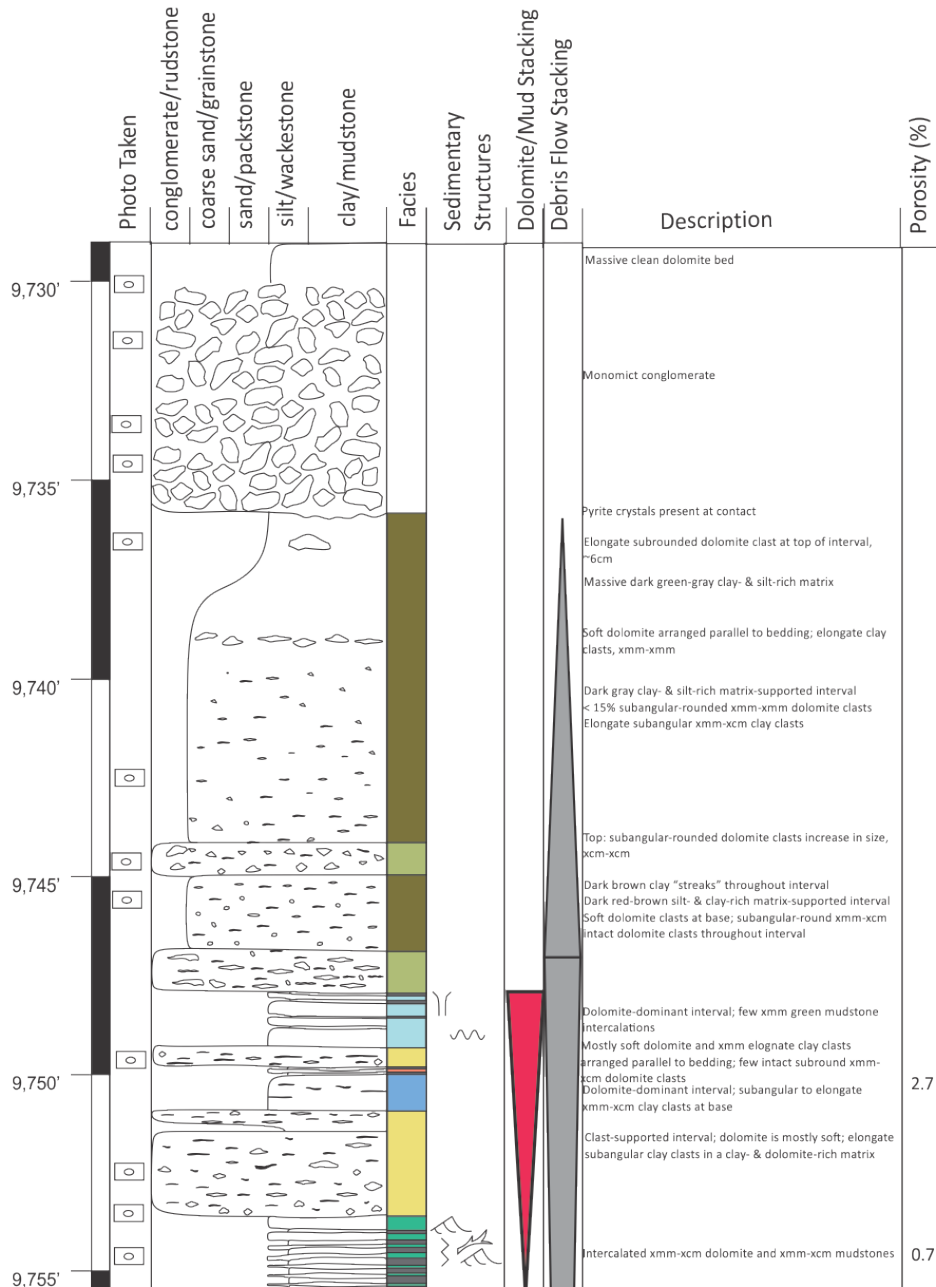
Well: Liberty 2-11H

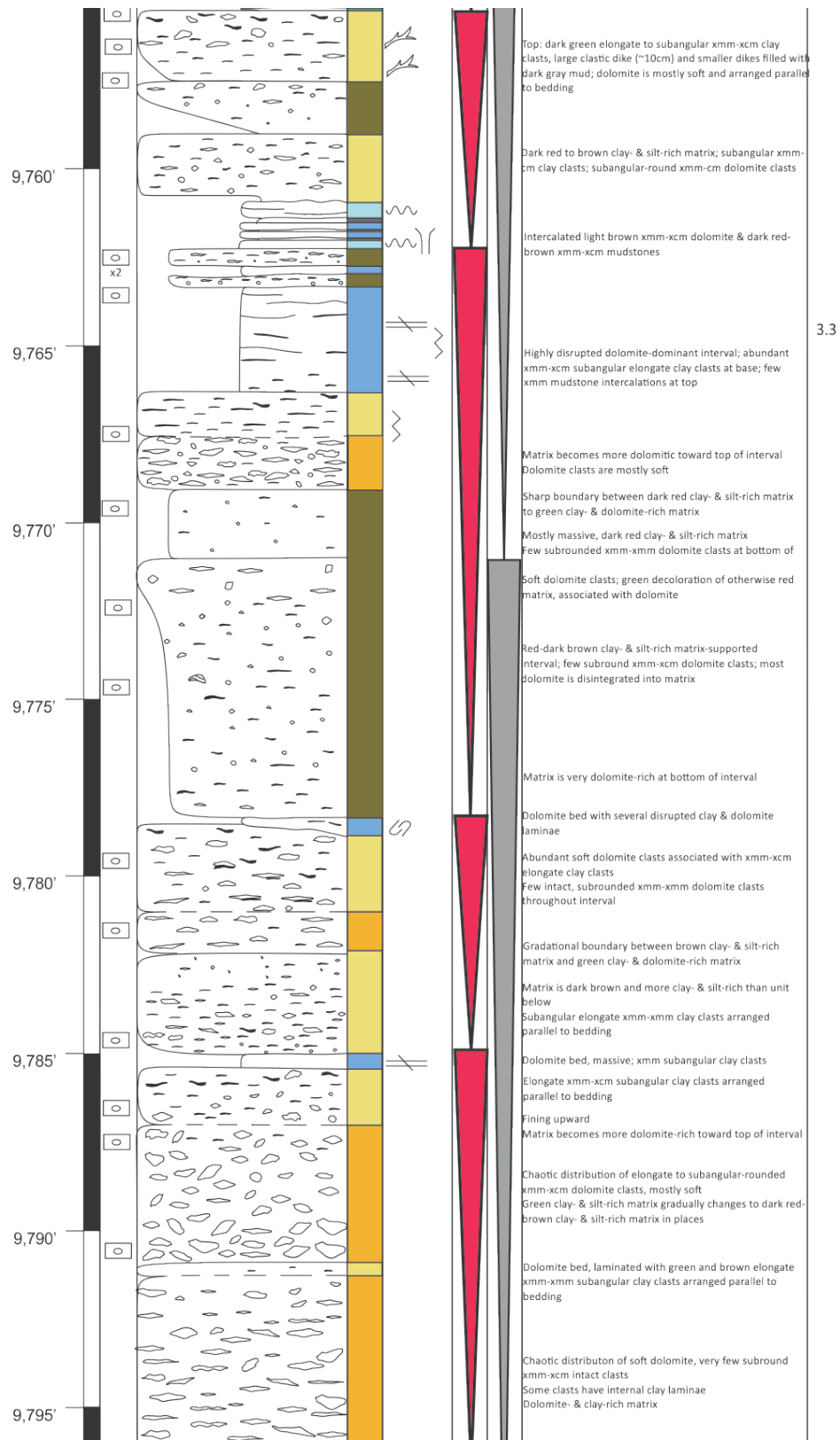
Stratigraphic Interval: Middle Three Forks Formation

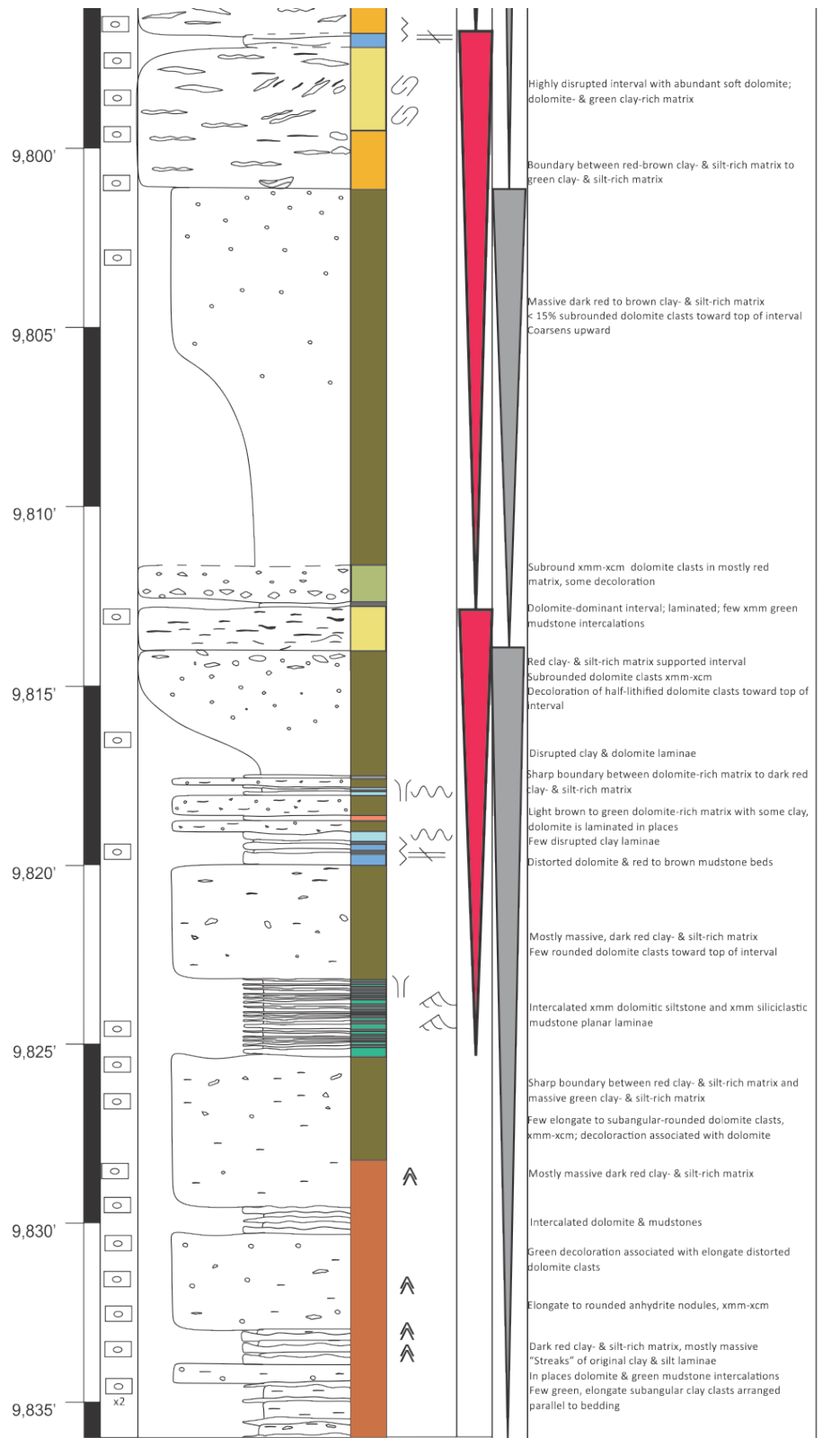
Date: August 13, 2012

Core Analyst: Lauren Droege

County, State: Mountrail Co., North Dakota

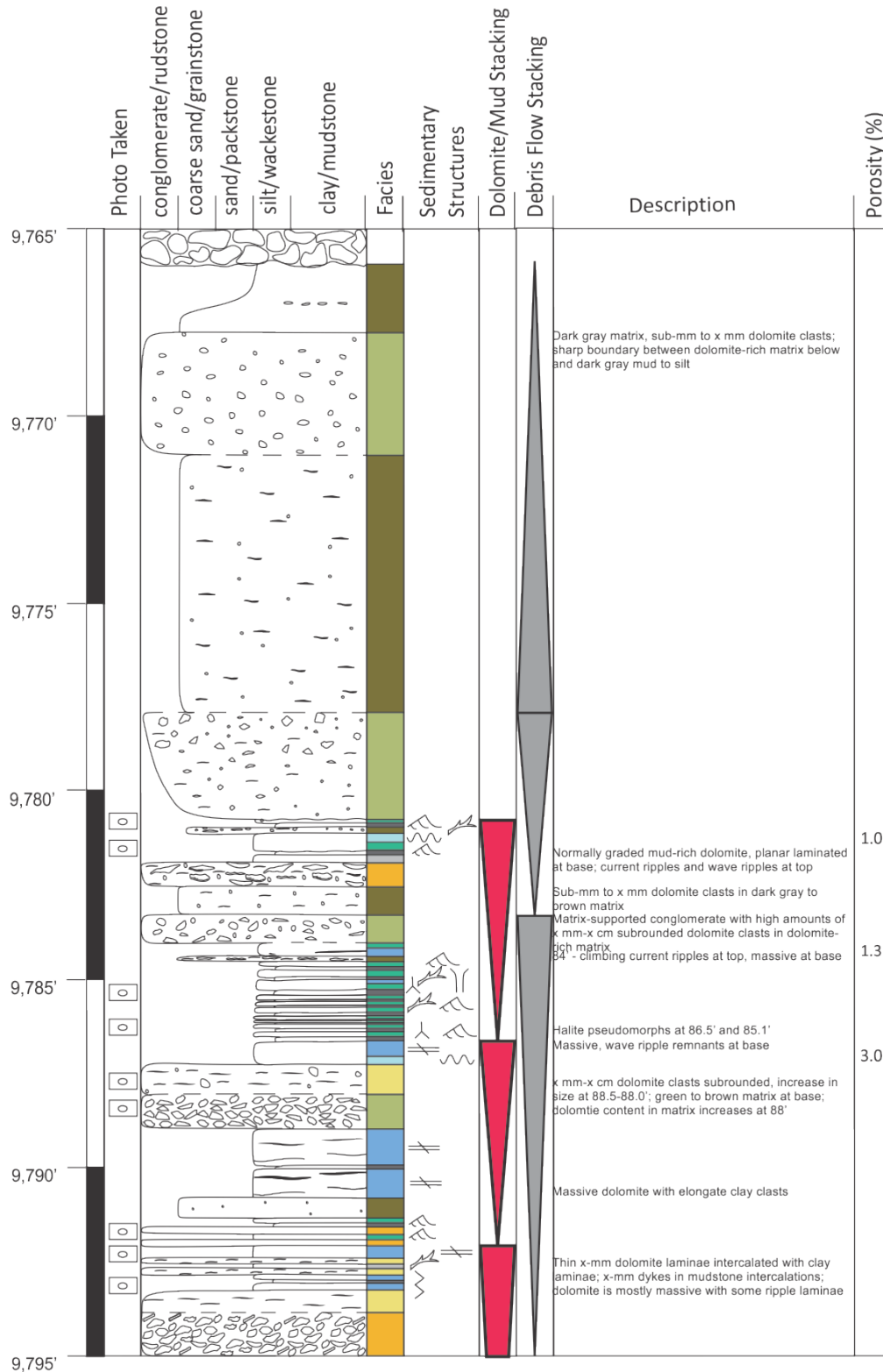






Operator: North Plains Energy, LLC
Well: Comfort 9-12H
Stratigraphic Interval: Middle Three Forks Formation

Date: November 18, 2013
Core Analyst: Lauren Droege
County, State: Williams County, North Dakota



Operator: Hess Corporation

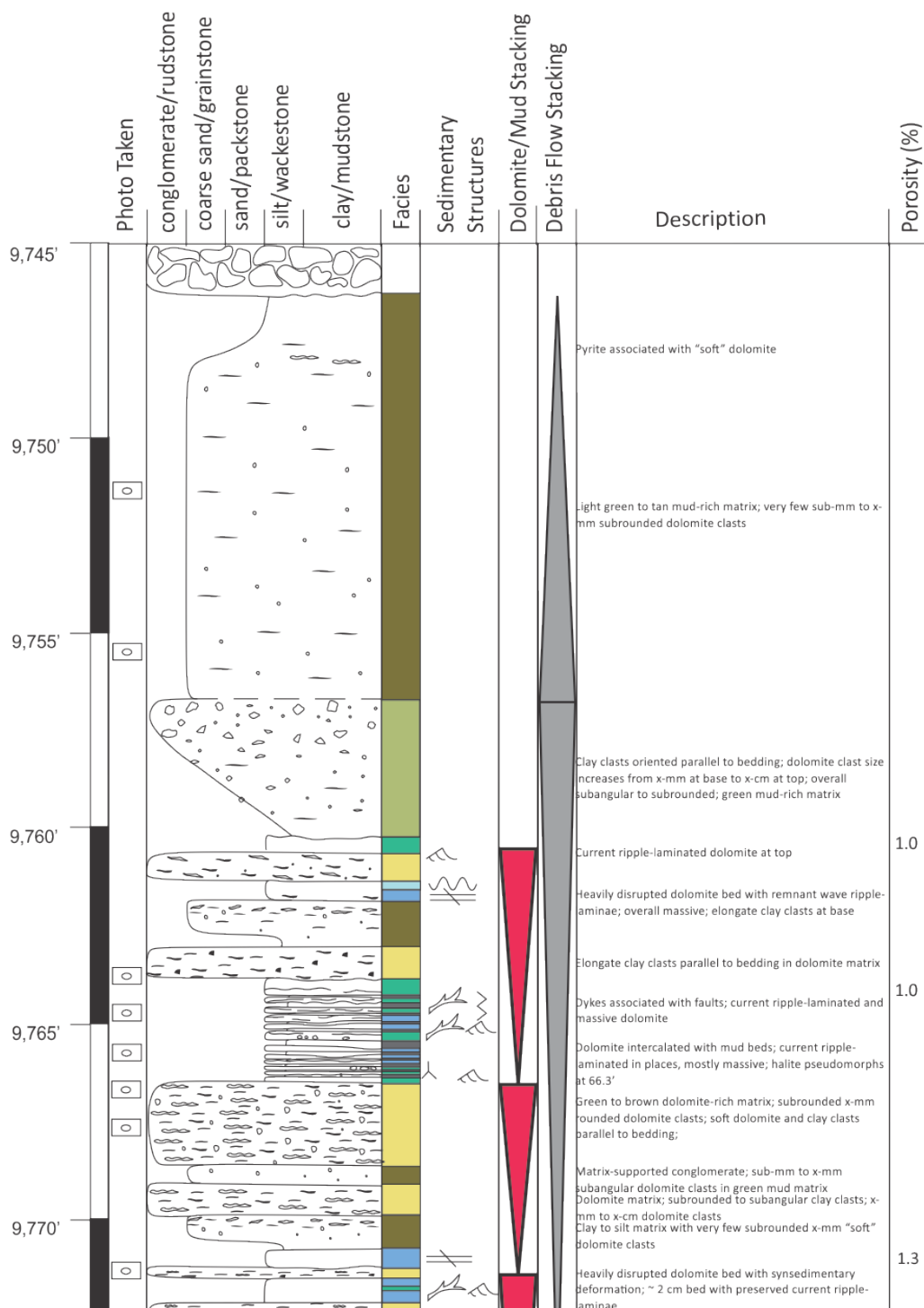
Well: H. Bakken 12-07H

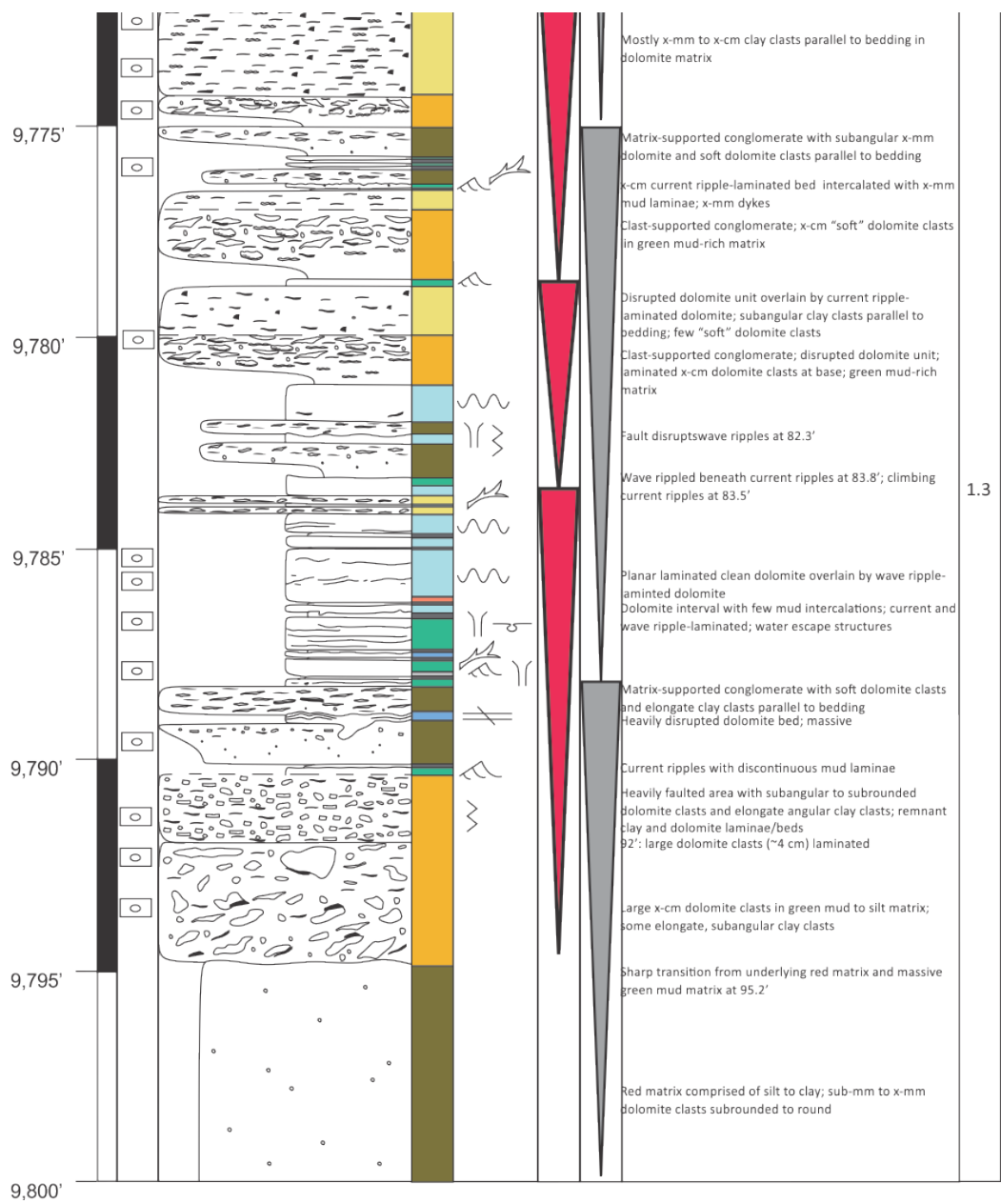
Stratigraphic Interval: Middle Three Forks Formation

Date: November 17, 2013

Core Analyst: Lauren Droege

County, State: Williams County, North Dakota





Operator: Hess Corporation

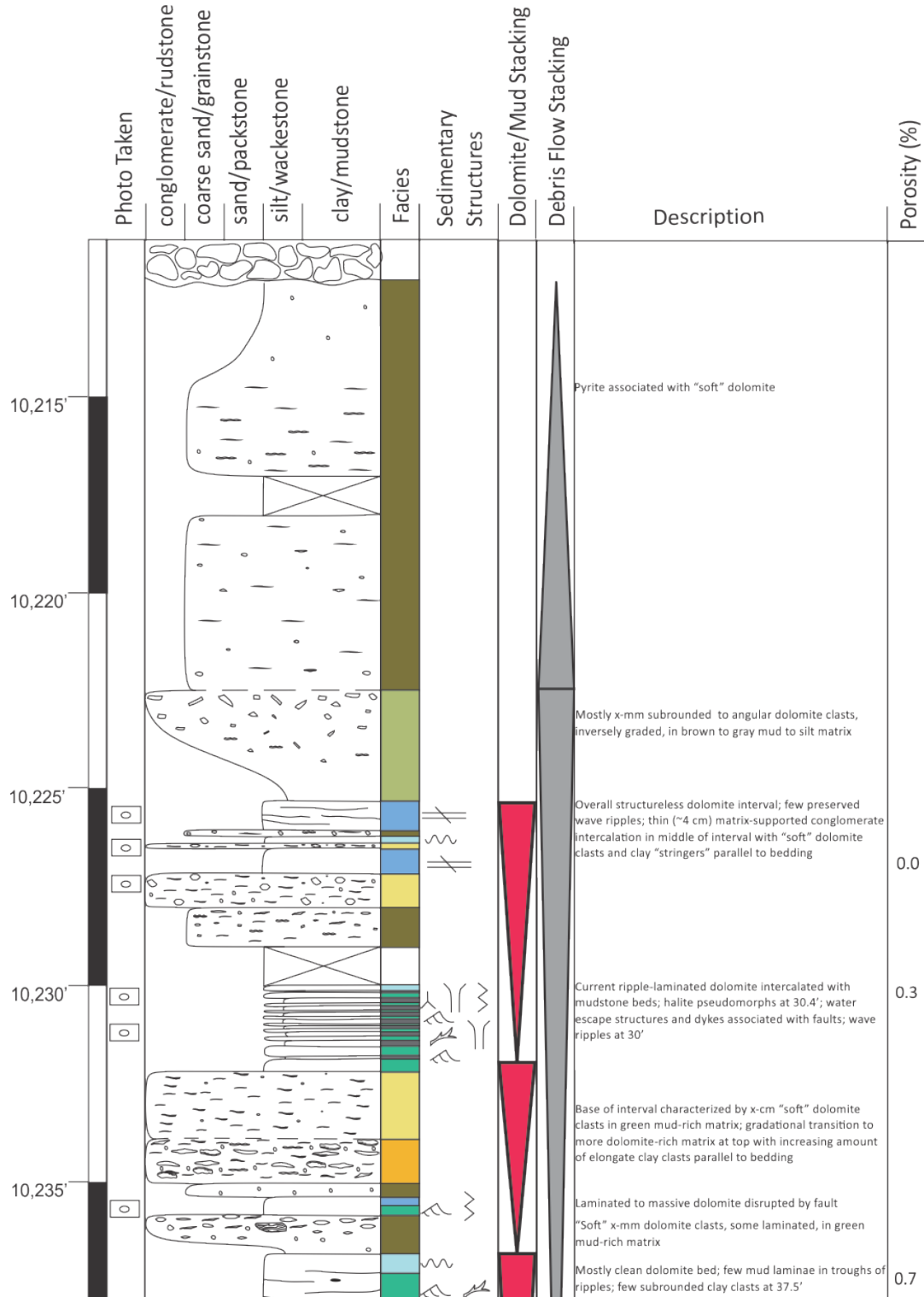
Well: En-Person Observation 11-22

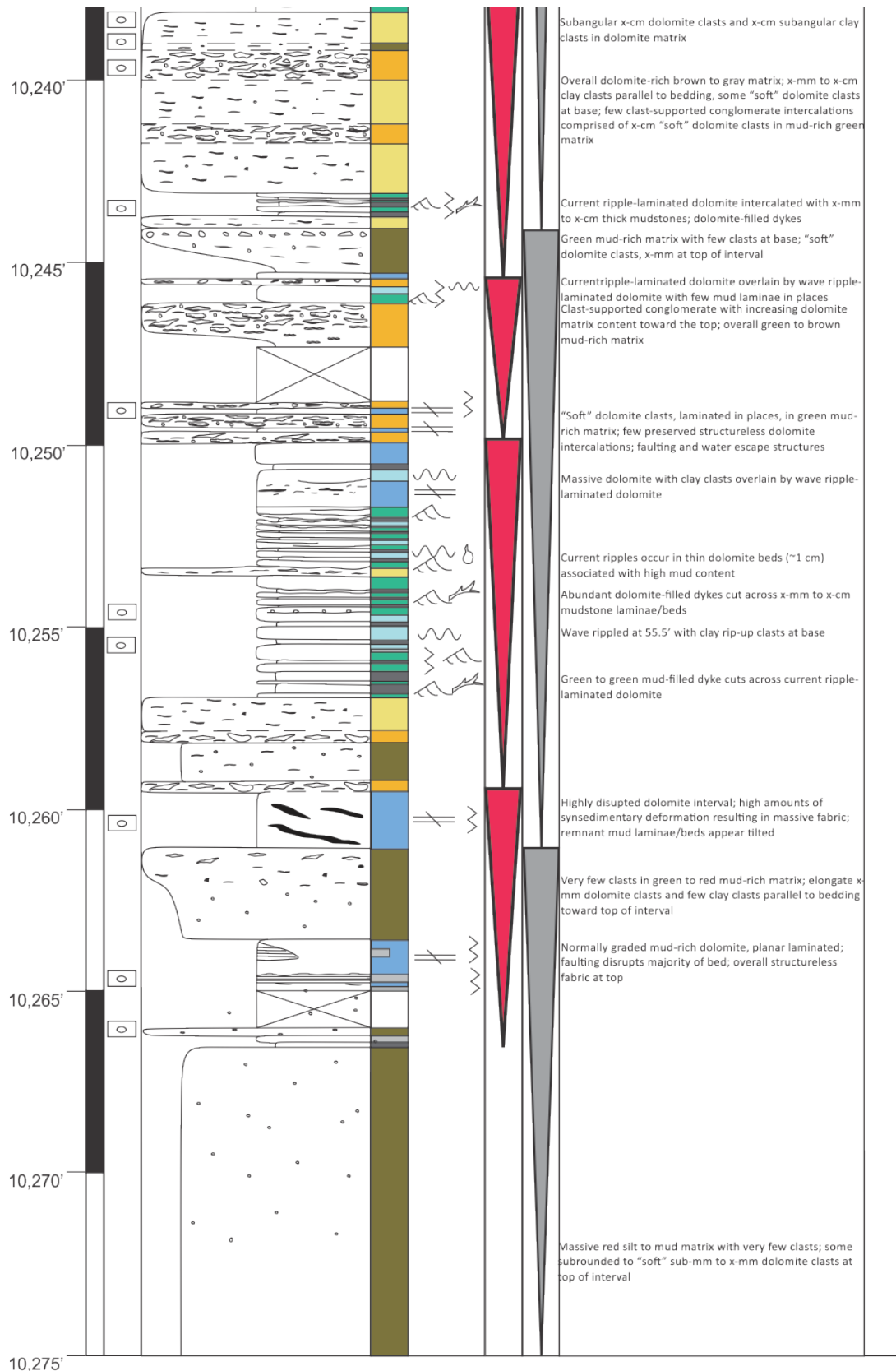
Stratigraphic Interval: Middle Three Forks Formation

Date: November 16, 2013

Core Analyst: Lauren Droeger

County, State: Mountrail County, North Dakota





Operator: Hess Corporation

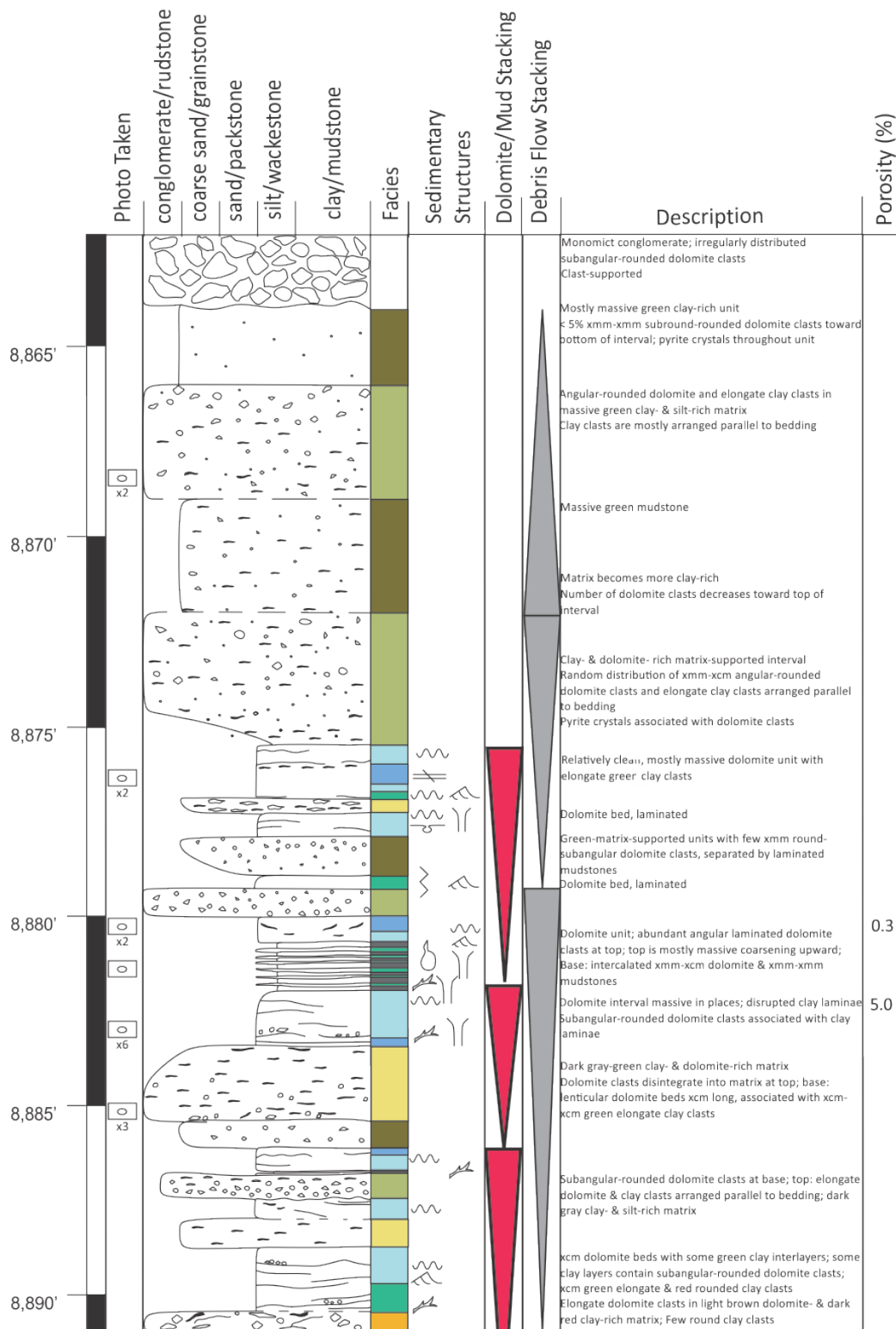
Well: RS State C3603 H-1

Stratigraphic Interval: Middle Three Forks Formation

Date: August 15, 2012

Core Analyst: Sven Egenhoff

County, State: Mountrail Co., North Dakota



Operator: Brigham Oil & Gas

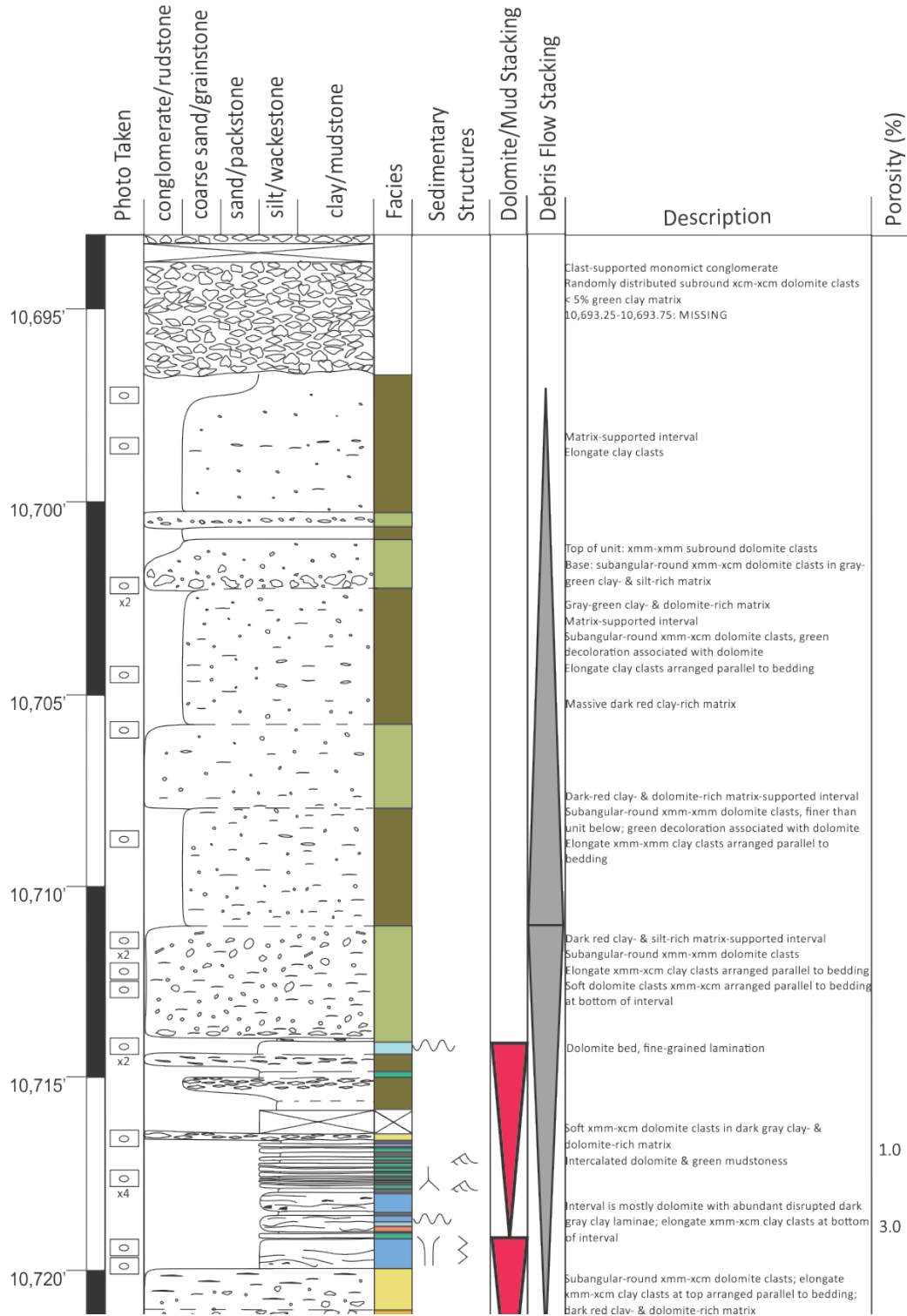
Well: Olson 10-15H

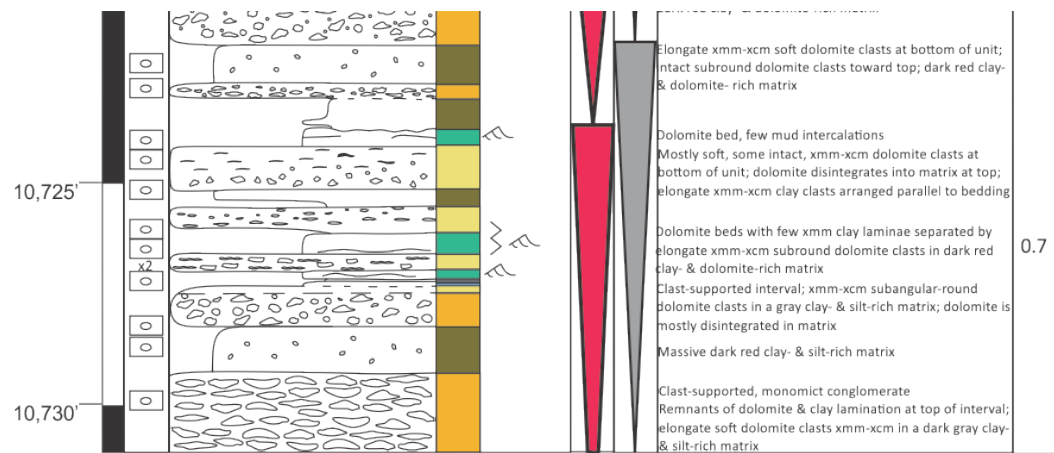
Stratigraphic Interval: Middle Three Forks Formation

Date: August 15, 2012

Core Analyst: Lauren Droege

County, State: Williams Co., North Dakota





Operator: Brigham Oil and Gas, L.P.

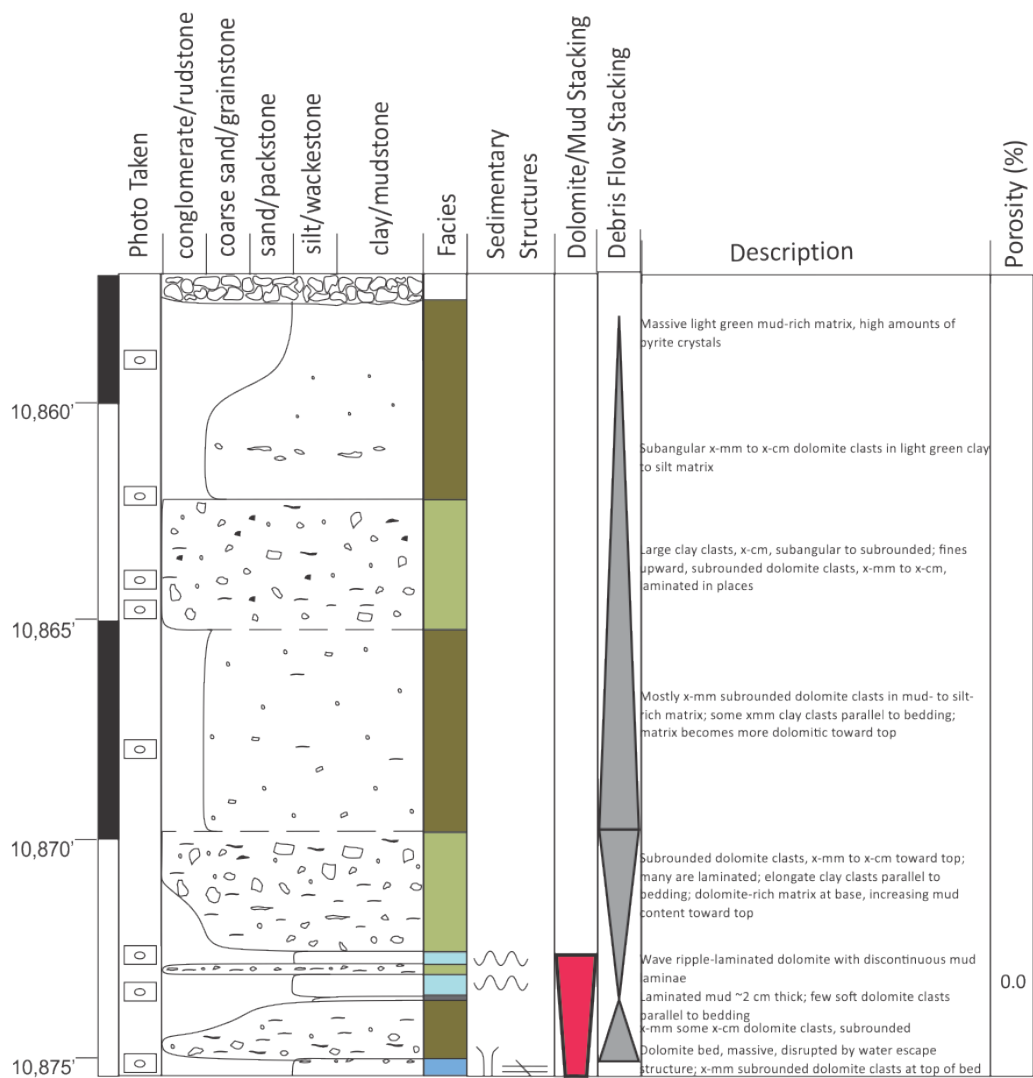
Well: State 36-1 2H

Stratigraphic Interval: Middle Three Forks Formation

Date: November 17, 2013

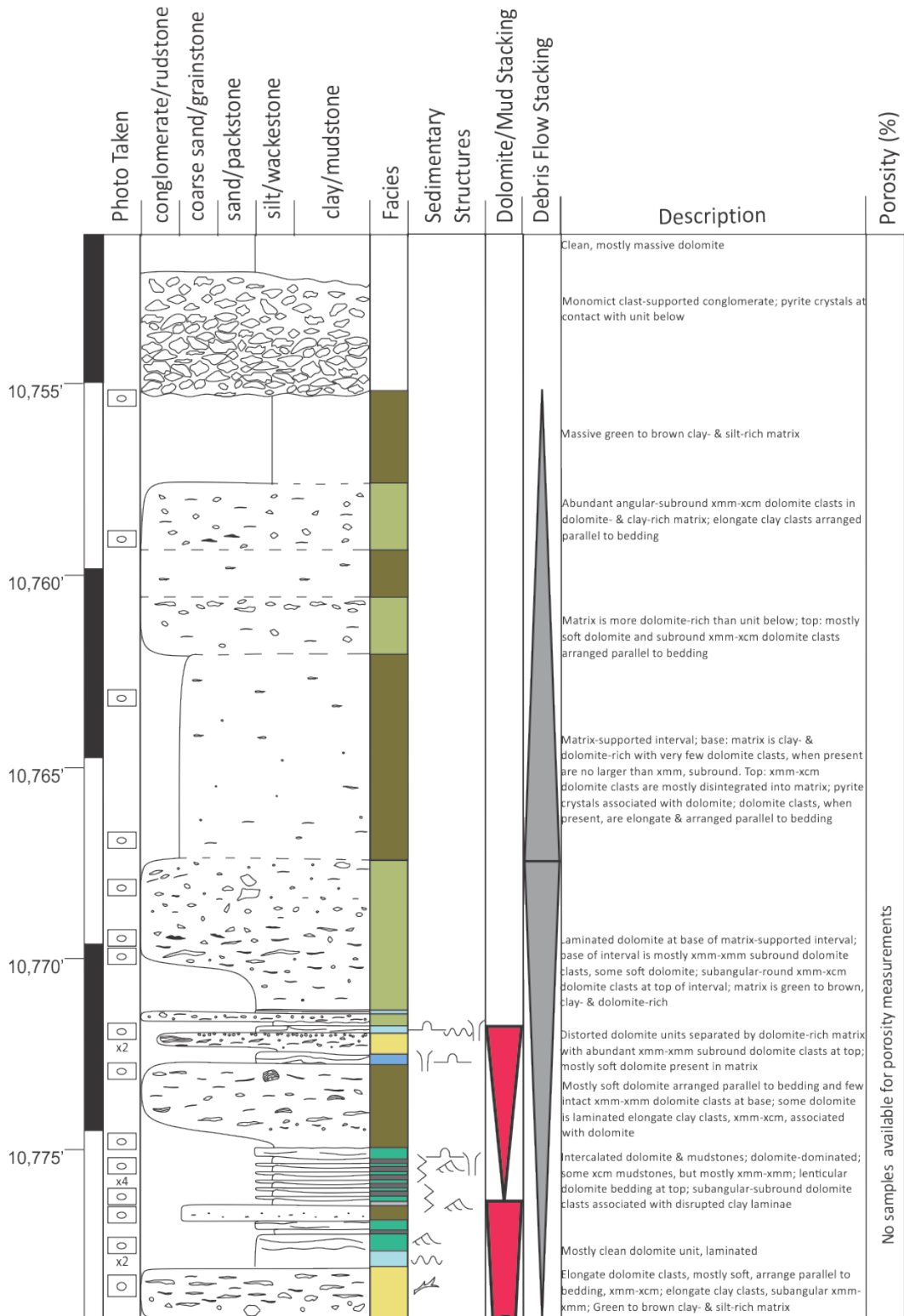
Core Analyst: Lauren Droege

County, State: Williams County, North Dakota



Operator: Newfield Production
Well: Heidi 1-4H
Stratigraphic Interval: Middle Three Forks Formation

Date: August 17, 2012
Core Analyst: Lauren Droege
County, State: Williams Co., North Dakota



Operator: SM Energy Company

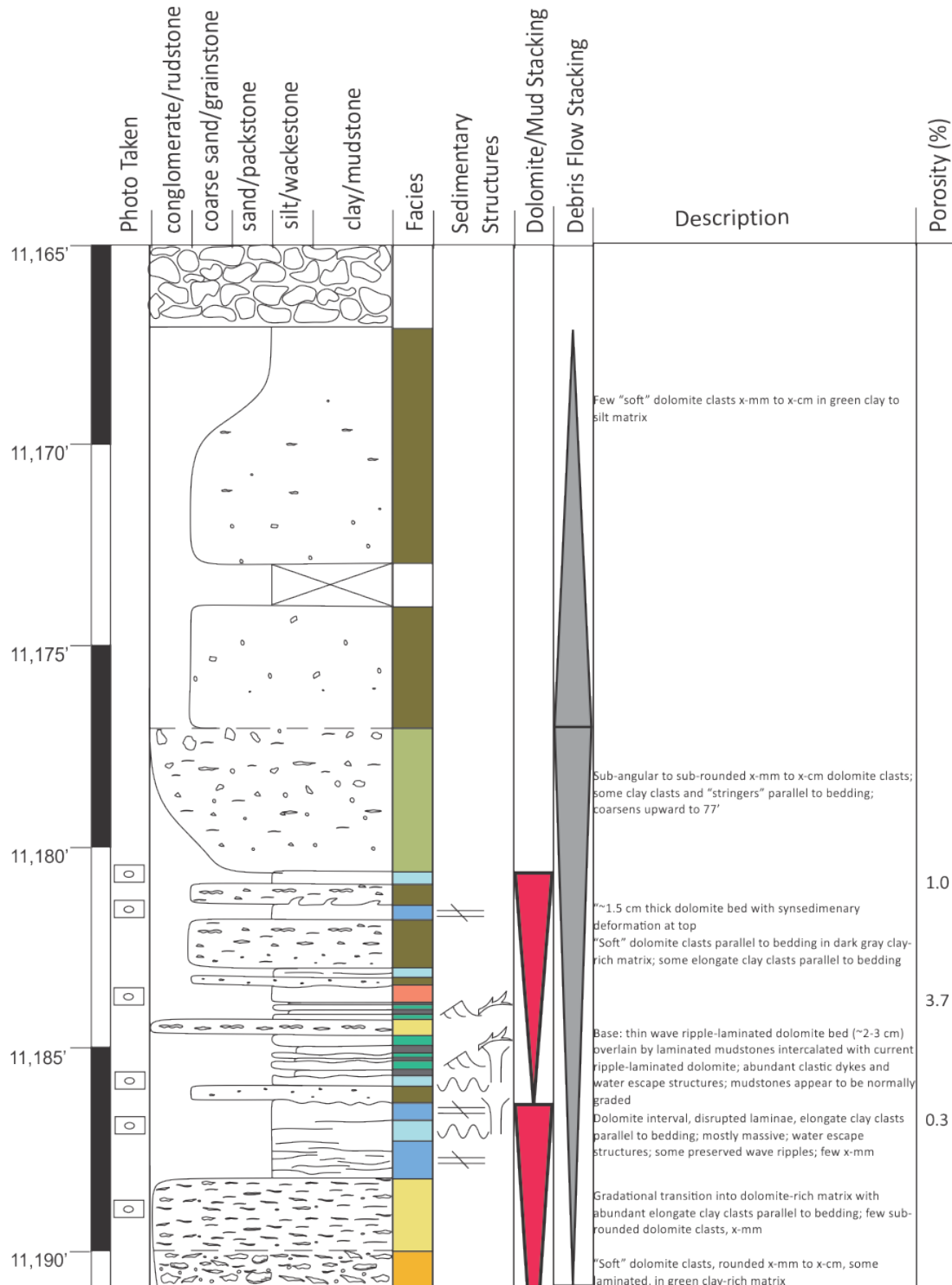
Well: Jaynes 16-12H

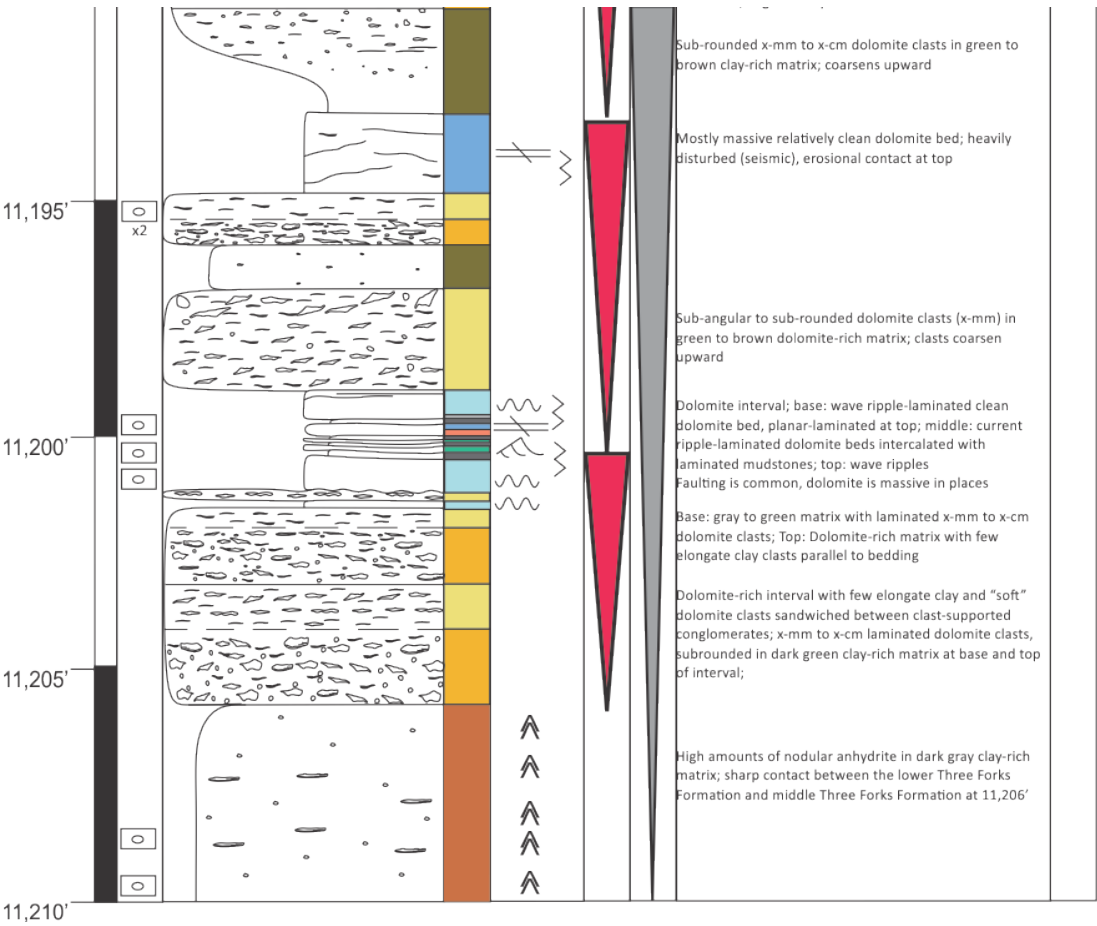
Stratigraphic Interval: Middle Three Forks Formation

Date: November 16, 2013

Core Analyst: Lauren Droege

County, State: McKenzie County, North Dakota





Operator: North Plains Energy, LLC

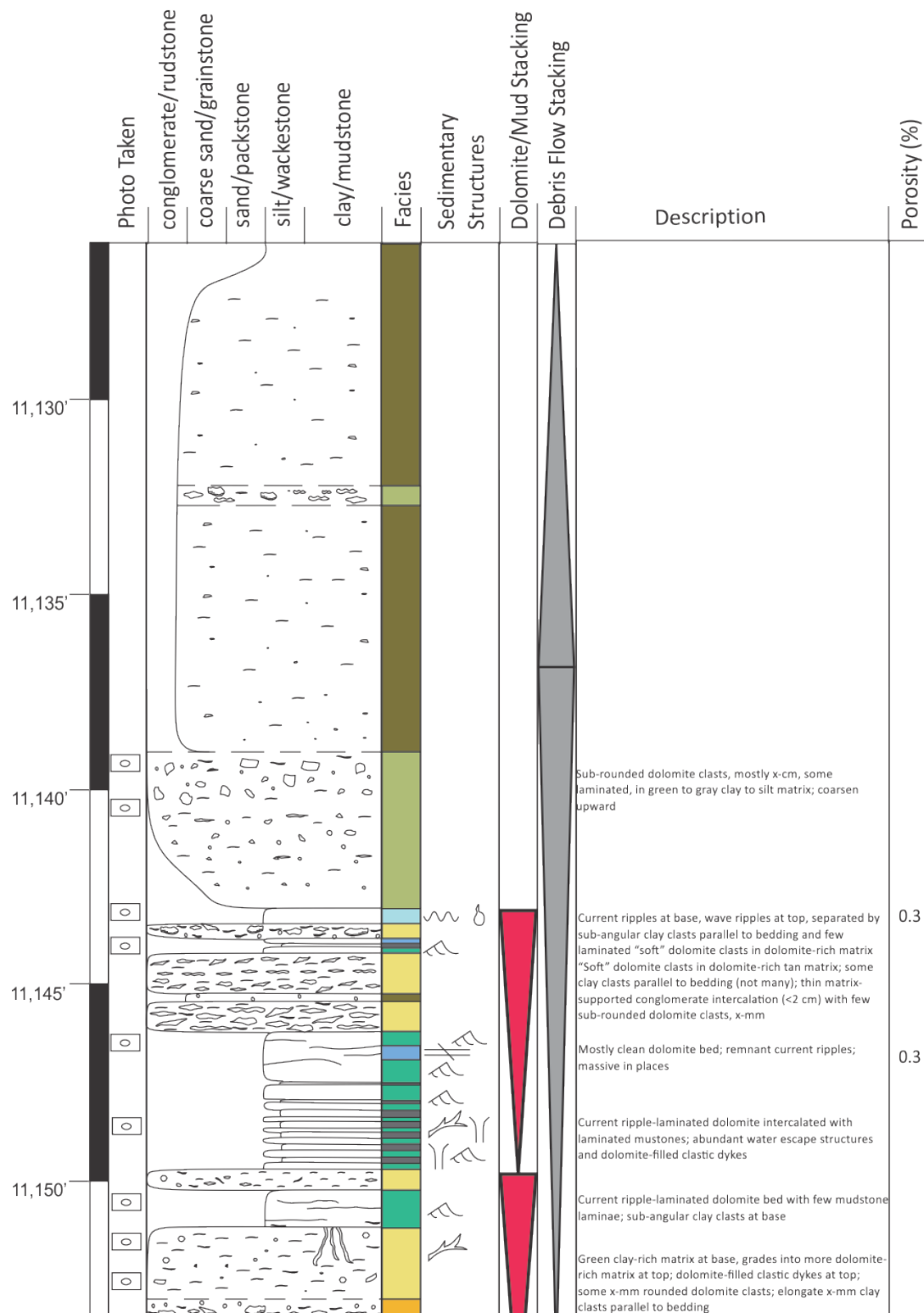
Well: Scanlan 3-5H

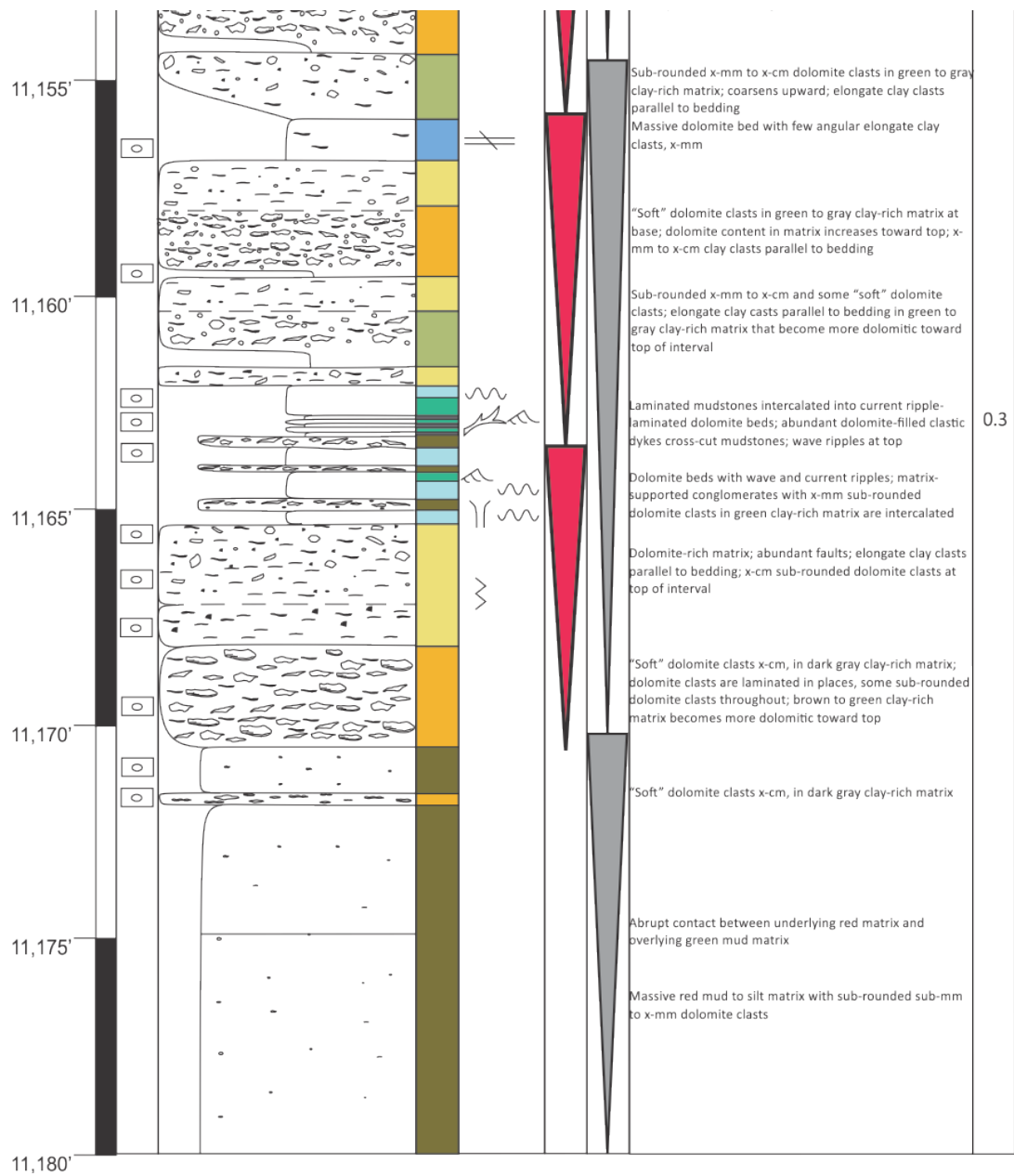
Stratigraphic Interval: Middle Three Forks Formation

Date: November 18, 2013

Core Analyst: Lauren Droege

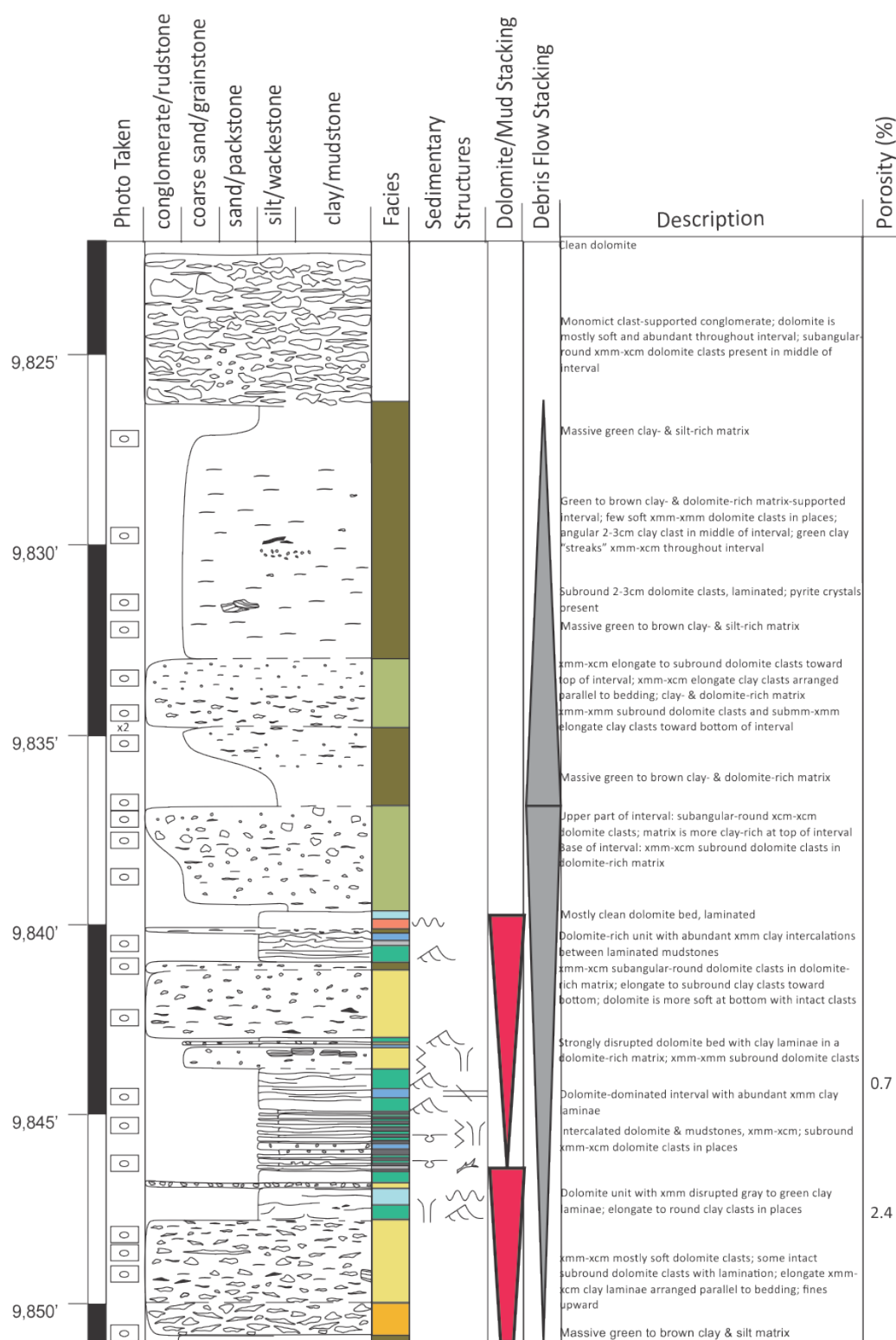
County, State: Williams County, North Dakota





Operator: Amerada Hess
Well: Anderson Smith 1-26H
Stratigraphic Interval: Middle Three Forks Formation

Date: August 16, 2012
Core Analyst: Lauren Droege
County, State: Williams Co., North Dakota



Operator: Headington Oil

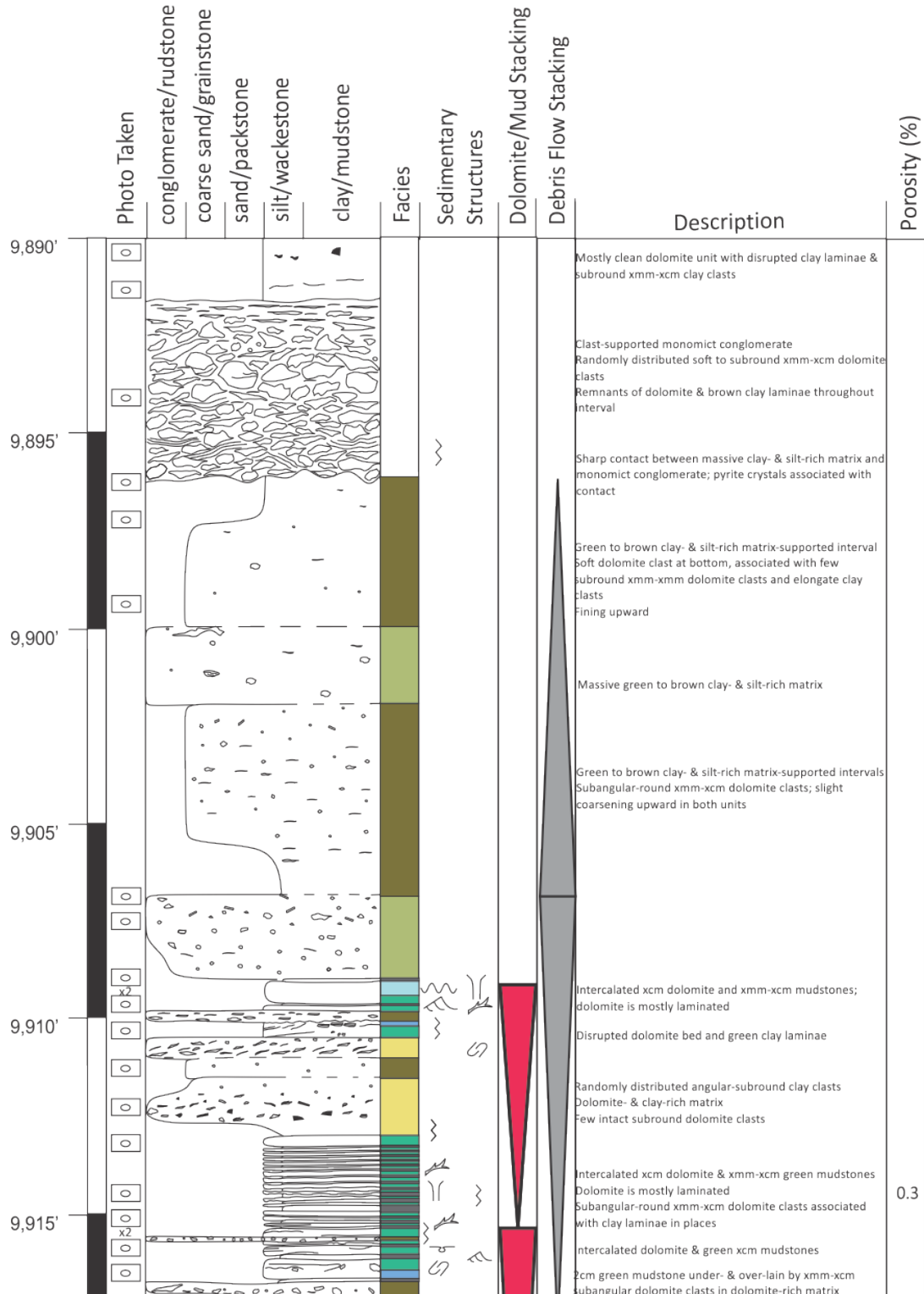
Well: Sak.Fed. 13X-35

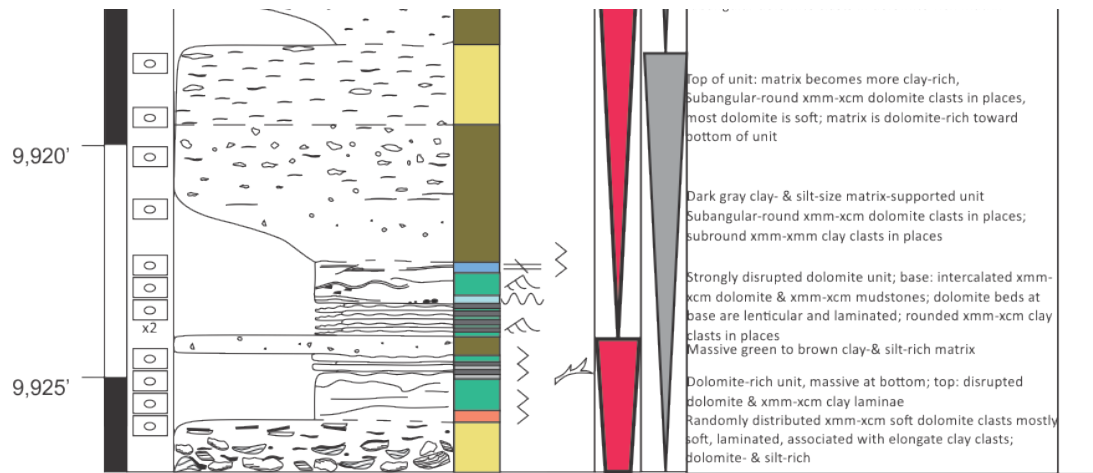
Stratigraphic Interval: Middle Three Forks Formation

Date: August 17, 2012

Core Analyst: Lauren Droege

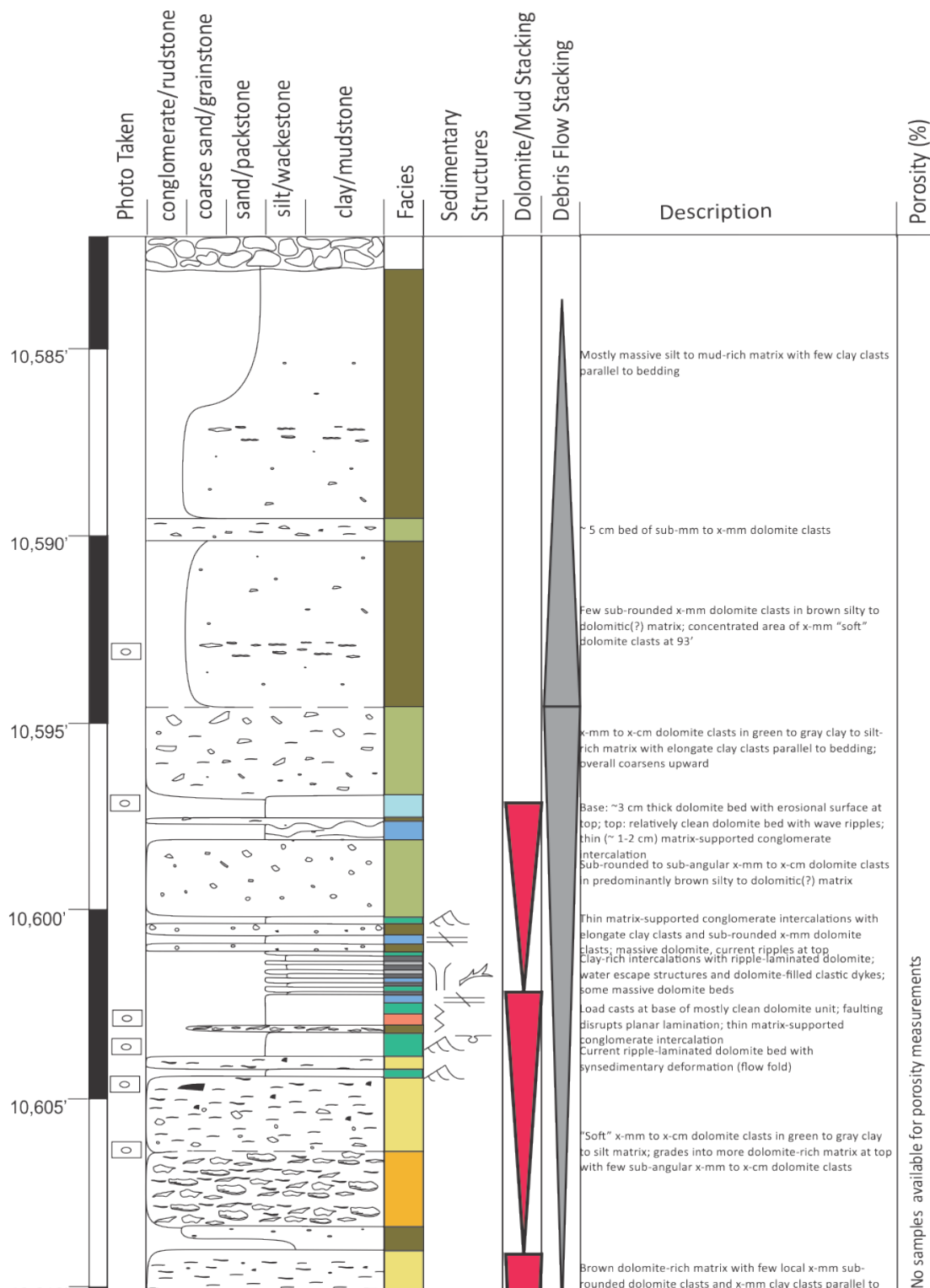
County, State: McKenzie Co., North Dakota

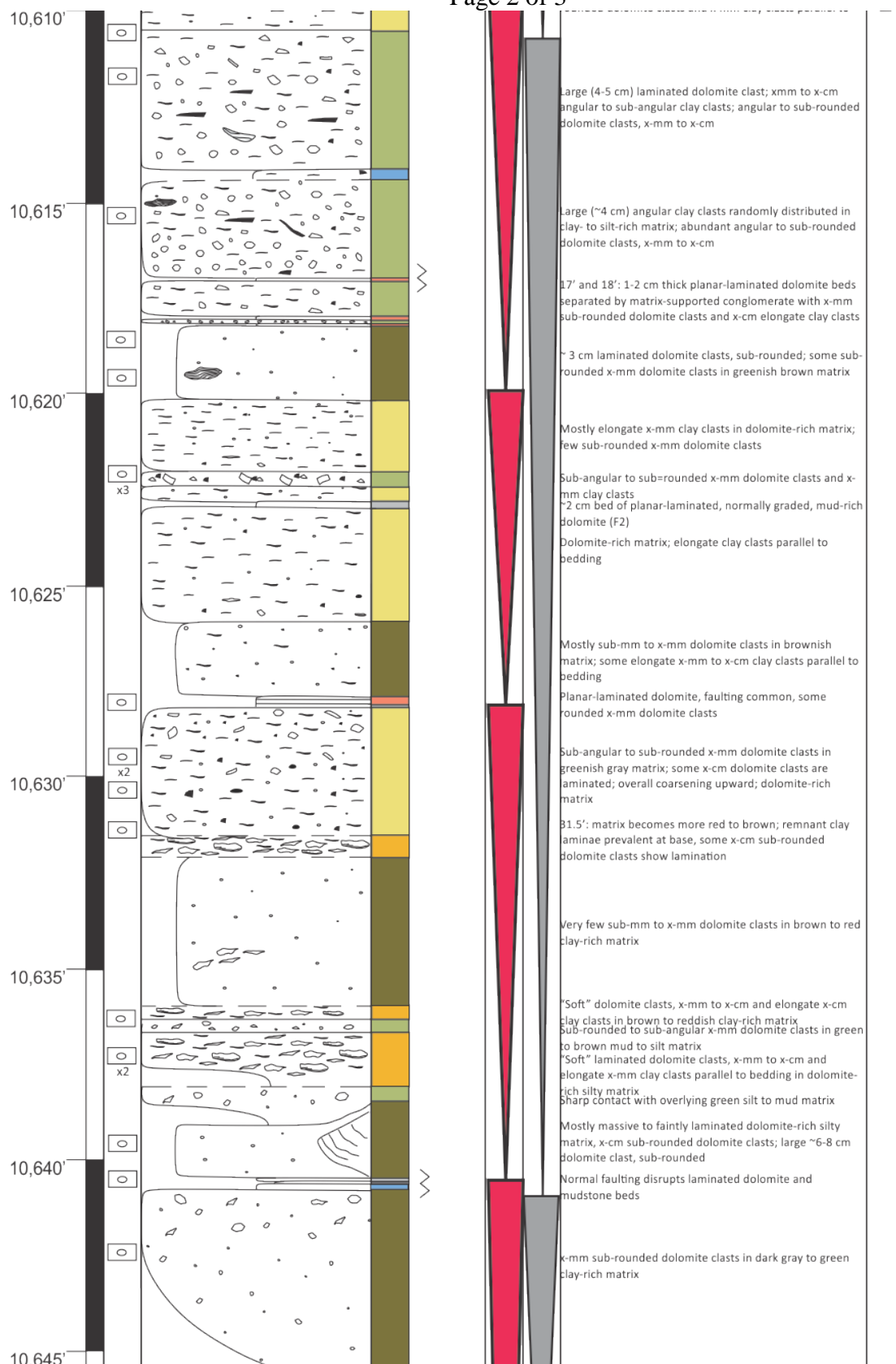


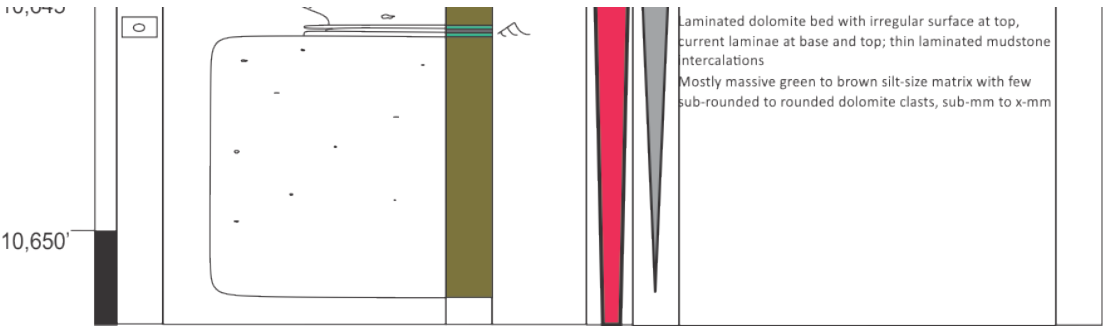


Operator: Burlington Resources Oil and Gas Company
Well: Washburn 44-36H
Stratigraphic Interval: Middle Three Forks Formation

Date: November 15, 2013
Core Analyst: Lauren Droege
County, State: McKenzie County, North Dakota







Appendix 6: Thin section index

Well Number and Sample Depth	Facies Association (FA)	Coarse silt to very fine sand-size dolomite (%)	Fine to medium silt-size dolomite (%)	Coarse silt to very fine sand-size detrital quartz (%)	Clay-size material (%)	Porosity (%)	Muscovite (%)	Pyrite (%)	Anhydrite (%)
16083-9844.1	FA1	3.7	61.3	5.7	28.3	0.7	0.3	0.0	0.0
16083-9847.6	FA1	11.2	64.1	13.2	9.2	2.4	0.0	0.0	0.0
16160-9569.9	FA3	6.3	46.0	5.7	42.0	0.0	0.0	0.0	0.0
16160-9581.5	FA1	5.3	48.0	20.3	20.7	5.7	0.0	0.0	0.0
16565- 9760.3	FA2	2.0	58.3	36.7	2.0	1.0	0.0	0.0	0.0
16565- 9771.0	FA2	0.0	90.0	7.7	1.0	1.3	0.0	0.0	0.0
16565- 9783.6	FA2	0.0	86.0	12.0	0.7	1.3	0.0	0.0	0.0
16565- 9763.9	FA2	3.7	85.0	10.0	0.3	1.0	0.0	0.0	0.0
16586-9948.6	FA1	1.3	70.2	6.0	16.7	4.3	0.3	1.0	0.0
16586-9957.7	FA2	4.0	68.0	7.3	20.3	0.3	0.0	0.0	0.0
16824-9329.9	FA2	3.0	72.0	11.7	12.3	1.0	0.0	0.0	0.0
16841-10249.0	FA1	3.3	54.0	6.0	35.7	0.0	0.7	0.3	0.0
16841-10249.9	FA2	8.7	76.3	4.3	7.7	2.3	0.7	0.0	0.0
17023-10020.6	FA1	4.0	33.8	15.7	41.5	5.0	0.0	0.0	0.0
17067-9914.0	FA1	7.3	56.7	4.0	31.3	0.3	0.3	0.0	0.0
17071-8881.0	FA1	4.0	49.0	18.5	27.5	0.3	0.7	0.0	0.0
17071-8882.3	FA1	7.0	62.5	3.7	21.1	5.0	0.7	0.0	0.0
17096-9791.0	FA2	12.3	72.7	0.3	10.3	0.0	0.3	4.0	0.0
17096-9793.9	FA2	9.0	67.0	10.3	9.7	4.0	0.0	0.0	0.0
17351-10219.4	FA1	0.7	62.7	6.0	30.0	0.3	0.3	0.0	0.0
17351-10227.4	FA2	4.7	71.9	13.4	8.0	1.3	0.0	0.3	0.3
17513-10716.9	FA1	2.0	74.7	5.7	16.5	1.0	0.0	0.0	0.0
17513-10718.8	FA2	18.4	59.9	13.4	5.0	3.0	0.3	0.0	0.0
17513-10726.4	FA2	13.7	64.3	19.3	2.0	0.7	0.0	0.0	0.0

17676-8850.8	FA2	7.7	55.4	11.7	20.8	4.4	0.0	0.0	0.0
17676-8855.9	FA1	16.1	52.8	18.7	8.7	3.7	0.0	0.0	0.0
18101-9750.1	FA2	4.7	61.0	12.3	18.7	2.7	0.7	0.0	0.0
18101-9754.5	FA1	3.0	16.8	5.1	74.1	0.7	0.3	0.0	0.0
18101-9764.5	FA2	9.0	77.7	6.3	3.7	3.3	0.0	0.0	0.0
18770- 11143.2	FA2	0.3	84.0	14.0	1.0	0.3	0.0	0.3	0.0
18770- 11146.8	FA2	2.3	90.0	6.7	0.3	0.3	0.0	0.3	0.0
18770- 11162.9	FA2	1.7	88.3	9.7	0.0	0.3	0.0	0.0	0.0
19060- 9781.3	FA2	0.7	77.3	19.0	2.0	1.0	0.0	0.0	0.0
19060- 9784.2	FA2	2.3	80.3	12.3	3.3	1.3	0.0	0.3	0.0
19060- 9787.0	FA2	0.7	93.3	3.0	0.0	3.0	0.0	0.0	0.0
19215- 10873.2	FA2	1.3	93.3	1.3	3.3	0.0	0.0	0.0	0.7
20022- 11180.9	FA2	1.3	68.6	29.1	0.0	1.0	0.0	0.0	0.0
20022- 11183.9	FA2	7.7	65.3	23.3	0.0	3.7	0.0	0.0	0.0
20022- 11186.9	FA2	3.0	91.3	2.0	2.3	0.3	0.0	0.0	1.0
20315- 10230.1	FA2	2.0	92.0	5.7	0.0	0.3	0.0	0.0	0.0
20315-10226.8	FA2	0.0	83.7	8.3	8.0	0.0	0.0	0.0	0.0
20315-10237.3	FA2	0.7	88.3	5.7	4.7	0.7	0.0	0.0	0.0
21928- 9948.8	FA2	2.0	67.3	16.7	12.7	1.3	0.0	0.0	0.0
21928- 9954.5	FA2	0.3	93.0	4.7	1.7	0.3	0.0	0.0	0.0
DN39564- 8410.1	FA3	1.2	84.9	2.3	11.6	0.0	0.0	0.0	0.0
DN39564-8418.2	FA1	2.3	51.7	7.3	38.3	0.0	0.0	0.3	0.0
DN39564-8418.7	FA1	1.3	70.3	3.0	23.7	0.0	0.7	1.0	0.0

Appendix 7: Scanning electron microscope (SEM) report

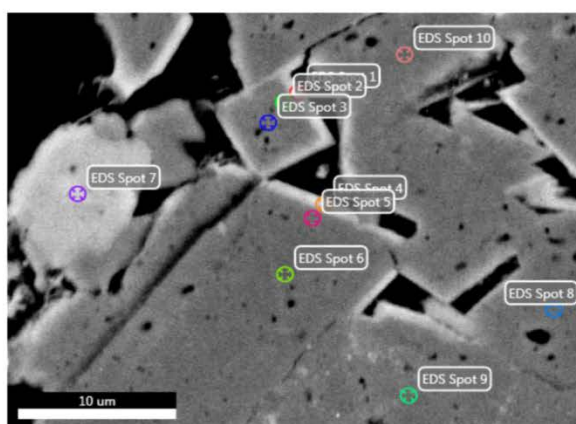
EDAX TEAM

Page 1

Middle Three Forks

Author: segenhoff
Creation: 3/7/2014
Sample Name: 20315- 10237.3

Area 2

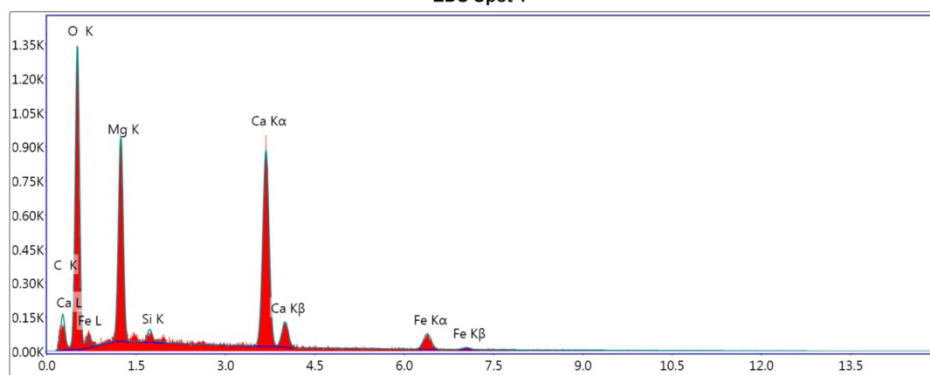


Notes:

EDS Spot 1

kV: 15 Mag: 4513 Takeoff: 35.3 Live Time(s): 30 Amp Time(μs): 0.5 Resolution:(eV) 141.9

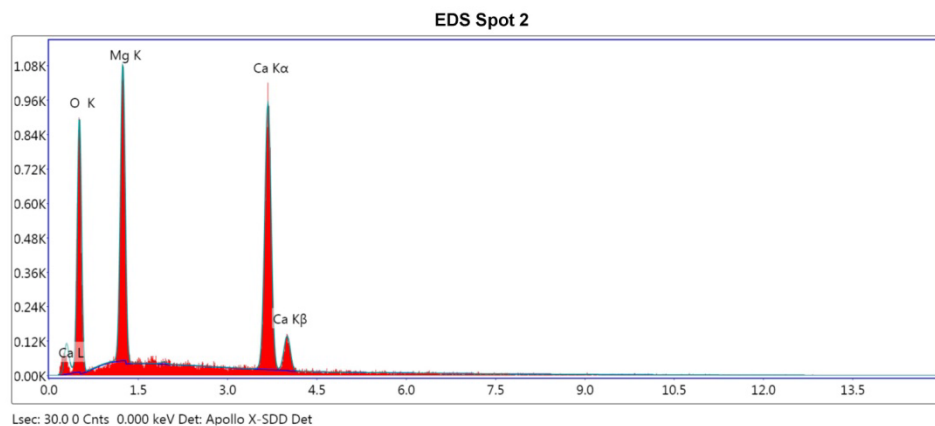
EDS Spot 1

eZAF Smart Quant Results

Element	Weight %	Atomic %	Net Int.	Error %
C K	7.24	12.32	39.44	11.71
O K	48.39	61.79	380.22	9.7
MgK	12.31	10.35	296.4	6.73
SiK	0.77	0.56	21.61	15.5
CaK	24.5	12.49	369.89	2.9
FeK	6.78	2.48	35.27	12.1

EDS Spot 2

kV: 15 Mag: 4513 Takeoff: 35.3 Live Time(s): 30 Amp Time(μs): 0.5 Resolution:(eV) 141.9

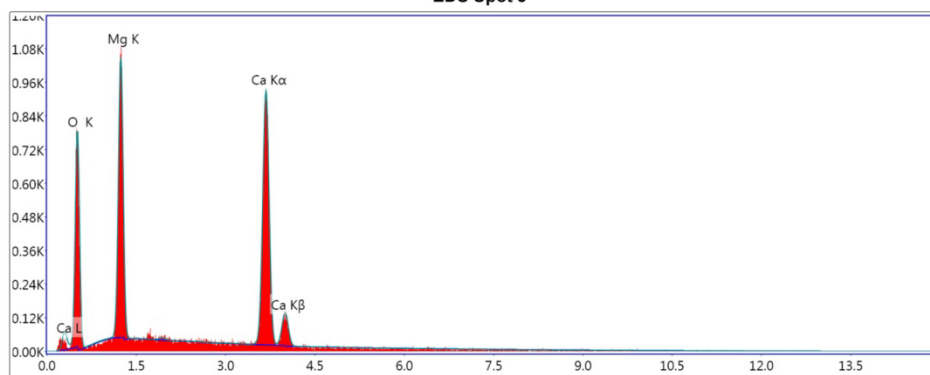
**eZAF Smart Quant Results**

Element	Weight %	Atomic %	Net Int.	Error %
O K	48.36	65.84	252.33	10.32
MgK	17.3	15.5	335.14	6.42
CaK	34.34	18.66	396.52	2.83

EDS Spot 3

kV: 15 Mag: 4513 Takeoff: 35.3 Live Time(s): 30 Amp Time(μs): 0.5 Resolution:(eV) 141.9

EDS Spot 3



Lsec: 30.0 0 Cnts 0.000 keV Det: Apollo X-SDD Det

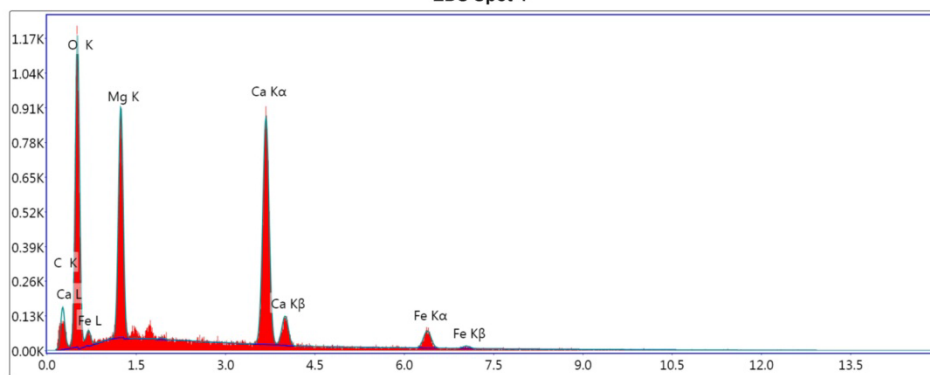
eZAF Smart Quant Results

Element	Weight %	Atomic %	Net Int.	Error %
O K	46.75	64.41	222.23	10.49
MgK	17.65	16.01	322.8	6.44
CaK	35.6	19.58	387.08	2.9

EDS Spot 4

kV: 15 Mag: 4513 Takeoff: 35.3 Live Time(s): 30 Amp Time(μs): 0.5 Resolution:(eV) 141.9

EDS Spot 4



Lsec: 30.0 0 Cnts 0.000 keV Det: Apollo X-SDD Det

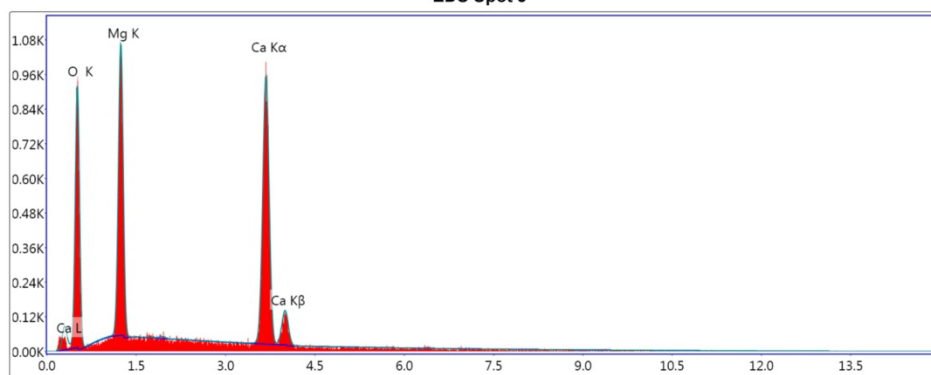
eZAF Smart Quant Results

Element	Weight %	Atomic %	Net Int.	Error %
C K	7.62	13.05	39.9	11.55
O K	47.2	60.67	334.74	9.87
MgK	12.39	10.48	277.93	6.92
CaK	25.77	13.22	364.07	2.96
FeK	7.01	2.58	34.08	13.3

EDS Spot 5

kV: 15 Mag: 4513 Takeoff: 35.3 Live Time(s): 30 Amp Time(μs): 0.5 Resolution:(eV) 141.9

EDS Spot 5



Lsec: 30.0 0 Cnts 0.000 keV Det: Apollo X-SDD Det

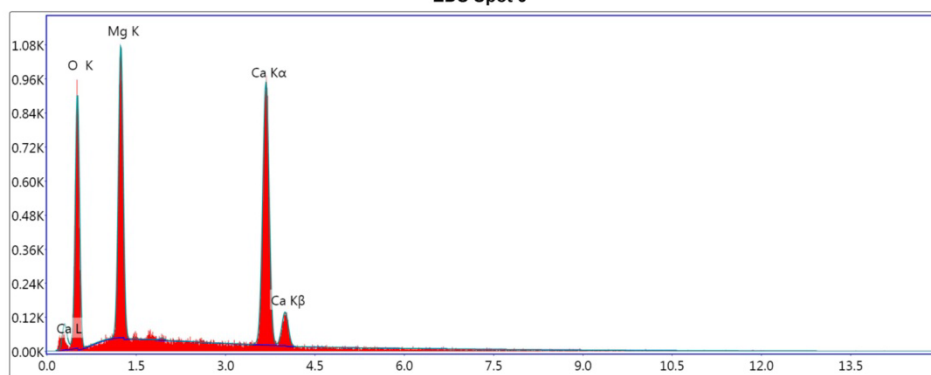
eZAF Smart Quant Results

Element	Weight %	Atomic %	Net Int.	Error %
O K	48.99	66.45	258.72	10.29
MgK	16.88	15.07	328.08	6.45
CaK	34.13	18.48	396.3	2.94

EDS Spot 6

kV: 15 Mag: 4513 Takeoff: 35.3 Live Time(s): 30 Amp Time(μs): 0.5 Resolution:(eV) 141.9

EDS Spot 6



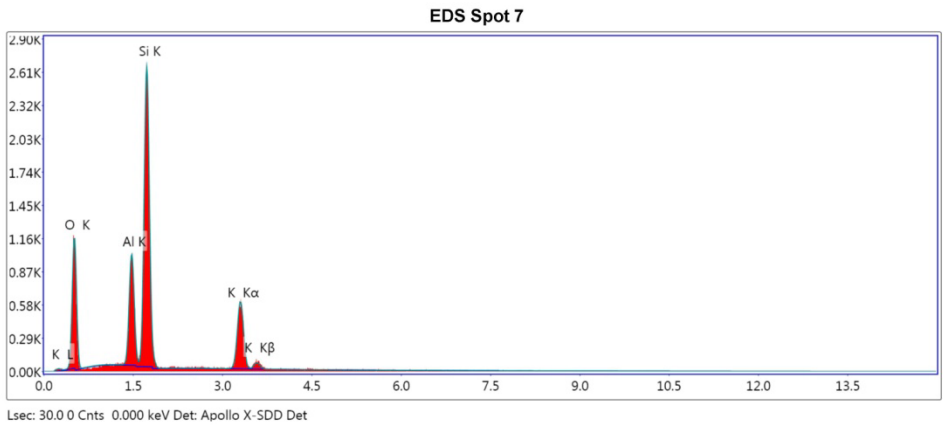
Lsec: 30.0 0 Cnts 0.000 keV Det: Apollo X-SDD Det

eZAF Smart Quant Results

Element	Weight %	Atomic %	Net Int.	Error %
O K	48.59	66.06	254.13	10.3
MgK	17.18	15.37	332.43	6.43
CaK	34.22	18.57	394.85	2.88

EDS Spot 7

kV: 15 Mag: 4513 Takeoff: 35.3 Live Time(s): 30 Amp Time(μs): 0.5 Resolution:(eV) 141.9



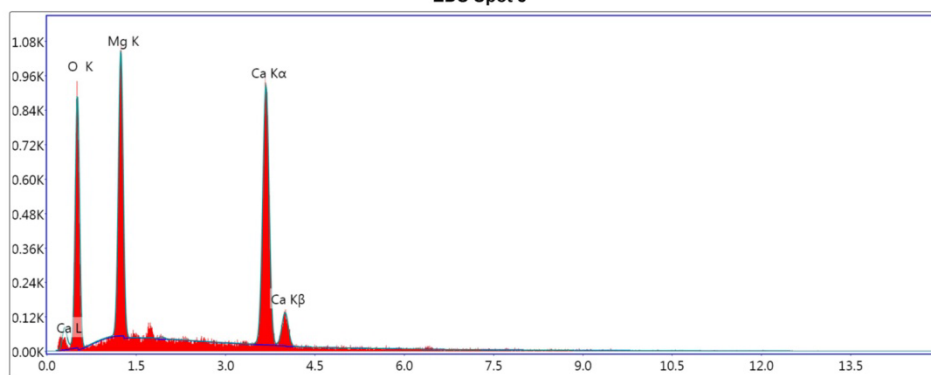
eZAF Smart Quant Results

Element	Weight %	Atomic %	Net Int.	Error %
O K	40.36	55.97	331.05	9.37
AlK	11.2	9.21	325.84	4.51
SiK	32.94	26.02	902.22	3.88
K K	15.5	8.8	241.17	3.96

EDS Spot 8

kV: 15 Mag: 4513 Takeoff: 35.3 Live Time(s): 30 Amp Time(μs): 0.5 Resolution:(eV) 141.9

EDS Spot 8



Lsec: 30.0 0 Cnts 0.000 keV Det: Apollo X-SDD Det

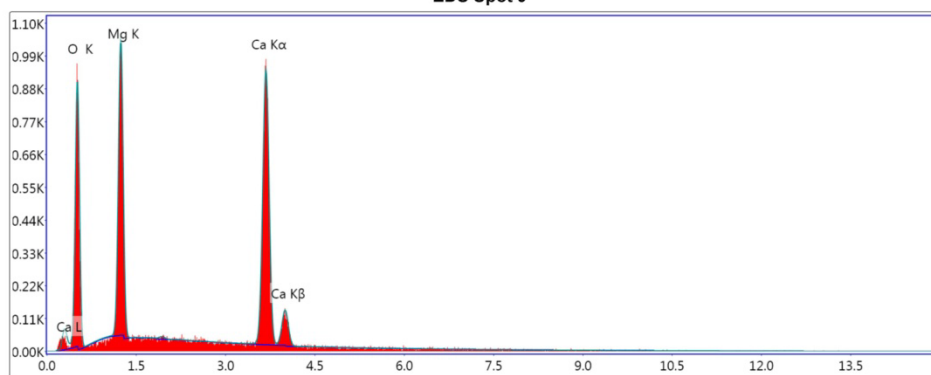
eZAF Smart Quant Results

Element	Weight %	Atomic %	Net Int.	Error %
O K	48.79	66.26	249.91	10.32
MgK	16.98	15.18	321.22	6.46
CaK	34.23	18.56	386.61	2.89

EDS Spot 9

kV: 15 Mag: 4513 Takeoff: 35.3 Live Time(s): 30 Amp Time(μs): 0.5 Resolution:(eV) 141.9

EDS Spot 9

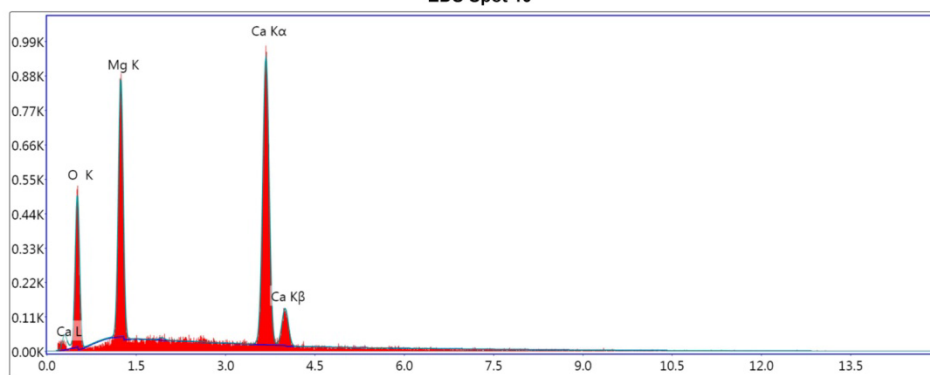
eZAF Smart Quant Results

Element	Weight %	Atomic %	Net Int.	Error %
O K	48.98	66.47	255.6	10.31
MgK	16.77	14.97	322.62	6.46
CaK	34.25	18.55	393.98	2.88

EDS Spot 10

kV: 15 Mag: 4513 Takeoff: 35.3 Live Time(s): 30 Amp Time(μs): 0.5 Resolution:(eV) 141.9

EDS Spot 10

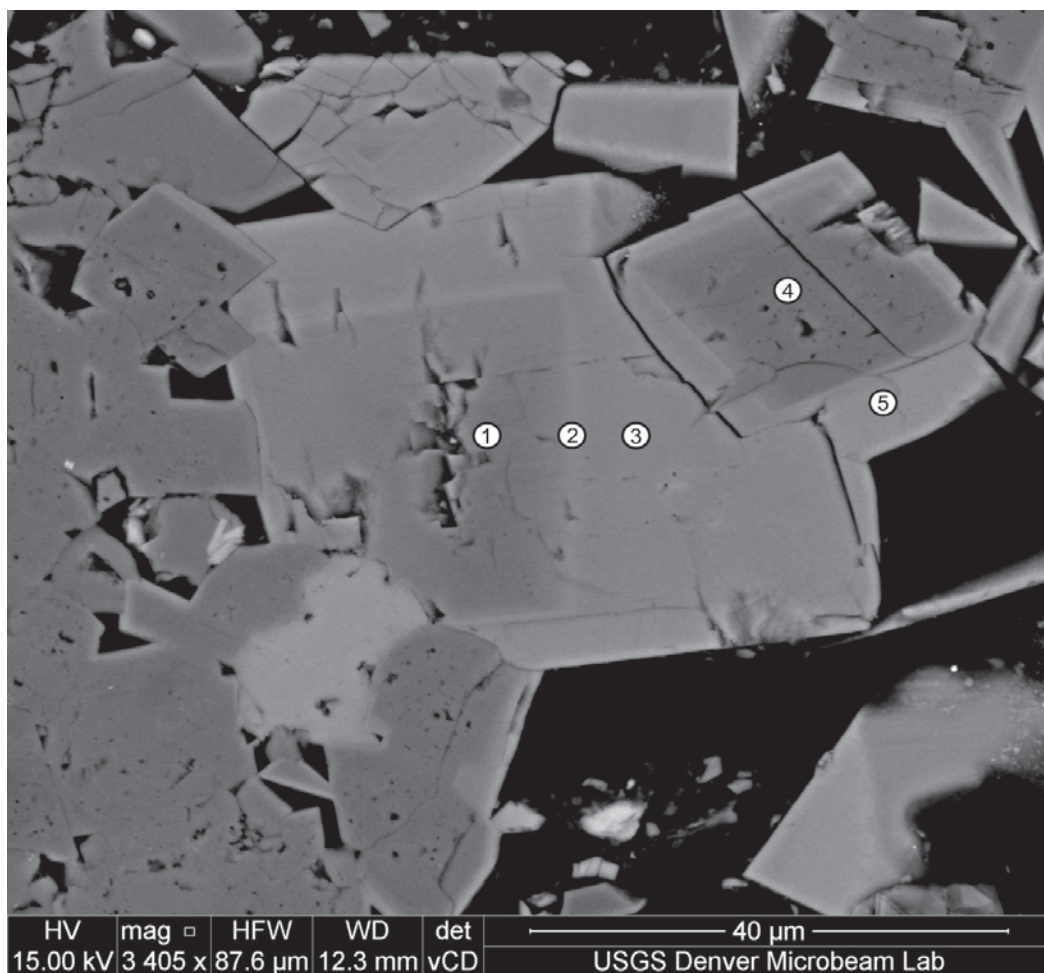


Lsec: 30.0 0 Cnts 0.000 keV Det: Apollo X-SDD Det

eZAF Smart Quant Results

Element	Weight %	Atomic %	Net Int.	Error %
O K	40.35	58.81	140.19	11.4
MgK	17.21	16.51	267.25	6.7
CaK	42.44	24.69	392.63	2.9

Appendix 8: Electron Microprobe quantitative results



Datapoint	Well number and sample depth (ft)	FeO WT%	MnO WT%	BaO WT%	MgO WT%	CaO WT%	SO ₃ WT%	SrO WT%	SiO ₂ WT%	CO ₂ WT%
1	17071-8882.3	3.6	0.74	0.00	20.3	34.5	0.00	0.01	0.03	40.8
2	17071-8882.3	6.0	0.42	0.03	18.0	35.3	0.01	0.02	0.03	40.1
3	17071-8882.3	5.2	0.04	0.00	17.9	35.0	0.00	0.00	0.04	41.8
4	17071-8882.3	0.4	0.08	0.18	22.1	33.2	0.05	0.00	0.90	43.0
5	17071-8882.3	6.7	0.41	0.04	15.0	30.5	0.01	0.00	0.26	47.1